PB-227 029

ANALYTICAL AND EXPERIMENTAL INVESTIGATION OF AN AMMONIA/AIR OPPOSED REACTING JET

Gary Scott Samuelsen

California University
Berkeley, California

September 1970

DISTRIBUTED BY:

NTIS
National Technical Information Service
U. S. DEPARTMENT OF COMMERCE
5285 Port Royal Road, Springfield Va. 22151

PB 227 029

Analytical and Experimental Investigation of an Ammonia/Air Opposed Reacting Jet

By

Gary Scott Samuelsen

B.S. (University of California) 1964
M.S. (University of California) 1965

DISSERTATION

Submitted in partial satisfaction of the requirements for the degree of

DOCTOR OF PHILOSOPHY

in

Engineering

in the

GRADUATE DIVISION

of the

UNIVERSITY OF CALIFORNIA, BERKELEY

Approved:
E. Starkman
R F Sawyer
Theodore Vermeulen

Committee in Charge

Reproduced by
NATIONAL TECHNICAL
INFORMATION SERVICE
U S Department of Commerce
Springfield VA 22151

Analytical and Experimental Investigation of an Ammonia/Air Opposed Reacting Jet

G. Scott Samuelsen

ABSTRACT

The point-by-point properties of an ammonia/air opposed-reacting-jet flow field are described by solving the governing partial differential elliptic equations. Solutions are compared to three experimental conditions including both reacting and non-reacting flows. The analytical results for the reacting flow are compared to experimentally measured profiles of temperature and composition. Calculated distributions of stream function, temperature and fuel mole fraction are presented.

ACKNOWLEDGEMENTS

Appreciation is extended to E. S. Starkman for his support and faith, R. F. Sawyer for his encouragement and guidance, D. B. Spalding for his inspiration and direction, and T. Vermeulen for his continued interest and helpful suggestions.

A special debt of gratitude is due V. Locke and J. DeCosta for the fabrication of the experiment, and W. Coleman for assistance in the collection of experimental data, and A. D. Gosman and W. M. Pun for valuable discussions with regard to the numerical procedure.

The computer facilities of the University of California Computer Center are gratefully acknowledged.

This work was supported by a grant from the U.S. Public Health Service.

TABLE OF CONTENTS

Page

SECTION 1 - Introduction 1

SECTION 2 - The Opposed Reacting Jet as a Flameholder 3

- 2.1 Flameholding Concepts 3
- 2.2 Previous Work 10

SECTION 3 - The Opposed Reacting Jet as a Research Tool 24

- 3.1 Fundamental Characteristics 24
- 3.2 Relation to Real Combustors 25
- 3.3 Summary of the State-of-the-Art 27

SECTION 4 - Analytical Investigation 29

- 4.1 Conditions Investigated 29
- 4.2 Numerical Calculations 34
  - 4.2.1 Theory 34
  - 4.2.2 Finite Difference Formulation 44
  - 4.2.3 Physical Inputs 54
  - 4.2.4 Computational Procedure 60
  - 4.2.5 Analytical Results 66

SECTION 5 - Experimental Investigation 71

- 5.1 Experimental Facility 71
- 5.2 Inlet Velocity and Composition Profiles 74
- 5.3 Blowout Map 80
- 5.4 Jet Exit Temperature and Velocity 82
- 5.5 Composition and Temperature Measurements 83

SECTION 6 - Analytical and Experimental Results Compared 93

SECTION 7 - Conclusions 100

TABLE OF CONTENTS (Continued)

Page

References 101

Symbols 108

APPENDIX A - Experimental Facility 111

APPENDIX B - Thermocouple Reading Errors 117

APPENDIX C - Adiabatic Approximation 119

APPENDIX D - Description of Computer Program 123

APPENDIX E - Experimental Data Reduction Program 176

LIST OF FIGURES

Figure Page

1.1 Opposed jet combustor 2

2.1 Physical flameholders 4

2.2 Aerodynamic flameholder, the opposed reacting jet 7

2.3 Blowout map 8

2.4 Blowout map: effect of jet composition 9

3.1 Gas turbine combustor 26

4.1 Blowout map: ammonia/air opposed reacting jet 32

4.2 Turbulent velocity 39

4.3 Computer flow diagram 62

4.4 Grid schematic 64

4.5 Distributions of stream function, $\psi \times 10^3$ 67

4.6 Distributions for Case 3 69

4.7 Temperature and fuel mole fraction profiles, predicted . . 70

5.1 Opposed reaction jet: cross-section 73

5.2 Vycor combustion chamber with lagging 75

5.3 Stagnation probe 77

5.4 Inlet velocity profiles 78

5.5 Blowout map: ammonia/air opposed reacting jet 80

5.6 Location of composition and temperature measurements . . . 84

5.7 Composition probe 85

5.8 Composition profile, experimentally measured 89

5.9 Thermocouple probe 90

5.10 Temperature profile, experimentally measured 92

6.1 Temperature profiles, adiabatic jet wall 94

LIST OF FIGURES (Continued)

Figure		Page
6.2	Temperature and composition profiles, adiabatic jet wall	96
6.3	Temperature and composition profiles, diabatic jet wall	98
A.1	Experimental facility	112
C.1	Lagging wall temperatures	120

LIST OF TABLES

TABLE PAGE

2.1 Historical summary of opposed reacting jet work 12

4.1a Components of the laminar stress tensor for Newtonian fluids in Cartesian coordinates 41

4.1b Components of the turbulent stress tensor in Cartesian coordinates 41

4.2 Functions a_ϕ, b_ϕ, c_ϕ, and d_ϕ of Equations 4.11 and 4.12 45

SECTION 1

Introduction

An opposed-reacting-jet (ORJ) is shown in Figure 1.1. The flame is stabilized by a jet directly opposing the premixed combustible main flow. The jet stream can be air, a fuel/air mixture or an inert gas. The flame will blow out when the jet is shut-off. Because the flame is stabilized by the jet, the opposed-reacting-jet is classified as a flameholder.

In this investigation, the governing partial differential equations are solved for an ammonia/air opposed-reacting-jet. Solutions are compared to three experimental conditions. The objective is to demonstrate that the governing equations can be solved for a reacting, turbulent flow with recirculation while obtaining satisfactory correlation with experiment. A theoretical prediction of the point-by-point properties of the reacting flow is valuable to the study of air pollution emissions from continuous combustion sources.

In Sections 2 and 3, the opposed-reacting-jet is discussed as a flameholder and as a potential research tool. The analytical investigation is presented in Section 4 and the experimental study is described in Section 5. The analytical solutions and the experimental observations are compared in Section 6. Section 7 contains the conclusions of the investigation.

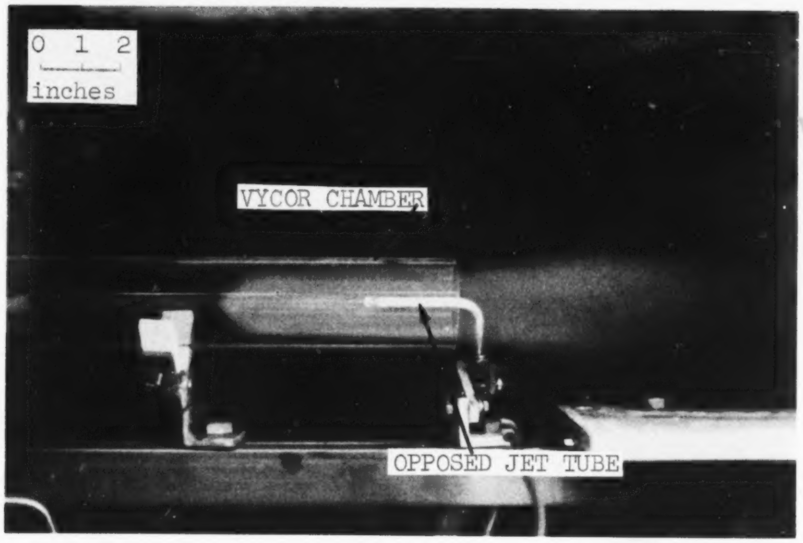
0 1 2
inches
VYCOR CHAMBER
OPPOSED JET TUBE

FIGURE 1.1 OPPOSED JET COMBUSTOR

SECTION 2

The Opposed-Reacting-Jet as a Flameholder

2.1 Flameholding Concepts
2.2 Previous Work

2.1 Flameholding Concepts

A flame requires a reactive composition and an igniting condition. To occur, a flame needs a continuing feed of reactant mixture and a sufficient reflux of energy and/or active species.

A steady-state flame represents a balance between chemical reaction, fluid mechanics, mass diffusion, and heat conduction. The balance cannot be sustained indefinitely as the mass flow rate of reactants is increased. A critical velocity will be reached above which sufficient energy cannot be recirculated upstream to sustain the flame, and the flame will consequently blow out. The critical velocity is on the order of the flame propagation rate. Velocities higher than the flame propagation rate occur often in combustion systems (e.g., the ramjet and the afterburner of a gas-turbine engine) and special devices called flameholders must be used to stabilize the flame.

In Figure 2.1, streamlines (ψ = constant) are plotted for a variety of flameholders. The flameholder 1) decelerates the stream locally and 2) produces a zone of recirculation. The recirculation zone is characterized by a reverse flow. Partially or completely reacted species are recirculated upstream to the region of decelerated flow. The zone of recirculation provides the necessary energy to sustain the flame.

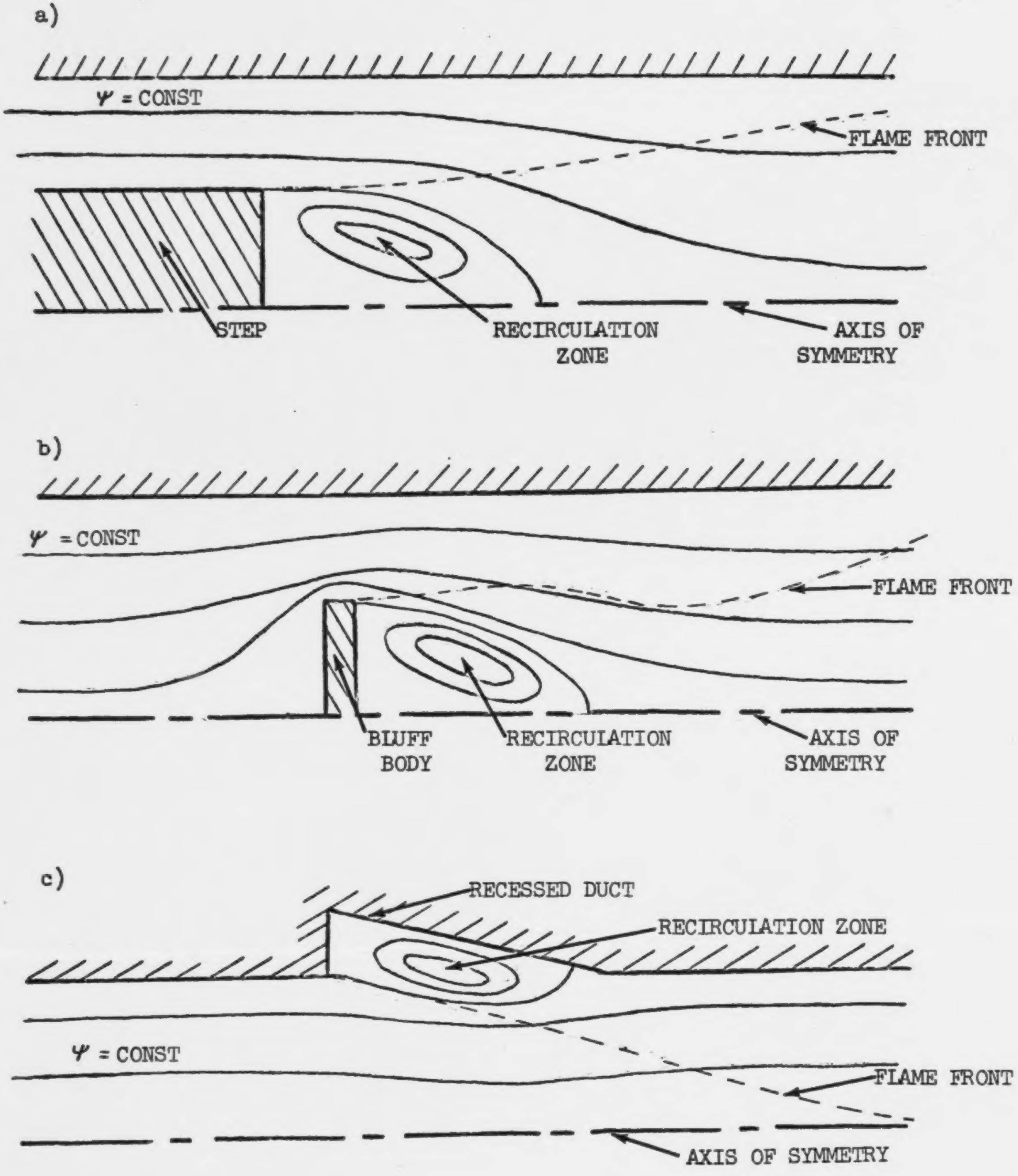
a)
Ψ = CONST
FLAME FRONT
STEP
RECIRCULATION ZONE
AXIS OF SYMMETRY
b)
Ψ = CONST
FLAME FRONT
BLUFF BODY
RECIRCULATION ZONE
AXIS OF SYMMETRY
c)
RECESSED DUCT
RECIRCULATION ZONE
Ψ = CONST
FLAME FRONT
AXIS OF SYMMETRY

FIGURE 2.1 PHYSICAL FLAMEHOLDERS
a) STEP
b) BLUFF BODY
c) RECESSED DUCT
d) AFTERBURNER OR RAMJET (Hill and Peterson-1967)

d)

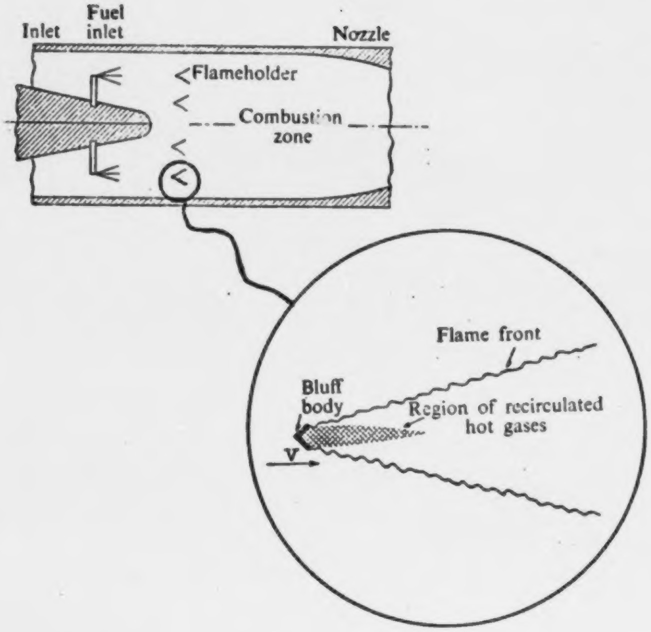
Inlet
Fuel inlet
Nozzle
Flameholder
Combustion zone
Flame front
Bluff body
Region of recirculated hot gases
V

The flameholders shown in Figure 2.1 are referred to as "physical" flameholders. Another class of flameholders are classified as "aerodynamic" flameholders. The opposed-reacting-jet shown in Figure 2.2 is an example of an aerodynamic flameholder. The flame is stabilized near the stagnation region of the main and jet streams. The zone of recirculation is located along the edge of the jet. The stream exiting the jet tube entrains and recirculates partially and completely reacted species back to the region of stagnation.*

Although a flameholder will stabilize a flame at a velocity in excess of the flame propagation rate, the flame will eventually blow out as the approach stream velocity is increased. The velocity at which the flame blows out is called the blowout velocity. The blowout velocity depends on the equivalence ratio** of the approach stream. This dependency is illustrated by the blowout map shown in Figure 2.3 for a propane/air ORJ with a stoichiometric jet. As shown in Figure 2.4, the blowout velocity depends on the jet composition as well as the main stream composition. The influence of the jet composition distinguishes the ORJ from a physical flameholder. Only one blowout map can be generated for a physical flameholder whereas a series of blowout maps can be generated for an ORJ by changing the jet composition.

---

*The mass flow rate of the jet is much less than the mass flow rate of the main stream ($\dot{m}_j/\dot{m}_p << 1$). The opposed-reacting-jet should not be confused with the opposed-diffusion-jet (Kushida-1968). The jet mass flow rate in the opposed-diffusion-jet is approximately equal to the mass flow rate of the main stream ($\dot{m}_j/\dot{m}_p \approx 1$).

**The equivalence ratio, Φ, is defined as the actual fuel/air ratio divided by the stoichiometric fuel/air ratio

$$\Phi = m_{fu}/m_a \Big/ (m_{fu}/m_a)_{stoich}$$

A stoichiometric mixture has an equivalence ratio of unity.

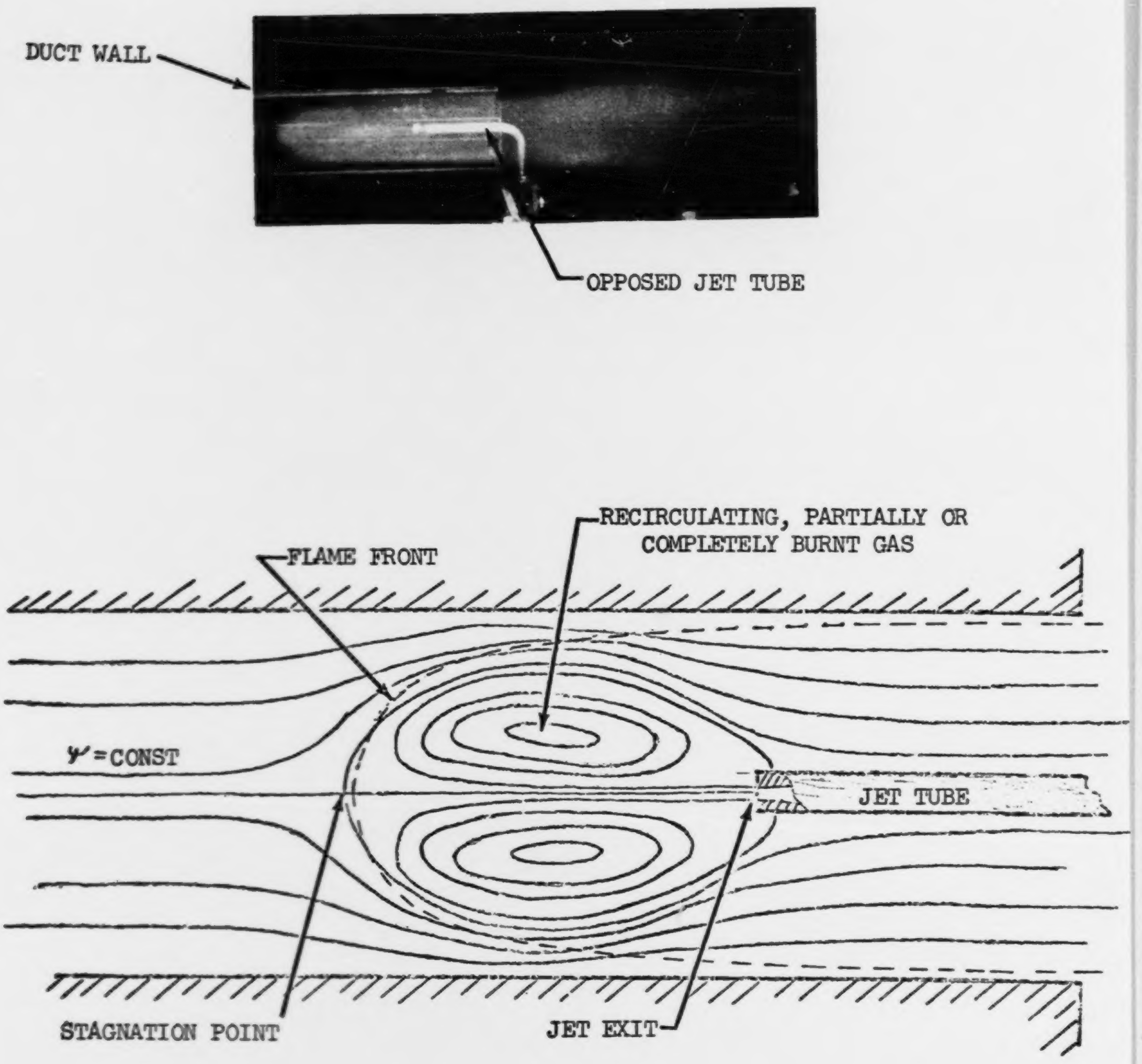
DUCT WALL
OPPOSED JET TUBE
RECIRCULATING, PARTIALLY OR COMPLETELY BURNT GAS
FLAME FRONT
ψ = CONST
JET TUBE
STAGNATION POINT
JET EXIT

FIGURE 2.2 AERODYNAMIC FLAMEHOLDER, THE OPPOSED REACTING JET

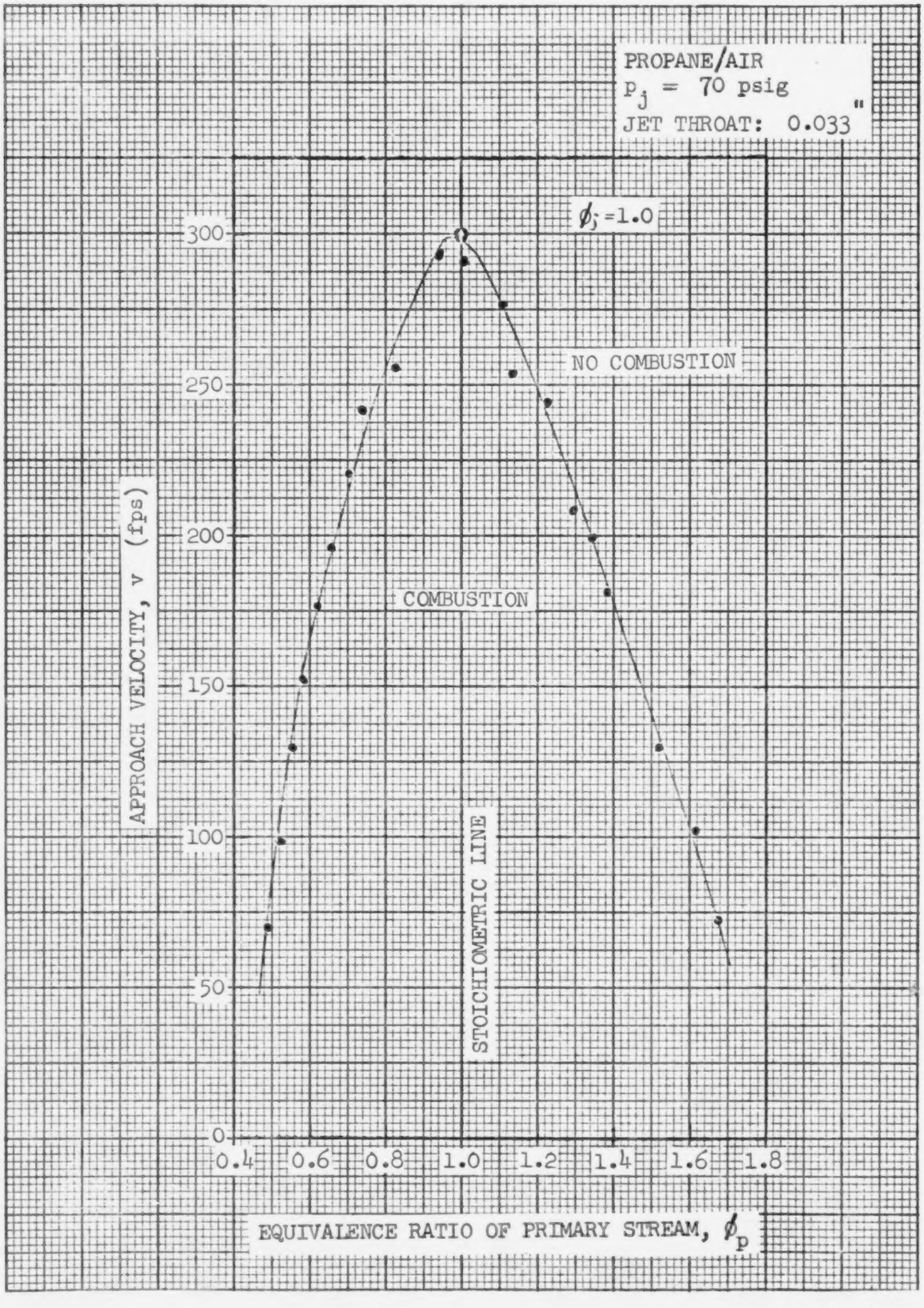

FIGURE 2.3 BLOWOUT MAP (Schaffer-1957)

PROPANE/AIR
p_j = 70 psig
JET THROAT: 0.033"

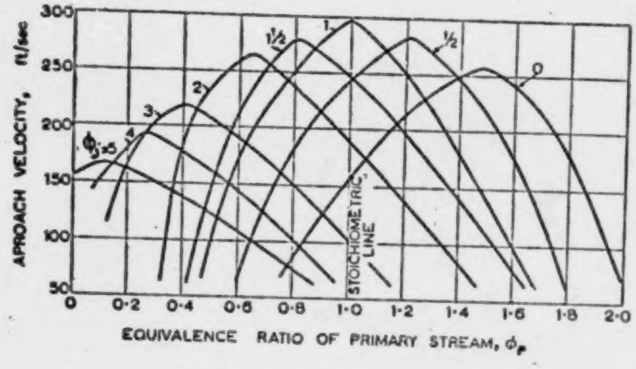

FIGURE 2.4 BLOWOUT MAP: EFFECT OF JET COMPOSITION (Schaffer-1957)

In summary:

1. A flameholder stabilizes a flame in a high velocity stream by a) decelerating the stream and b) producing a zone of recirculation.

2. The velocity at which a flameholder is no longer effective in stabilizing a flame is called the blowoff velocity.

3. The ORJ has a broader operating range than the physical flameholder.

2.2 Previous Work

The ORJ, first introduced in the open literature by Schaffer and Cambel (1955), was conceived as a potential flameholder in an afterburner of a gas turbine engine. Although physical flameholders had been used in afterburners, the ORJ offered certain advantages. For example:

1. The highest velocity at which a flame can be stabilized by a physical flameholder occurs for an approach stream composition near stoichiometric. It is often desirable in practical situations to operate at high velocities, but at lean mixtures. The ORJ has the advantage of allowing this range of operation. Flames can be stabilized over a broad range of approach stream equivalence ratios by varying the composition of the jet.

2. To provide stability over a wide range of operation, a physical flameholder is sized for the most critical condition (e.g., minimum pressure and minimum velocity). In normal operation, the physical flameholder is oversized and this results in excessive aerodynamic losses. The physical obstacles also cause drag losses when the afterburner is not in use. To negate these aerodynamic losses, Schaffer and Cambel proposed that the ORJ be used as the flameholder. Introduced at

an angle from the wall of the afterburner, the jets could operate with bleed compressor air. When the afterburner is not in use, the jets could be shut off, leaving a streamlined wall.

The use of the ORJ in an afterburner never proved practical because the flameholding capacity falls drastically as the angle of the jet to the direction of flow is increased a few degrees (Duclos, Schaffer and Cambel-1957).

A few studies have been made in which jets were used under conditions representative of afterburner operation. Bertin and Salmon (1958) used transverse jets with apparent success.* Butze and Metzler (1959) used flow rates and injection pressures representative of those available from compressor-bleed air and found that opposed-jets alone, regardless of composition, failed to maintain a stable flame.

The main contributions to the development of the ORJ are summarized in Table 2.1. Nearly all the work to date has been experimental. In the late 1950's, the Aircraft Division of General Electric sponsored a three-year investigation at Northwestern University under the guidance of Professor A. B. Cambel. During the same period, the Air Force sponsored a program at Stanford Research Institute. Partly because interest swung to high-temperature gas dynamics in the early 1960's and partly because the potential of the ORJ as a flameholder in afterburners was not realized, ORJ-studies were essentially curtailed until the Army funded a three-year program at Tulane University under the director of Professor J. R. O'Loughlin. The studies given in Table 2.1 are presented below in chronological order with a summary statement

---

*Neither the manner in which the jets were introduced into the main stream nor the composition of the jet streams were described in the paper.

TABLE 2.1 HISTORICAL SUMMARY OF OPPOSED REACTING JET WORK

YEAR	PRINCIPAL INVESTIGATOR	AGENCY	MAIN STREAM	JET STREAM	MAIN CONTRIBUTION
1954	Schaffer	Northwestern University	Propane/Air	Air Nitrogen Oxygen	Introduction of jet flame stabilization
	Pohlmann	Northwestern University	Propane/Air Air	Propane Air Propane/Air	Effect of jet(uncooled) pressure, diameter, and composition All-fuel jet ineffective
1956	Eustis	Stanford Research Institute	Natural Gas/Air	Natural Gas/Air	Transverse jet ineffective
	Schaffer	Northwestern University	Propane/Air	Propane/Air Nitrogen Oxygen	Introduction of "Critical Zone"
	Snyder	Northwestern University	Propane/Air	Air	Photographic study using tracers
1957	Putnam	Battelle Memorial Institute	Propane/Air Methane/Air	Air	Drag compared for aerodynamic and bluff body flameholder
	Bohrer	Northwestern University	Propane/Air	Air	Effect of jet (cooled) temperature jet pressure
	Noon	Stanford Research Institute	Natural Gas/Air Air	Air Propane/Air Propane	All-fuel jet ineffective
	Schaffer	Northwestern University	Propane/Air	Propane/Air	Critical zone concept correlated to experiment
	Noreen	General Electric	Natural Gas/Air	Methane/Air	Well-stirred reactor analysis of critical zone Effect of main stream temperature and pressure

TABLE 2.1 (Continued)

YEAR	PRINCIPAL INVESTIGATOR	AGENCY	MAIN STREAM	JET STREAM	MAIN CONTRIBUTION
1957	Duclos	Northwestern University	Propane/Air	Air	Effect of jet inclination
1958	Cambel	Northwestern University	Propane/Air Air	Propane/Air Propane Air Nitrogen Argon	A review of work through 1958 Stabilization possible with inert gas in jet
	Agoston	Stanford Research Institute	Natural Gas/Air	Natural Gas/Air	Visual observations of jet field New location proposed for critical zone
1960	Fuhs	California Institute of Technology	Propane/Air	Propane/Air Air Oxygen	Spectroscopic study of critical zone
1966	Massaro	Northwestern University	Propane/Air	Air	Flameholding using convergent jets
	Bellamy	Tulane University	Propane/Air	Air Propane/Air	Effect of chemical inhibition Well-stirred reactor analysis of critical zone
1967	Douglas	Tulane University	Propane/Air	Air	Combustion efficiency versus flame shape
1968	Fluker	Tulane University	Propane/Air	Air	Effects of unsteady flow in main and jet streams
1969	O'Loughlin	Tulane University			Review of Tulane work, 1966-1968

regarding the contribution each has made to opposed-jet technology. Unless stated otherwise, propane was used as the fuel and the diameter of the combustion chamber was 2 inches. The diameter of the jet was nominally 1/32 to 1/16 inch.

1. Alan Schaffer - 1954: The first documented work using the opposed-jet as a flameholder.

The feasibility of the opposed-jet to stabilize a flame was evaluated and the flameholding potential of the opposed jet was compared to that of a physical flameholder and no flameholder. An all-oxygen jet performed better than an air jet. An increase in the jet supply enhanced the flameholding capacity. A summary of this work was published in Jet Propulsion by A. Schaffer and A. B. Cambel (1955).

2. Edward Pohlman - 1954: A study of the effect of jet properties on flameholding.

A colleague of Schaffer at Northwestern University, Pohlman expanded on the initial ORJ work. The influence of the jet fuel/air ratio, the jet pressure, and the jet exit diameter were evaluated. An optimum pressure was found to exist for a particular jet exit diameter.

3. Allan Schaffer and Ali Bulent Cambel - 1956: An important paper in the historical development of the ORJ introducing the concept of a "critical zone."

The authors suggested that the conditions in a small zone located at the nose of the flame determined the stability of the flame. They hypothesized that the flame would not be stabilized if the conditions were not stable in the small zone. The zone was labeled "critical zone."

Schaffer and Cambel suggested that the mass flowing into the critical zone was composed of three parts: the primary mixture and jet media entering the zone, and the products of combustion entrained in the jet stream. By assuming that all the jet flow enters this zone, the authors calculated that three percent of the main stream entered the critical zone. This argument satisfactorily answered the reason for the great influence the jet conditions (composition, temperature, pressure) have on flame stability.

A stoichiometric jet was found to have higher blowout velocity than an air jet. Heating of the jet flow also aided the flameholding capacity.

4. Robert H. Eustis and Charles L. Mraz - 1956: The first of three reports covering work at Stanford Research Institute from 1956 to 1958.

This study was the first directed toward a practical application of the opposed-jet. The research was funded by the Air Force to investigate the possibility of using an opposed-jet to stabilize a flame in a turbojet afterburner or ramjet. Both transverse and opposing-jets were studied using natural gas as a fuel. Transverse jets were ineffective as stabilizers for the conditions investigated.

Among the various jet stream variables studied, stabilization was slightly aided by an increase in jet exit size, moderately aided by an increase in jet manifold pressure or an increase in jet temperature and greatly influenced by jet composition. A major part of this work was a photographic and theoretical water channel study.

5. William T. Snyder - 1956: A photographic study of the opposed-reacting-jet.

The effect of jet pressure and approach velocity on the flow field was investigated visually using photographs. At each condition, a series of three photographs was taken, one with combustion and two without combustion. In the two without combustion, tracers were used alternately in the jet and main streams. The length of the jet stream in cold flow did not change appreciably in the presence of combustion. The qualitative picture provided by this flow visualization is similar to that obtained by Eustis and Mraz in their water channel analysis.

6. William A. Putnam - 1957: A comparison of the drag force imparted to the approach stream at blowoff by the ORJ and physical flameholders.

Putnam suggests that a minimum force is required to hold a flame under any particular condition and because the force may be applied by an opposed jet, a V-gutter, a bluff body or by other means, the particular method of flameholding is unimportant.

7. Lionel C. Bohrer - 1957: A study of jet temperature and jet supply pressures using a water-cooled jet holder.

Prior to this study jet holders had not been cooled and the jet temperatures could neither be controlled nor accurately measured. With a water-cooled jet, jet temperatures could be maintained constant over a range of operation.

Correlation of the data with key variables was attempted. The effect of jet nozzle geometry was also studied. A converging-nozzle and a converging-diverging nozzle were compared for the same inlet conditions. No appreciable change in stabilization was observed.

8. A. W. Noon - 1957: The second in a series of three reports covering an investigation of opposed-jet flameholders conducted at Stanford Research Institute.

Parameters studied included the jet temperature, jet composition at various temperatures and non-uniformities in the composition of the main stream. Both propane and natural gas were used.

An increase in jet temperature improved the stability of an air jet. An increase in the temperature of a fuel/air jet, however, yielded little difference in the flameholding capacity. The author concluded that jet composition was more important to stability than temperature.

To assess the feasibility of using the jet as a combined fuel injector and flameholder, stabilization was attempted using an all-fuel jet. Various fuel/air mixtures of the main stream were investigated in conjunction with a variation in jet diameter and fuel pressure. Both pure and vitiated air were used in the main stream. It was not possible to stabilize a flame using a pure fuel jet under any condition.

Under some conditions of controlled non-uniformities in the composition of the main stream the flame extinguished.

9. Allan B. Schaffer - 1957: A doctoral thesis documenting most of the work completed at Northwestern University since the opposed-jet was first investigated.

Schaffer's work was primarily directed toward substantiating the "critical zone" concept (Schaffer and Cambel-1956). Three of the more important studies considered by Schaffer were:

1) The location of the critical zone.

2) An analytical study using the properties of the critical zone to generate generalized blowout curves.

3) Temperature measurements in the critical zone using the sodium line reversal technique.

Temperatures in the latter study were measured for systematic variations in jet equivalence ratio, approach velocity, and approach equivalence ratio. The temperature measurements indicated a region of uniform temperature in the nose of the flame lending credance to the critical zone concept.

10. S. S. Penner and F. Williams - 1957: A review of flame stabilization in premixed turbulent flows.

The mechanism of flame stabilization was discussed in relation to the bluff body flameholder. Blowoff characteristics were compared for the bluff body, opposed-jet, and recessed-duct flameholders. The theoretical studies of flame stabilization were also reviewed.

11. A. E. Noreen and W. T. Martin - 1957: First investigation of the effect of main stream pressure and main stream temperature.

With natural gas as the fuel, experimental results indicated that the flameholding capacity was aided by increasing the main stream temperature or pressure. The investigations were restricted to stoichiometric jets.

Noreen and Martin also developed the first of two theoretical analyses concerned with the stability limits of the opposed-jet. The other analysis is by Bellamy (1968). In both studies a model was used to describe the stability limits of the opposed-jet. Following the hypothesis of Schaffer and Cambel (1956) that the critical zone was a small pilot reactor from which the flame spreads and following the observation of Schaffer (1957) that the "critical zone" was homogeneous, these investigators took the model for the critical zone to be a well-stirred reactor. The stability of the opposed-jet was hypothesized to be wholly determined by the stability of the stirred reactor. Using this model, Noreen and Martin computed the maximum main stream velocity as a function of the main stream pressure and main stream temperature, and compared the computed results to experimental values.

12. D. P. Duclos, A. Schaffer, A. B. Cambel - 1957: A study of the effect of inclining an opposed air jet to the main stream.

If opposed jets were to be used for flameholders in afterburners, introduction of the jets from the wall at an angle to the main stream would be most practical. The flameholding capacity of the opposed-jet when inclined to the main flow must be considered. The results of this study demonstrated that the flameholding capacity drops drastically at small angles of inclination. For example, the maximum velocity decreased 20 percent for an inclination of 7 degrees,* 70 percent at an inclination of 14 degrees.

13. G. A. Agoston, R. H. Eustis, A. W. Noon, T. D. Witherly - 1958: The final report in a three part series of research conducted at Stanford Research Institute.

Visual observations of the flow field were recorded by means of time exposure photographs, spark shadowgraphs and high-speed (Fastax)

---

[*] Angle is measured from the centerline:

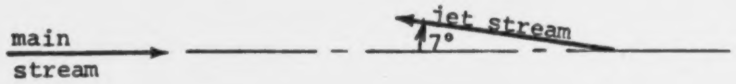

motion pictures. Based on 1) the results from these observations and 2) the effects of non-uniform concentration patterns in the main stream, an alternative mechanism for opposed-jet flame stabilization was proposed. The authors suggested that the critical zone is toroidial in shape and located along the outer boundary of the recirculation zone. This work was also reported by the authors in Combustion and Flame (1958).

14. A. B. Cambel - 1958: A review of the opposed-jet technology in 1958.

One result noted by Cambel that had not been previously reported was the ability to stabilize a flame using an inert gas in the jet. Stabilization was effected using both nitrogen and argon, with argon showing markedly better flameholding capacity. The maximum velocities using the inert gas were about 1/2 those obtained using air for an equivalent jet supply pressure. The results were also presented by Choudhury and Cambel in the ARS Journal (1960). These findings contradicted an earlier report which suggested that a flame could not be stabilized using an inert gas (Schaffer and Cambel-1956). The ability to hold a flame in a jet of inert gas suggested that the critical zone as initially conceived by Schaffer and Cambel (1956) may not be singularly critical.

15. A. E. Fuhs - 1960: A limited but intriguing spectroscopic study of the opposed jet.

Equivalence ratios were measured in the critical zone as a function of radius using the spectral-intensity-ratio method. Three jet compositions were considered: an oxygen jet, an air jet, and a stoichiometric fuel/air jet. Only a portion of the lean blowoff regime was investigated. The results indicated that there may be one unique blowoff map in the critical zone (blowoff velocity as a function of equivalence ratio in the critical zone) regardless of jet composition. This is an interesting suggestion worthy of more substantiative work.

16. D. J. Massaro - 1966: A study of the flame stabilization of convergent jets.

Because a single opposed-jet loses its flameholding capacity when introduced into a stream at an angle (Duclos-1957), the author proposed that a number of jets impinging on one point might create a stagnation zone that would give flameholding performance comparable to one opposed-jet. A 4-jet manifold was used. Stabilization was studied as a function of injection angle, jet mass flow rate, and jet supply pressure. To match the performance of one single opposed-jet, the jet pressure had to be sufficiently high for the four-impinging jet streams to form one stream opposing the main flow. This work was also reported by Massaro and Trezek in Combustion and Flame (1967).

17. Lynn Bellamy - 1966: An experimental and theoretical study of the critical zone of the opposed-jet flameholder.

A chemical inhibition investigation was conducted to determine the importance of chemical processes in the critical zone. By using a stirred reactor to model the stabilization, Noreen and Martin (1957) deduced that chemical rate processes were dominant. To establish the validity of the stirred reactor model, Bellamy introduced a small percentage (2-8 percent by weight) of a chemical inhibitor (chlorine) into the jet flow. The flameholding capacity dropped proportionally and the author concluded that the chemical rate processes were important. The inhibitor study was also reported by Bellamy, Barron and O'Loughlin (1968).

The theoretical study was based on modeling the critical zone by a well-stirred reactor. Bellamy's study and the work of Noreen and Martin (1957) are the only theoretical investigations of the stability of an opposed-reacting-jet. Both used the stirred-reactor model. There are some basic differences between the two studies, however. Bellamy used kinetic rate data from an actual well-stirred reactor; Noreen and Martin also used an Arrhenius form for the kinetics, but determined the constants from experimental, opposed-jet data. Bellamy predicted the lean blowout of velocity as a function of primary-stream equivalence ratio for a stoichiometric jet. Noreen and Martin predicted only the maximum blowout velocity for various jet equivalence ratios, and main-stream temperatures. Noreen and Martin assumed a-priori critical zone size, shape and relative contribution of jet and main-stream flow into the zone. Bellamy calculated the volume of the critical zone and the contribution of the jet and main-stream flow, using kinetic rate data, reactor theory, and the assumption that all the jet flow enters the critical zone unreacted. The latter is the main assumption that the two stirred-reactor analyses had in common. This work was also reported by Bellamy, Brown and O'Loughlin in Combustion and Flame (1968).

18. Douglas - 1967: An experimental study to determine combustion efficiency of an opposed-reacting-jet downstream of the jet exit.

The mass crossing the flame front was found to be not immediately burnt. The combustion efficiency (fraction of reactants converted into equilibrium products) was about 25 percent 3 diameters downstream of the flame tip. The results were also reported by Douglas and O'Loughlin (1968).

19. B. J. Fluker - 1968: A study of unsteady flow on the flameholding capacity of the opposed-jet flameholder.

Flow velocities were systematically perturbed, both with step and periodic functions, in the primary and jet flow. For the conditions investigated, the fluctuation in the main stream had little effect on the flameholding capacity, whereas stabilization was markedly improved by transients in the jet stream.

20. J. R. O'Loughlin - 1968: A summary of the work conducted at Tulane University on the opposed jet flameholder for the U. S. Army Research Office, Durham, North Carolina.

SECTION 3

The Opposed Reacting Jet as a Research Tool

3.1 Fundamental Characteristics

3.2 Relation to Real Combustors

3.3 Summary of the State-of-the-Art

3.1 Fundamental Characteristics

The opposed-reacting-jet has certain characteristics that make it attractive as a research tool for the study of reacting, mixing flows: 1) the ORJ is a relatively simple combustion system, yet very versatile, and 2) the reacting flowfield of the ORJ combustor is easy to observe visually.

The versatility of the ORJ is shown in Figure 2.4. Small changes in the composition of the jet have a significant influence on the performance of the ORJ. A flame can be stabilized in a very lean main stream by using a rich jet. A flame can also be stabilized in a rich main stream by using a lean jet. Although the jet mass flow rate is one percent of the main stream mass flow rate, the performance of the combustor is influenced by the properties of the jet stream. The influence of the jet makes the ORJ a valuable potential research tool for investigating reacting flows and the interaction between chemical kinetics, mass diffusion, and heat transfer.

An attractive feature of the ORJ is the ease with which the reacting flow may be visually observed. The ORJ combustor of the present investigation consists of a high-temperature glass duct. As shown in Figure 1.1, the reacting flowfield may be studied optically. The ORJ also lends itself readily to spectroscopic studies.

The analytical description of the opposed-reacting-jet developed in this investigation complements the experimental features of the ORJ.

3.2 Relation to Real Combustors

The study of fundamental processes in reacting flows using the ORJ is relevant to real combustor systems. The ORJ has many properties in common with real combustion devices. The gas-turbine combustor is a good example of a real device to which the ORJ is related. The reacting-flow fields in the ORJ and the gas-turbine both feature recirculation. A schematic cross-section of a gas-turbine combustor is shown in Figure 3.1a. Fuel is introduced at the entrance to the combustor and mixed with a near-stoichiometric equivalent of air. Downstream, additional air is introduced along the periphery of the combustor to cool the gaseous stream to a temperature compatible with the turbine blade material. The overall equivalence ratio at the exit of the combustor is typically 0.2.

The gas-turbine combustor is divided into a primary zone and a secondary zone. The primary zone, characterized by intense mixing, is the region in which the major part of the reaction occurs. As shown in Figure 3.1b, the equivalence ratio is near unity in the primary zone. Excess air is introduced in the secondary zone. This addition of dilution air is reflected in Figure 3.1b by a decrease in the equivalence ratio.

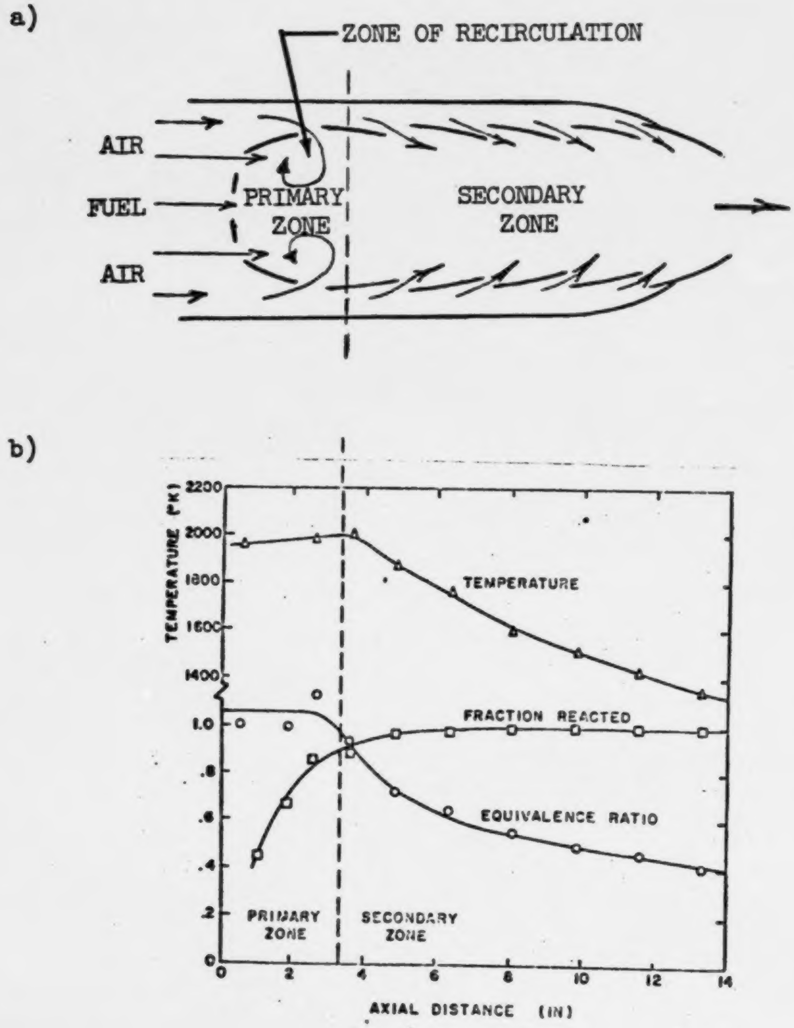

FIGURE 3.1 GAS TURBINE COMBUSTOR (Sawyer-1969)
a) SCHEMATIC
b) PROPERTY CONTOURS

In Figure 3.1a, the primary zone is seen to be a zone of recirculation, an important feature which the gas-turbine combustor and the ORJ have in common.

Study of the combustion processes in an ORJ gives insight into the processes occurring in real combustors. For example, the ORJ is a valuable tool for broadening the understanding of those mechanisms controlling the formation of pollutants in continuous combustion processes.

3.3 Summary of the State-of-the Art

Solution of the governing partial differential equations for the opposed-reacting-jet has not been attempted heretofore because neither the motivation for such an analysis nor the numerical techniques have been available. Continuous-combustion devices have been developed primarily by trial and error using empirical data for guidelines. Because performance has been the main consideration in combustor development, more sophisticated techniques than overall energy, mass and momentum balances or simple modeling have not been necessary. However, the advent of concern over emissions now provides the motivation to develop a more sophisticated analysis.

Most theory has been limited to modeling because of inherent difficulties in solving the governing equations for reacting flows. For example, the stabilization of the bluff body and opposed-jet flameholders has been likened to that of a stirred reactor. Similarly, a gas-turbine combustor has been modeled by considering a number of stirred reactors in series (Hammond and Mellor-1970).

Modeling is effective in establishing the performance of combustion systems, but it is not wholly adequate in describing the detail of the flow field.* The point-by-point properties of a reacting flow can only be described by a solution of the governing partial differential equations. In the case of flows with recirculation, similar to those of the opposed-jet and gas-turbine combustor, these equations are "elliptic."

To obtain a solution of the governing equations, the numerical technique must be developed. Elliptic partial differential equations have been solved numerically for low-velocity flows, but difficulties are encountered with stability for Reynolds numbers above 400. In practice, the Reynolds number is often much higher. For the opposed-jet, Reynolds numbers based on the diameter of the combustor in excess of 10^4 are typical.

By giving special consideration to the formulation of the finite-difference equation, Runchal and Wolfshtein (1966) were successful in obtaining solutions to the elliptical equations that were stable for all Reynolds numbers. Instead of using the central difference formulation, they employed the upwind difference formulation, a procedure suggested by Spalding (1966). The work of Runchal and Wolfshtein has led to the numerical technique adopted in the present study. The numerical procedure, developed at Imperial College in London under the guidance of Professor D. B. Spalding, is described in a book by Gosman, Pun, Runchal, Spalding and Wolfshtein (1969) entitled "Heat and Mass Transfer in Recirculating Flows."

---

*Prediction of the point-by-point properties of a reacting flow is valuable to the understanding of air pollution emissions. The distribution of nitric oxide (NO), for example, can be calculated from the predicted distribution of temperature. The effect of parametric variation on the nitric oxide distributions within the combustor can thereby be established.

SECTION 4

Analytical Investigation

4.1 Conditions Investigated

4.2 Numerical Calculations

  4.2.1 Theory

  4.2.2 Finite Difference Formulation

  4.2.3 Physical Inputs

  4.2.4 Computational Procedure

  4.2.5 Analytical Results

4.1 Conditions Investigated

Two parameters are invariant in this investigation: the equivalence ratio of the jet, and the equivalence ratio of the main stream. Although differing equivalence ratios (such as an air jet and a fuel/air main stream) may be handled readily, the equivalence ratios of the two streams are chosen to be unity for the following reasons:

1. Non-equal equivalence ratios necessitate solution for a fifth dependent variable. The four that must be considered in the numerical calculations are one for conservation of mass, one for conservation of momentum, one for conservation of energy, and one for conservation of an individual species, say fuel mass fraction. Usually the oxidizer mass fraction must also be considered. However, in the case of a uniform equivalence ratio throughout the flow field, the oxidizer mass fraction is related to the fuel mass fraction by a simple algebraic relation and need not be solved for separately. When the equivalence ratio of the jet and main stream are not equal, the oxidizer mass fraction must be solved for as an additional dependent variable, increasing computation

time and making it more difficult to obtain convergence.

2. Similar equivalence ratios in both the jet and main stream reduce the effect of molecular diffusion. This is a desirable condition because of the difficulty in modeling transport processes.

The fuel selected for this study is ammonia, since the ammonia/air reaction is well represented by a single-step or global reaction rate. The amount of equilibrium dissociation of the reactants is small at the temperatures and near-atmospheric pressures of interest in this investigation (Newhall-1964). The use of ammonia is in contrast to previous work on the ORJ where hydrocarbons have been used exclusively, especially propane. In the numerical analysis, hydrocarbon/air reactions are not as simple to describe as the ammonia/air reaction. Intermediates, such as aldehydes and carbon monoxide, play an important role in hydrocarbon/air reactions, and at least two or three reactions and many species must be considered. Although it is plausible that an analysis that includes many reactions and many species may be performed successfully, a one-step reaction is a more reasonable choice for the initial solution.

The ammonia/air reaction is assumed to follow the stoichiometry

$$4NH_3 + \overbrace{3[O_2 + (3.77)N_2]}^{\text{air}} \rightarrow 6\,H_2O + 2N_2 + (3)(3.77)N_2 \qquad (4.1)$$

The fuel mass fraction that corresponds to the stoichiometric inlet conditions of the jet and main stream is 0.1416; the fuel volume or mole fraction is 0.218. The corresponding values for propane are 0.060 and 0.040 respectively.

The pressure of the combustion chamber is assumed to be constant and equal to the ambient pressure. Pressure gradients do exist in the combustor but they are on the order of a few inches of water for the ammonia/air system and may be neglected. The uniformity of pressure across the chamber has been shown by Douglas (1967) for a propane/air opposed-reacting-jet. Douglas also measured the static pressure along the length of the flame. The maximum pressure ranged from 2.6 inches-H_2O (0.094 psi) for an inlet velocity of 66.6 fps to 6.1 inches-H_2O (0.22 psi) for an inlet velocity of 132.8 fps.

Normally in opposed-reacting-jet studies the pressure of the jet supply is sufficiently high to choke the stream at the jet exit. A jet supply pressure of 70 psig is typical. As a result, compressibility effects are important in the region surrounding the jet exit. Compressibility effects are not easily handled numerically, however. When the effect of pressure on density is large, the convergence of the numerical solution may be threatened and the character of the governing equations may change from elliptic to parabolic (Gosman, et al-1969, pg. 52). Compressibility effects are avoided in this study by using a subsonic jet. The jet supply pressure of 3.2 psig produces a Mach number at the jet exit less than 0.5.

The blowout map for the ammonia/air opposed-reacting-jet investigated is given in Figure 4.1. Solutions to the governing equations are obtained for three cases:

Case 1: Cold flow* for the blowout conditions represented by point A

Case 2: Cold flow for the conditions represented by point B

---

*Cold flow: Non-reacting, isothermal flow
Hot flow: Reacting flow

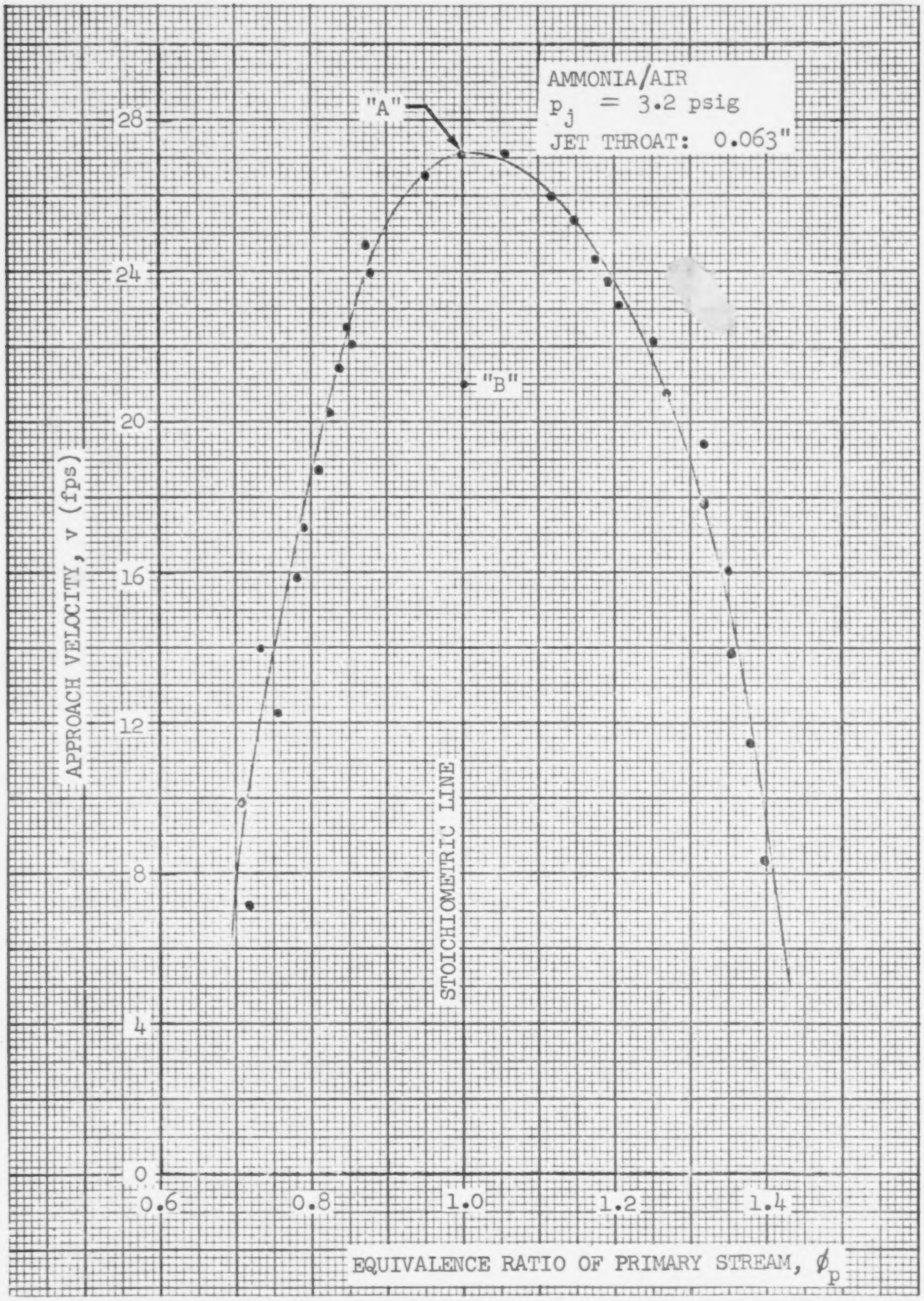

FIGURE 4.1 BLOWOUT MAP: AMMONIA/AIR OPPOSED REACTING JET

Case 3: Hot flow for the conditions represented by point B
The expression for the chemical kinetics is refined to predict blowout at point A. The refined kinetics expression is then used to obtain a solution for the case of reacting flow at point B. A cold-flow solution is obtained for point B for comparison to the hot-flow solution.

4.2 Numerical Calculations

The main thrust of this thesis is the numerical calculations, developed and used to predict the point-by-point properties throughout the flow field of an opposed-reacting-jet. The experimental measurements of composition and temperature in the reaction zone, described in Section 5, are used to evaluate the accuracy of the numerical technique in predicting the flow properties.

The section on numerical calculations is presented in four parts:

- 4.2.1 Theory
- 4.2.2 Finite Difference Formulation
- 4.2.3 Physical Inputs
- 4.2.4 Computational Procedure and Results

The theory is transformed into finite-difference equations for the numerical computations. Before numerical computations can be performed, physical inputs such as specific heat and molecular weights are required. With these ingredients, the computations can proceed and results obtained.

4.2.1 Theory

Governing Equations. The partial differential equations that must be considered in solving the opposed-jet flow field in the absence of combustion (cold flow) are the conservation of mass and the conservation of momentum.

When the flow field is nonisothermal due to chemical reaction, the conservation of energy must be added. Because individual species are created as well as destroyed through chemical reaction, conservation equations for each species must likewise be considered in a reacting flow.

Using tensor form, the governing conservation equations may be written in the absence of body forces as:

Conservation of mass

$$\operatorname{div} \rho\vec{v} = 0 \tag{4.2a}$$

Conservation of momentum

$$- \operatorname{div} \rho\, \vec{v}\vec{v} - \operatorname{grad} \rho - \operatorname{div} \underline{\underline{\tau}} = 0 \tag{4.2b}$$

Conservation of energy

$$\operatorname{div} \{\rho\vec{v}\bar{h} - \Gamma_h c_p \operatorname{grad} T - h_{fu}\Gamma_{fu} \operatorname{grad} m_{fu} - \sum_{i=1}^{3} v_i \vec{\tau}_i\} = 0 \tag{4.2c}$$

Fuel mass species conservation

$$\operatorname{div} (\rho\vec{v}m_{fu} - \Gamma_{fu} \operatorname{grad} m_{fu}) - R_{fu} = 0 \tag{4.2d}$$

where

$\underline{\underline{\tau}}$ = stress tensor

$\Gamma_h = k/c_p$

k = thermal conductivity

$\Gamma_{fu} = \rho\mathcal{D}_{fu}$

$\mathcal{D}_{fu}$ = fuel diffusivity

R_{fu} = reaction rate of fuel

Normally a mass-species conservation equation would be required for all the species involved in the reacting flow. The species-conservation equation for the other species need not be solved here because:

1. The products are lumped together and considered as a whole, and
2. The equivalence ratio is uniform throughout the flow field as explained in Section 4.1

When the products are considered as a whole, the reaction assumes the following form*

$$4NH_3 + 3O_2 \rightarrow \text{"product"}$$

The oxidizer mass fraction need not be solved for because it is related algebraically to the fuel mass fraction through the equivalence ratio, Φ

$$m_{ox} = m_{fu} \frac{\Phi}{(m_{fu}/m_{ox})_{stoich}}$$

The equivalence ratio is uniform and equal to unity throughout the flow field.

For a nonuniform equivalence ratio (e.g., a jet equivalence ratio different than the main stream equivalence ratio), the distribution of the equivalence ratio throughout the flow field is not known a-priori and the species conservation equation for the oxidizer mass fraction must be solved in addition to the fuel mass species conservation equation. In either case, the product mass fraction is known from

$$m_{prod} = 1 - m_{fu} - m_{ox}$$

and need not be solved for separately as a dependent variable.

No time-derivatives appear in Equations 4.1. The equations are written for the steady-state condition. This may seem inappropriate when turbulence is being considered. Turbulence is unsteady, and it would be valuable to solve the governing equations with the time-derivative included. Unfortunately, for the present state of knowledge, excessive computer resources are required, both in time and capacity. Initial attempts are now being made at unsteady-state solutions for certain simplified models of turbulent flow; however, it will be some time before unsteady problems of turbulence with reaction can be handled economically.

---

*The atmospheric nitrogen in the ammonia/air reaction is accounted for by considering it a constituent of the product. In cold flow, the product is entirely atmospheric nitrogen. In hot flow, the product consists of atmospheric nitrogen and the products of combustion, H_2O and N_2.

A procedure commonly used in calculations involving turbulent flows is adopted for this investigation. If the turbulent motion is random, a solution based on the "time-smoothed" or "time-averaged" motion is quite adequate. When this procedure is adopted, the steady-state governing equations introduced initially and written strictly for laminar flow may be used for the turbulent problem with little modification. Essentially, the modification entails replacing the transport properties (viscosity, mass diffusivity and thermal conductivity) with "effective" or turbulent properties.

The continuity equation and the equation of motion in rectangular coordinates are*

Conservation of mass

$$\frac{\partial}{\partial x}(\rho v_x) + \frac{\partial}{\partial y}(\rho v_y) + \frac{\partial}{\partial z}(\rho v_z) = 0 \qquad (4.3a)$$

Conservation of momentum (z-direction)

$$\left[\frac{\partial}{\partial x}(\rho v_x v_z) + \frac{\partial}{\partial y}(\rho v_y v_z) + \frac{\partial}{\partial z}(\rho v_z v_z)\right] + \left[\frac{\partial}{\partial x}\tau_{xz} + \frac{\partial}{\partial y}\tau_{yz} + \frac{\partial}{\partial z}\tau_{zz}\right] - \frac{\partial p}{\partial z} = 0 \qquad (4.3b)$$

---

*Reference: Bird, Stewart and Lightfoot (1960), p. 153.

Written in this form, v_x, v_y, v_z and ρ represent the instantaneous values of velocity and pressure. For steady laminar flow, the values of velocity and pressure at any point are fixed. For turbulent flow, the velocity and pressure at any point are not fixed. In Figure 4.2 the instantaneous values v_z can be seen to oscillate irregularly.

Adopting the "time-smoothed" approach, the time-smoothed velocity, $\bar{v}_z$, is introduced

$$\bar{v}_z = \frac{1}{t_o} \int_t^{t+t_o} v_z \, dt$$

where t_o is large with respect to the time of turbulent oscillation. The instantaneous velocity can be written as the sum of the time-smoothed velocity $\bar{v}_z$ and a velocity fluctuation v_z'

$$v_z = \bar{v}_z + v_z' \qquad (4.4a)$$

similarly for pressure

$$p = \bar{p} + p' \qquad (4.4b)$$

When the instantaneous values of velocity and pressure in the governing equations are replaced by Equations (4.4a,b), an interesting result is obtained which is important to the theoretical work developed here.

time-smoothed conservation of mass

$$\frac{\partial \bar{v}_x}{\partial x} + \frac{\partial \bar{v}_y}{\partial y} + \frac{\partial \bar{v}_z}{\partial z} = 0 \qquad (4.5a)$$

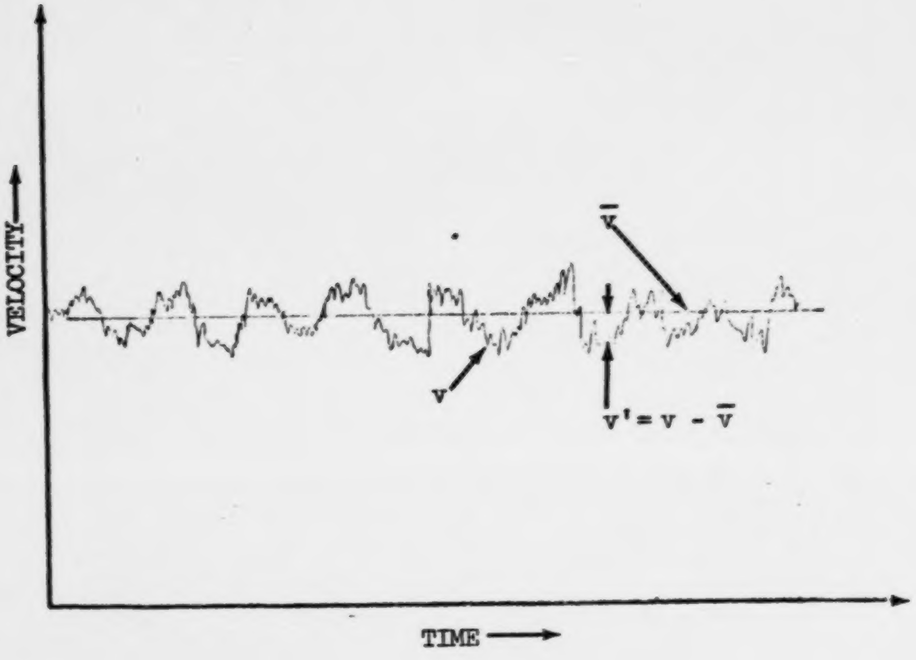

FIGURE 4.2 TURBULENT VELOCITY

time-smoothed conservation of momentum

$$\begin{aligned}
&-\frac{\partial \bar{p}}{\partial z} - \left(\frac{\partial}{\partial x}\rho \bar{v}_x \bar{v}_z + \frac{\partial}{\partial y}\rho \bar{v}_y \bar{v}_z + \frac{\partial}{\partial z}\rho \bar{v}_z \bar{v}_z\right) \\
&\underline{-\left(\frac{\partial}{\partial x}\rho \overline{v'_x v'_z} + \frac{\partial}{\partial y}\rho \overline{v'_y v'_z} + \frac{\partial}{\partial z}\rho \overline{v'_z v'_z}\right)} \\
&-\left(\frac{\partial}{\partial x}\tau_{xz} + \frac{\partial}{\partial y}\tau_{yz} + \frac{\partial}{\partial z}\tau_{zz}\right) = 0 \qquad (4.5b)
\end{aligned}$$

By comparing the time-smoothed conservation of mass to the governing equation presented in Equation 4.3a, it is apparent that the two are identical except that the instantaneous velocity has been replaced by the time-smoothed value.

The result is similar for the conservation of momentum. In addition, a new series of terms (underlined) appears, often referred to as the "Reynolds stresses". This name follows from using the following notation for these terms

$$\tau^t_{xz} = \rho \overline{v'_x v'_z}\,, \qquad \tau^t_{yz} = \rho \overline{v'_y v'_z}\,, \quad \text{etc.}$$

Using this convention, the conservation of momentum can be written in tensor form

$$-\operatorname{div} \rho \vec{v}\,\vec{v} - \operatorname{grad} p - \operatorname{div} \underline{\underline{\tau}}^{\ell} - \operatorname{div} \underline{\underline{\tau}}^{t} = 0 \qquad (4.6)$$

For $\underline{\underline{\tau}}^{\ell}$, the laminar stress tensor, the components are generally specified based on the hypothesis of a Newtonian fluid. These components are given in Table 4.1a. One of the earliest and most convenient proposals for the turbulent stress tensor was to specify that $\underline{\underline{\tau}}^{t}$ has the same dependency on the velocity gradients as the laminar stress tensor (Boussinesq-1877). With this assumption, the turbulent and laminar stress tensors can be combined into one with components as presented in

TABLE 4.1a COMPONENTS OF THE LAMINAR STRESS TENSOR FOR NEWTONIAN FLUIDS IN CARTESIAN COORDINATES

$$\tau_{xx} = -\mu[2\frac{\partial v_x}{\partial x} - \frac{2}{3}(\nabla\cdot\vec{v})]$$

$$\tau_{yy} = -\mu[2\frac{\partial v_y}{\partial y} - \frac{2}{3}(\nabla\cdot\vec{v})]$$

$$\tau_{zz} = -\mu[2\frac{\partial v_z}{\partial z} - \frac{2}{3}(\nabla\cdot\vec{v})]$$

$$\tau_{xy} = \tau_{yx} = -\mu[\frac{\partial v_x}{\partial y} + \frac{\partial v_y}{\partial x}]$$

$$\tau_{yz} = \tau_{xy} = -\mu[\frac{\partial v_y}{\partial z} + \frac{\partial v_z}{\partial y}]$$

$$\tau_{zx} = \tau_{xz} = -\mu[\frac{\partial v_z}{\partial x} + \frac{\partial v_x}{\partial z}]$$

$$(\nabla\cdot\vec{v}) = \frac{\partial v_x}{\partial x} + \frac{\partial v_y}{\partial y} + \frac{\partial v_z}{\partial z}$$

TABLE 4.1b COMPONENTS OF THE TURBULENT STRESS TENSOR IN CARTESIAN COORDINATES

$$\tau_{xx} = -\mu_{eff}[2\frac{\partial \bar{v}_x}{\partial x} - \frac{2}{3}(\nabla\cdot\vec{\bar{v}})]$$

$$\tau_{yy} = -\mu_{eff}[2\frac{\partial \bar{v}_y}{\partial y} - \frac{2}{3}(\nabla\cdot\vec{\bar{v}})]$$

$$\tau_{zz} = -\mu_{eff}[2\frac{\partial \bar{v}_z}{\partial z} - \frac{2}{3}(\nabla\cdot\vec{\bar{v}})]$$

$$\tau_{xy} = \tau_{yx} = -\mu_{eff}[\frac{\partial \bar{v}_x}{\partial y} + \frac{\partial \bar{v}_y}{\partial x}]$$

$$\tau_{yz} = \tau_{zy} = -\mu_{eff}[\frac{\partial \bar{v}_y}{\partial z} + \frac{\partial \bar{v}_z}{\partial y}]$$

$$\tau_{zx} = \tau_{xz} = -\mu_{eff}[\frac{\partial \bar{v}_z}{\partial x} + \frac{\partial \bar{v}_x}{\partial z}]$$

$$(\nabla\cdot\vec{\bar{v}}) = \frac{\partial \bar{v}_x}{\partial x} + \frac{\partial \bar{v}_y}{\partial y} + \frac{\partial \bar{v}_z}{\partial z}$$

Table 4.1b. The expressions for the components of the combined stress tensor are identical to those of the laminar stress tensor except that μ, the laminar viscosity is replaced by μ_{eff}, the effective viscosity. The effective viscosity is many times larger than the laminar value. The evaluation of μ_{eff} is discussed on page 55.

Use of time-smoothed properties allows the governing equations, developed for laminar flow, to be used for turbulent flow. The conservation of mass is not effected by the time-smoothed method, but the conservation of momentum is changed and a new variable, μ_{eff}, must be used in place of the laminar viscosity. When an identical exercise is applied to the energy and species conservation equations, an extra series of terms analogous to the "Reynolds stresses" also appear. Again, these terms are handled by simply replacing the transport properties with "effective" values.

The exchange coefficients, Γ_h, and Γ_{fu} in the energy and species conservation equations as initially presented (Equations 4.2c,d) relate the mass diffusivity and thermal conductivity respectively to the viscosity through the Schmidt and Prandtl Numbers. Defined for laminar flow, the exchange coefficients are

$$\Gamma_h = \frac{k}{c_p} \quad , \qquad \Gamma_{fu} = \rho \mathcal{D}_{fu} \tag{4.7a}$$

and the Schmidt and Prandtl Numbers are respectively

$$\sigma_{fu} = \frac{\Gamma_{fu}}{\mu} = \frac{\rho \mathcal{D}_{fu}}{\mu} \; ; \qquad \sigma_h = \frac{\Gamma_h}{\mu} = \frac{k}{c_p \mu} \tag{4.7b}$$

For turbulent flow, following the convention of using effective transport properties in place of the laminar properties:

$$\sigma_{fu\ eff} = \frac{\Gamma_{fu\ eff}}{\mu_{eff}} \; ; \qquad \sigma_{h\ eff} = \frac{\Gamma_{h\ eff}}{\mu_{eff}} \tag{4.8}$$

The effective exchange coefficients, $\Gamma_{fu\ eff}$ and $\Gamma_{h\ eff}$, are used in the energy and species conservation equations for turbulent flow and are simply related to the effective viscosity through the Schmidt and Prandtl Number. The effective Schmidt and Prandtl Numbers are treated on page 56. Once the effective viscosity is established, all the transport properties are known.

It is normal procedure to transform or combine various of the governing equations into more convenient forms. The momentum equations in the r and z direction are combined to eliminate the pressure terms and most of the velocity terms. Performing this operation creates instead a new variable, vorticity.

The vorticity, ω, is a measure of the anticlockwise rotation of the fluid and is defined as

$$\omega = \frac{\partial v_r}{\partial z} - \frac{\partial v_z}{\partial r} \tag{4.9}$$

In the cylindrical geometry, it is convenient to replace ω as the dependent variable by ω/r, referred to as the "vorticity variable." The introduction of the vorticity results in one momentum equation instead of two, and one principle variable, ω/r, instead of the velocity and pressure. The pressure field can easily be recovered from the solution to the vorticity field.

The second manipulation normally undertaken is to introduce the stream function, ψ, into the continuity equation. The stream function is defined by

$$\rho v_z = \frac{1}{r}\frac{\partial\psi}{\partial r}; \qquad \rho v_r = -\frac{1}{r}\frac{\partial\psi}{\partial z} \tag{4.10}$$

Thus ψ describes the behavior of both v_z and v_r, and its use reduces the number of unknowns from two to one. The stream function is also introduced into the other governing equations wherever velocity appears.

The preceding manipulations result in four equations and four dependent variables:

Stream function, ψ

Vorticity variable, ω/r

Stagnation enthalpy, $\tilde{h}$

Fuel mass fraction, m_{fu}

The equations for each of these dependent variables have a similar structure. For axi-symmetric flow, the general form is represented by:

$$\boxed{\begin{aligned} &a_\phi\{\frac{\partial}{\partial z}(\phi\,\frac{\partial\psi}{\partial r}) - \frac{\partial}{\partial r}\,(\phi\,\frac{\partial\psi}{\partial z})\} - \frac{\partial}{\partial z}\,\{b_\phi\,\frac{\partial}{\partial z}(c_\phi\phi)\} \\ &\qquad - \frac{\partial}{\partial r}\,\{b_\phi\,\frac{\partial}{\partial r}(c_\phi\phi)\} + d_\phi = 0 \end{aligned}} \qquad \text{GENERAL GOVERNING PARTIAL DIFFERENTIAL EQUATION} \qquad (4.11)$$

The functions a_ϕ, b_ϕ, c_ϕ, and d_ϕ are given in Table 4.2 for each of the dependent variables, ϕ, considered.

4.2.2 Finite-Difference Formulation

No simple solution exists for the equations presented in Equation 4.11. A typical approach to solving a simultaneous set of equations with this complexity is to convert them to finite-difference form, and evaluate them numerically on a computer by iterating over a grid that covers the flow field in question.

The numerical procedure restricts attention to a finite number of points systematically distributed over the flow field as the nodal points of a grid. At each node, the differential equation (Equation 4.11)

TABLE 4.2 FUNCTIONS a_ϕ, b_ϕ, c_ϕ, AND d_ϕ OF EQUATIONS 4.11, 4.12

ϕ	a_ϕ	b_ϕ	c_ϕ	d_ϕ
ψ	0	$\frac{1}{\rho r}$	1	$-\omega$
ω/r	r^2	r^3	μ_{eff}	$-r^2[\frac{\partial}{\partial z}(\frac{v_z^2+v_r^2}{2})\cdot\frac{\partial\rho}{\partial r}$ $-\frac{\partial}{\partial r}(\frac{v_z^2+v_r^2}{2})\cdot\frac{\partial\rho}{\partial z}]$
$\tilde{h}$	1	$r\Gamma_{h,eff}$	1	$-\frac{\partial}{\partial z}(\mu_{eff}r\{(1-\frac{1}{\sigma_h})\frac{\partial v^2/2}{\partial z}$ $+\sum_{fu}(\frac{1}{\sigma_{fu}}-\frac{1}{\sigma_h})h_{fu}\frac{\partial m_{fu}}{\partial z}\}]-\frac{\partial}{\partial r}[\mu_{eff}r$ $\{(1-\frac{1}{\sigma_h})\frac{\partial v^2/2}{\partial r}+\sum_{fu}(\frac{1}{\sigma_{fu}}-\frac{1}{\sigma_h})h_{fu}\frac{\partial m_{fu}}{\partial r}\}]$
m_{fu}	1	$r\Gamma_{fu,eff}$	1	$-rR_{fu}$

is replaced by an algebraic finite-difference equation.

For each of the governing equations, the finite difference equation takes the general form (ref: Gosman et al-1969)

$$\boxed{\phi_P = C_E\phi_E + C_W\phi_W + C_N\phi_N + C_S\phi_S + D} \qquad (4.12)$$

GENERAL
GOVERNING FINITE
DIFFERENCE
EQUATION

where

$$C_E + (A_E + B_E c_{\phi,E})/\Sigma_{AB} \quad ,$$

$$C_W = (A_W + B_W c_{\phi,W})/\Sigma_{AB} \quad ,$$

$$C_N = (A_N + B_N c_{\phi,N})/\Sigma_{AB} \quad ,$$

$$C_S = (A_S + B_S c_{\phi,S})/\Sigma_{AB} \quad ,$$

$$D = -\, d_{\phi,P} V_P/\Sigma_{AB} \quad ,$$

$$\Sigma_{AB} = A_E + A_W + A_N + A_S + c_{\phi,P}(B_E + B_W + B_N + B_S)$$

$$A_E = \frac{a_{\phi,P}}{8}\{(\psi_{SE} + \psi_S - \psi_{NE} - \psi_N) + |\psi_{SE} + \psi_S - \psi_{NE} - \psi_N|\}$$

$$A_W = \frac{a_{\phi,P}}{8}\{(\psi_{NW} + \psi_N - \psi_{SW} - \psi_S) + |\psi_{NW} + \psi_N - \psi_{SW} - \psi_S|\}$$

$$A_N = \frac{a_{\phi,P}}{8}\{(\psi_{NE} + \psi_E - \psi_{NW} - \psi_W) + |\psi_{NE} + \psi_E - \psi_{NW} - \psi_W|\}$$

and

$$A_S = \frac{a_{\phi,P}}{8}\{(\psi_{SW} + \psi_W - \psi_{SE} - \psi_E) + |\psi_{SW} + \psi_W - \psi_{SE} - \psi_E|\}$$

$$B_E = \frac{b_{\phi,E} + b_{\phi,P}}{8} \cdot \frac{r_N - r_S}{z_E - z_P} \cdot (r_E + r_P) \quad ,$$

$$B_W = \frac{b_{\phi,W} + b_{\phi,P}}{8} \cdot \frac{r_N - r_S}{z_P - z_W} \cdot (r_W + r_P) \quad ,$$

$$B_N = \frac{b_{\phi,N} + b_{\phi,P}}{8} \cdot \frac{z_E - z_W}{r_N - r_P} \cdot (r_N + r_P) \quad ,$$

$$B_S = \frac{b_{\phi,S} + b_{\phi,P}}{8} \cdot \frac{z_E - z_W}{r_P - r_S} \cdot (r_S + r_P)$$

and

$$V_P = \frac{r_P}{4} (z_E - z_W) (r_N - r_S) .$$

The functions a_ϕ, b_ϕ, c_ϕ and d_ϕ are given in Table 4.2. The value of ϕ_P at a node, P, is then determined from the values of ϕ at the adjoining nodes: N, S, W and E. The coefficients A and B account for the effects of convection and diffusion respectively. The coefficient D accounts for the "source or sink" effects. For example, D encompasses the reaction rate term when ϕ is the fuel mass fraction.

Boundary Conditions. One requirement for the solution of a set of elliptic equations is that the boundary conditions must be specified on all boundaries enclosing the flow. Specifically, the values of the dependent variables must be specified on the boundaries that enclose the region for which a solution is sought. On many boundaries, the value of a dependent variable is known a-priori. For example, the stream function is zero along the wall of the combustion chamber, and the fuel mass fraction is usually known along the inlet plane. Along many boundaries, the value of the dependent variable may not be known. In this case, it is possible to specify the boundary condition in terms of an algebraic equation between the value of the variable on the boundary and the value of the variable at adjacent grid points. The boundary conditions are described below for each dependent variable considered: stream function, vorticity, stagnation enthalpy, and fuel mass fraction.

Stream Function

INLET PLANES: The distribution of stream function along the inlet plane of the jet and main streams is evaluated by integrating the relation for the stream function

$$\frac{\partial \psi}{\partial x} = - r \rho v_z \tag{4.10}$$

along the inlet planes. At the main stream inlet, the integration is performed from the wall to the centerline. The stream function is arbitrarily set to zero at the wall. At the jet inlet, the integration is performed from the centerline to the inner wall of the jet nozzle. The density and axial velocity are known a-priori from values measured experimentally.

SOLID WALLS AND CENTERLINE: The stream function is constant along solid walls and along the centerline because no net flux of mass crosses these boundaries. The constant values assumed by the stream function are those evaluated at the limits of the integration performed at the inlets.

EXIT PLANE: Along the exit plane the streamlines are assumed to be parallel to the axis. This implies that $\partial\psi/\partial z = 0$ in the exit plane. The assumption of parallel strealines is valid if the exit is bounded by walls parallel to the centerline and if the exit is a reasonable distance downstream of the region of recirculation.

Before evaluating the values of the stream function at the exit, a distribution between the value of the stream function at the exit and the value at nodes upstream of the exit must be assumed. Using the assumption of a zero normal gradient, the exit stream function may be calculated in terms of the upstream values.

A parabolic stream function is assumed between the stream function at the exit and the stream function two nodes directly upstream. By specifying $\partial\psi/\partial z = 0$, the value of the stream function at the exit is related to the values upstream by the relation

$$\psi_{exit} = \psi_3 \left[\frac{1}{1 - (\frac{n_2}{n_3})^2}\right] - \psi_2 \left[\frac{1}{1 - (\frac{n_2}{n_3})^2} - 1\right] \quad r = \text{const.} \qquad (4.13)$$

where n_2, distance between exit and first node upstream of exit

ψ_2, stream function at first node upstream of exit

n_3, distance between exit and second node upstream

ψ_3, stream function at second node upstream of exit

Vorticity

INLET PLANES: The vorticity at the inlet planes of the jet and main flow is determined from the definition of vorticity:

$$\omega = \frac{\partial v_r}{\partial z} - \frac{\partial v_z}{\partial r} \qquad (4.9)$$

The distribution of radial velocity, v_r, is taken to be zero (a non-zero radial velocity may be specified if desired). For a given profile of velocity at the inlet, $v_z(r)$, the vorticity is found directly by applying

$$\omega = - \frac{\partial v_z}{\partial r} \qquad (4.14)$$

The velocity distribution at the inlet plane of the main flow is determined experimentally. The velocity distribution at the jet inlet is assumed to be uniform.

EXIT PLANE: As above, the vorticity at the exit plane is determined from the velocity distribution at the exit. The radial velocity at the exit is zero because the streamlines are assumed to be parallel to the axis at that point (a convenient assumption in specifying the boundary conditions for the stream function at the exit). The velocity distribution, $v_z(r)$, is determined from the stream function distribution at the exit. The vorticity is found by applying Equation 4.14.

SOLID WALLS: The vorticity along a wall is not commonly specified as one would specify a value for the stream function. The vorticity at the wall is determined in terms of the vorticity at the adjacent node normal to the wall.

The vorticity at the wall is derived using the following three assumptions:

1. The flow between the wall and the node adjacent to the wall is parallel to the wall and the velocity varies as the "q" power of the distance between the two points.

2. The vorticity at the wall is contributed to only by the flow parallel to the wall.

3. The density varies linearly between the wall and the adjacent node.

For a horizontal wall (r = constant), the first assumption gives

$$v_z = S\left(\frac{n}{n_1}\right)^q \tag{4.15}$$

This profile is typical of turbulent flow in a smooth pipe where q assumes the value 1/6 to 1/7, depending on the Reynolds number of the flow. For the Reynolds number of 10^4 found experimentally, q assumes the value of 1/6 (Schlichting-1968).

From assumption 2

$$\omega = -\frac{\partial v_z}{\partial r} \tag{4.14}$$

and from assumption 3

$$\rho' = \rho_{wall} + (\rho_{n_1} + \rho_{wall}) \frac{n}{n_1} \tag{4.16}$$

The vorticity at the wall is now found by integrating the stream function relation

$$\frac{\partial \psi}{\partial r} = r \rho v_z \tag{4.10}$$

from the wall to the node adjacent using Equations 4.15 and 4.16 for v_z and ρ. The constant S is evaluated by solving the integrated equation in terms of the vorticity, ω_{n_1}, at the node adjacent to the wall. This gives the following relation for the vorticity at the wall

$$\left(\frac{\omega}{r}\right)_{wall} = \frac{\Delta\psi}{q^2 n_1^2 (kn_1+R) [\rho (\frac{kn}{2q+1} + \frac{R}{q+1}) + \Delta\rho (\frac{kn}{3q+1} + \frac{k}{2q+1})} \tag{4.17}$$

where

$\Delta\psi = \psi_{n_1} - \psi_{wall}$

$\Delta\rho = \rho_{n_1} - \rho_{wall}$

k = +1 when n and r are measured in the same direction

k = -1 when n and r are measured in opposite directions

The derivation for vertical walls (z = constant) is analogous.

AXIS OF SYMMETRY: The vorticity, ω, along the axis of symmetry is zero because the radial velocity, v_r, is zero along the axis and the axial velocity is symmetric around the axis,

$$\omega = \overset{0}{\cancel{\frac{\partial v_r}{\partial z}}} - \overset{0}{\cancel{\frac{\partial v_z}{\partial r}}}$$

However, the variable ω/r may be finite at r = 0 since

$$\frac{\omega}{r} = \frac{0}{0}$$

The vorticity variable is evaluated along the axis of symmetry using a quadratic approximation for the vorticity profile:

$$\omega = ar + br^2 \tag{4.18}$$

a and b are determined from values of ω/r and r at the two adjacent nodes normal to the axis. The solution is relatively insensitive to the specification of the vorticity variable at the axis.

PROTRUDING CORNERS: Special consideration must be taken at protruding corners for the vorticity because of the convention adopted for solid walls. Along solid walls the flow is assumed to be parallel to the wall and the vorticity at the wall is assumed to be contributed to only by the flow parallel to it. In the case of a protruding corner, it is not obvious along which wall, if either, the flow is parallel.

The one protruding corner in the ORJ is located at the intersection of the jet outer diameter and the face of the jet exit. The assumption is made that the dominant direction of flow past the corner is parallel to the axis of symmetry. With this assumption, the vorticity at the protruding corner is calculated as if the corner were situated on a horizontal (r = constant) wall.

Fuel Mass Fraction and Enthalpy

INLET PLANES: The values of the fuel mass fraction and enthalpy are specified at the main stream and jet inlet planes by values calculated from experimental measurements.

The theory and the experiment are developed in this study for stoichiometric mixtures in both the approach stream and the jet stream. The fuel mass fraction specified at the inlet planes is that corresponding to a stoichiometric mixture of ammonia and air. The stoichiometric fuel mass fraction is $(m_{fu})_{stoich} = 0.1416$.

The enthalpy along the inlet planes is evaluated from the experimentally measured temperature using the relation

$$\tilde{h} = c_{p_{mix}} T - m_{fu} HC \qquad (4.19)$$

where HC: heat of combustion of the fuel/air mixture

$c_{p_{mix}}$: specific heat of the mixture

A more accurate relation for the enthalpy would be one based on the heat of formation and sensible enthalpies of the species present. However, this involves terms which are temperature dependent and would require a more extensive iterative process.

SOLID WALLS, CENTERLINE AND EXIT: The values of the fuel mass fraction and enthalpy are specified on solid walls, the centerline, and at the exit plane by noting that there is no net flux of these quantities across the boundaries in question. This is true along solid, adiabatic walls and along the axis-of-symmetry, but it may not be valid along the exit plane. However, if the exit plane is reasonably downstream of the region of recirculation, then the assumption that the gradient normal to the exit plane is zero is reasonable.

With the additional assumption that the fuel mass fraction and enthalpy have a parabolic distribution adjacent to the boundaries in question, the condition $\partial\phi/\partial n = 0$ gives

$$\phi_{boundary} = \phi_3\left[\frac{1}{1 - (\frac{n_2}{n_3})^2}\right] - \phi_2\left[\frac{1}{1 - (\frac{n_2}{n_3})^2} - 1\right] \qquad (4.20)$$

where

n_2, normal distance between the boundary and the node adjacent

ϕ_2, value of the dependent variable at the node adjacent

n_3, normal distance between the boundary and two nodes away

ϕ_3, value of the dependent variable two nodes away

This expression is identical to Equation 4.13 for the stream function.

4.2.3 Physical Inputs

Before the governing equations are solved, certain parameters and thermodynamic data must be specified. The required inputs-density, effective viscosity, chemical kinetics and specific heat-are presented in this section.

Density: The density is related to the pressure and temperature of the mixture through the ideal gas equation of state:

$$\boxed{\rho = \frac{p\, m_{mix}}{R_u T}} \qquad (4.21)$$

where m_{mix}, the molecular weight of the mixture, is defined by:

$$m_{mix} = \frac{1}{\mathrm{m}_{fu}/m_{fu} + \mathrm{m}_{ox}/m_{ox} + \mathrm{m}_{prod}/m_{prod}} \qquad (4.22)$$

Effective Viscosity: In Section 4.2.1, the governing equations, written strictly for laminar flow, are applied to turbulent flow by replacing the transport properties with effective values. It is only necessary to establish a model for effective viscosity since the remaining transport properties are simply related to the effective viscosity through the effective exchange coefficients.

Evaluation of the effective viscosity is not straight forward. The effective viscosity has been the focus of much attention in recent years. Most of the emphasis has been directed toward models for parabolic flows. Effort has just recently been directed toward modeling the effective viscosity for elliptic flows. The object of these studies is to develop models that will be universally valid and not reliant upon an empirical input for the evaluation of various constants. The models are typically a function of the turbulence energy and some other characteristic parameter, such as the mixing length. Either or both of the turbulence energy and the mixing length may be dependent variables, requiring separate partial differential equations that must be solved simultaneously with those of the other dependent variables.

Because a more sophisticated model has not been developed for elliptic flow, a simplified model used previously by Pun and Spalding (1967) and Odlozinski (1968) is adopted:

$$\boxed{\mu_{eff} = KD^{2/3}\, L^{-1/3} \rho^{2/3} (\dot{m}v^2)^{1/3}} \qquad (4.23)$$

where K, a constant = 0.012

D, diameter

L, length of flow field being considered

ρ, local density

$\dot{m}v^2$, incoming kinetic energy

Equation 4.23 is derived by dimensional analysis after specifying that the effective viscosity is influenced by ρ, L, D and $(\dot{m}v^2)$ in the following manner (Odlozinski-1968):

ρ: μ_{eff} increases with local density

L: μ_{eff} diminishes with an increase in the length of the flow region

D: μ_{eff} increases with the diameter of the flow region

$\dot{m}v^2$: μ_{eff} increases with the incoming rate of kinetic energy

Effective Prandtl and Schmidt Numbers: The effective Prandtl and Schmidt Numbers

$$\boxed{\sigma_{h\ eff} = \Gamma_{h\ eff}/\mu_{eff}\ ; \qquad \sigma_{fu\ eff} = \Gamma_{fu\ eff}/\mu_{eff}} \tag{4.8}$$

are taken to be unity, a convention adopted in recent studies involving turbulent elliptic flows (Odlozinski-1968; Pun-1967). For gases in both laminar and turbulent flows, the effective Prandtl and Schmidt Numbers are typically in the vicinity of 0.7 (Shapiro-1954). Using a value of unity in lieu of 0.7 has the advantage of simplifying the governing partial differential equation for enthalpy (see Table 4.2).

Chemical Kinetics: The source term, d_ϕ, for the fuel mass fraction depends directly on the chemical reaction rate, R_{fu} (ref: Table 4.2). Adopting common convention, an Arrhenius form is used for the reaction rate,

$$\boxed{R_{fu} = A\, m_{fu}^{f}\, m_{ox}^{n-f}\, \rho^{n}\, e^{-E/RT}} \qquad \left[\frac{lbm_{fu}}{lbm\ ft^3\ sec}\right] \tag{4.24}$$

The constants A, n, f, and E are determined empirically. The rate data for the ammonia/air reaction are taken from a well-stirred reactor study (Pratt and Starkman-1968). Assuming the following stoichiometry,

$$4NH_3 + 3O_2 \rightarrow 6H_2O + 2N_2 \tag{4.25}$$

the constants in Equation 4.24 assume the following values:

$A = 2.5 \times 10^{10}$

$f = 0.75$

$n = 1.95$

$E = 6.26 \times 10^4$ Btu/lbm-mole

The reaction rate presented in the Arrhenius form depends on the local time-mean gas properties. As discussed in Section 4.2.1, the local gas properties (e.g., velocity, pressure, etc.) fluctuate due to the eddy motion of turbulent flow. Spalding (1970) suggests that the reaction rate is not simply dependent on the time-smoothed properties, but is strongly affected and, in fact, limited by the break-up of large eddies into small ones. The constants of the Arrhenius-type of rate function are found to be greatly exaggerated for turbulent flow. It might be expected then, to find that the Arrhenius equation and well-stirred reactor data given above do not give results quantitatively consistent with experimental findings. In anticipation of this, the data of Pratt and Starkman are used as first guesses. The constants A and E are refined by comparing the numerical prediction to the experimental results. This procedure is outlined in Section 6.

Heat of Combustion: The heat of combustion for the ammonia/air reaction is evaluated from an enthalpy balance between the reactants and products and assuming that they combine in the proportion given by Equation 4.1

$$4NH_3 + \overbrace{3O_2 + 3(3.77)N_2}^{\text{air}} \rightarrow 6H_2O + 2N_2 + 3(3.77)N_2 \qquad (4.1)$$

The heat of combustion is the decrease of enthalpy of the reacting mixture resulting in the most stable species, the pressures and temperature of the reactants being equal. Hence, the heat of combustion is the difference between the enthalpy of the reactants and the enthalpy of the products. Symbolically, this is represented by

$$HC = \Sigma\, b_j\, \Delta H_{f_{jT}} - \Sigma\, a_i\, \Delta H_{f_{iT}} \quad (4.26)$$

where

b_j: moles of product j

a_i: moles of reactant i

$\Delta H_{f_{jT}}$: heat of formation of species j at temperature T

The reference is taken to be 530°R, or about the inlet temperature of the mainstream. Using the data provided by the JANAF Tables (1960), Equation 4.26 gives:

$$\boxed{HC = -\ 8050\ \text{Btu/lbm}_{NH_3}} \quad (4.27)$$

The choice of the reaction temperature is not important. The heat of combustion is nearly independent of temperature. For example, at 3500°R the enthalpy of reaction is HC = -8091 Btu/lbm_{NH_3}.

Specific Heat: Assuming that the specific heat of all the species is constant and equal, the simplified temperature-rise relation given by Equation 4.19 is obtained,

$$T = \frac{\tilde{h} - m_{fu}\, HC}{c_{p_{mix}}} \quad (4.28)$$

The heat of combustion, HC, is evaluated in the previous section. The fuel mass fraction, m_{fu}, is calculated as a dependent variable. $\tilde{h}$, the enthalpy of the mixture is also a dependent variable. Hence, only the specific heat, $c_{p_{mix}}$, needs to be specified.

The specific heat is chosen to yield the adiabatic flame temperature for complete combustion (m_{fu} = 0.0). For a reactant temperature of 530°R, the adiabatic flame temperature for the ammonia/air reaction is 3460°R (McLean and Sawyer-1967). The value for the specific heat corresponding to these specifications is:

$$\boxed{c_{p_{mix}} = 0.395\ \text{Btu/lbm°R}} \qquad (4.29)$$

Using thermodynamic data from the JANAF Tables (1960), the specific heat of the mixture at the inlet conditions of the main stream [$4NH_3 + 3(O_2 + 3.77N_2)$] is

$$c_{p_{538°R}} = 0.290\ \text{Btu/lbm°R}$$

The specific heat corresponding to the fully reacted state [$6H_2O + 2N_2 + 3(3.77)N_2$] at the adiabatic temperature is

$$c_{p_{3460°R}} = 0.392\ \text{Btu/lbm°R}$$

The specific heat given by Equation 4.29 is adequate for the high-temperature regime. The assumption of a constant and equal specific heat is not wholly satisfactory at lower temperatures. The actual specific heat of the mixture at 538°R (0.290 Btu/lbm°R) is 73 percent of the value assumed (0.395 Btu/lbm°R).

Molecular Weight: In the numerical analysis, only three "species" are actually considered: fuel, oxidizer and product. To specify a molecular weight for the product, the species that comprise the product must be considered. The fuel and oxidizer are ammonia and oxygen. The product includes not only the products of combustion (H_2O and N_2), but also the 3.77 moles of inert nitrogen per mole of oxygen in the air.

The molecular weights of the fuel and oxidizer, ammonia and oxygen are 17.03 and 32.0 respectively. The molecular weight of the product is not as obvious. For cold flow, the product consists of atmospheric nitrogen only. The molecular weight then is 28.0. For hot flow, the combustion products H_2O and N_2 are also present but in varying amounts depending on the degree of reaction. For the completely reacted condition, the species that comprise the product are proportioned according to Equation 4.1, or

$$\text{reactants} \rightarrow \overbrace{6H_2O + 2N_2 + 3(3.77)N_2}^{\text{product}}$$

giving a product molecular weight of 24.8. From the cold-flow condition to the fully-reacted condition, the molecular weight of the product varies from 28.0 to 24.8. The variation of the product molecular weight is handled in the numerical program by assuming a linear variation:

$$\boxed{m_{prod} = 28.0 - \left(\frac{m_{fu_o} - m_{fu}}{m_{fu_o}}\right)(28.0 - 24.8)} \quad (4.31)$$

where:

$m_{fu_o} = (m_{fu})_{stoich} = 0.1416$, the initial fuel mass fraction

m_{fu} = local fuel mass fraction

4.2.4 Computational Procedure

The numerical program is developed in steps. The cold-flow solution is developed prior to the hot-flow solution. A uniform grid is used prior to a nonuniform grid. Each step introduces new problems, but because complications are introduced in steps, the problems are more readily isolated and cured. The information presented below describes the computer program in its final form.

Solutions are obtained for the two inlet main stream velocities. These two conditions are designated as points A and B in Figure 4.1.

Point A is located at the peak of the blowout curve, point B is located at an approach velocity about 20 percent lower.

Cold-flow solutions are obtained first. For cold flow, the two dependent variables considered are the stream function, ψ, and the vorticity variable, ω/r.

For hot flow, the enthalpy, $\tilde{h}$, and fuel mass fraction, m_{fu}, are also considered as dependent variables. The cold-flow solutions for the stream function and the vorticity variable are used for the initial values (or "guesses") in the hot-flow solution. The hot flow is "ignited" by specifying a small value of the fuel mass fraction (e.g., $m_{fu} = 5.0 \times 10^{-3}$) throughout a large area surrounding the stagnation point. If the "ignited" flow converges to the cold-flow solution, blowout is assumed.

Flow Diagram: The flow diagram of the computer program is given in Figure 4.3. Program MAIN reads in the data, calculates the grid sizing and calls two subroutines, INIT and HEADCT to calculate and print some of the initial information. To begin the iterative process, MAIN calls subroutine SOLVCT. In SOLVCT, the iteration process is controlled and the test for convergence is made. For each iteration, SOLVCT calls subroutine FDEQCT. For every dependent variable, FDEQCT sweeps the grid updating the value of the dependent variable at every node.

The computer program consists of another 20 subroutines in addition to the subroutines mentioned. Some support FDEQCT, some provide auxillary information, while others are used for printing the output in various forms. All the subroutines are described in Appendix D.

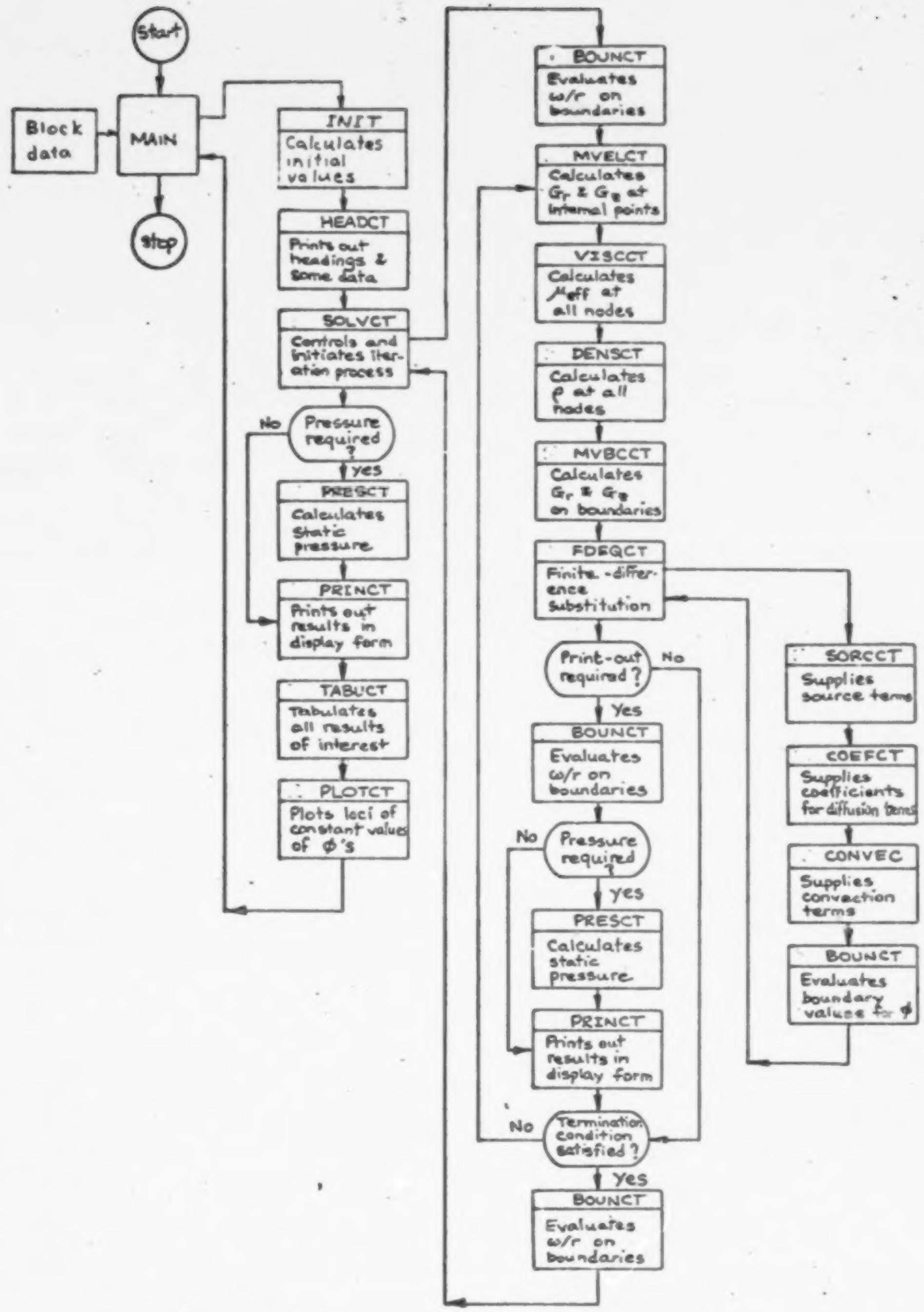
Start
Block data
MAIN
Stop
INIT
Calculates initial values
HEADCT
Prints out headings & some data
SOLVCT
Controls and initiates iteration process
Pressure required ?
No
yes
PRESCT
Calculates static pressure
PRINCT
Prints out results in display form
TABUCT
Tabulates all results of interest
PLOTCT
Plots loci of constant values of ϕ's
BOUNCT
Evaluates ω/r on boundaries
MVELCT
Calculates G_r & G_θ at internal points
VISCCT
Calculates μ_{eff} at all nodes
DENSCT
Calculates ρ at all nodes
MVBCCT
Calculates G_r & G_θ on boundaries
FDEQCT
Finite-difference substitution
Print-out required ?
No
Yes
BOUNCT
Evaluates ω/r on boundaries
Pressure required ?
No
Yes
PRESCT
Calculates static pressure
PRINCT
Prints out results in display form
Termination condition satisfied ?
No
Yes
BOUNCT
Evaluates ω/r on boundaries
SORCCT
Supplies source terms
COEFCT
Supplies coefficients for diffusion terms
CONVEC
Supplies convection terms
BOUNCT
Evaluates boundary values for ϕ

FIGURE 4.3 COMPUTER FLOW DIAGRAM

Grid: A schematic of the grid is given in Figure 4.4. In Figure 4.4b, the grid is expanded by a factor of two in the J-direction to accentuate the detail near the centerline. The grid is nonuniform in both directions. There are 15 nodes in the J-direction and 33 nodes in the I-direction. The jet exit plane is located at I = 27. The inner diameter of the jet exit is located at J = 3 and the outer diameter at J = 6.

The grid is nonuniform. A nonuniform grid allows the region of steep gradients to be covered with a fine mesh while including within the grid network the entire area of interest. Ideally, the entire area of interest should be covered with a small mesh. However, a small mesh results in a large number of grid points and excessive computer time. To minimize computational time and still effectively cover the area of steep gradients, a nonuniform grid is employed.

In the J-direction, the grid lines are closely spaced at the axis. The spacing between constant J-lines expands uniformly to the wall of the chamber. The spacing at the axis is about 0.016-inch, and at the wall, about 0.20-inch.

In the I-direction, the grid spacing decreases from the inlet to a small, uniform spacing, 0.2-inch in size. The uniform spacing is maintained until the plane of the jet exit. At that point, the grid spacing in the I-direction expands to a 0.5-inch spacing.

Iterative Process: For each iteration, the field is sweep from bottom to top (J = 1 to J = 15), and from left to right (I = 1 to I = 33) for each dependent variable. The new value of the dependent variable immediately replaces the old value. Reference to the finite-difference

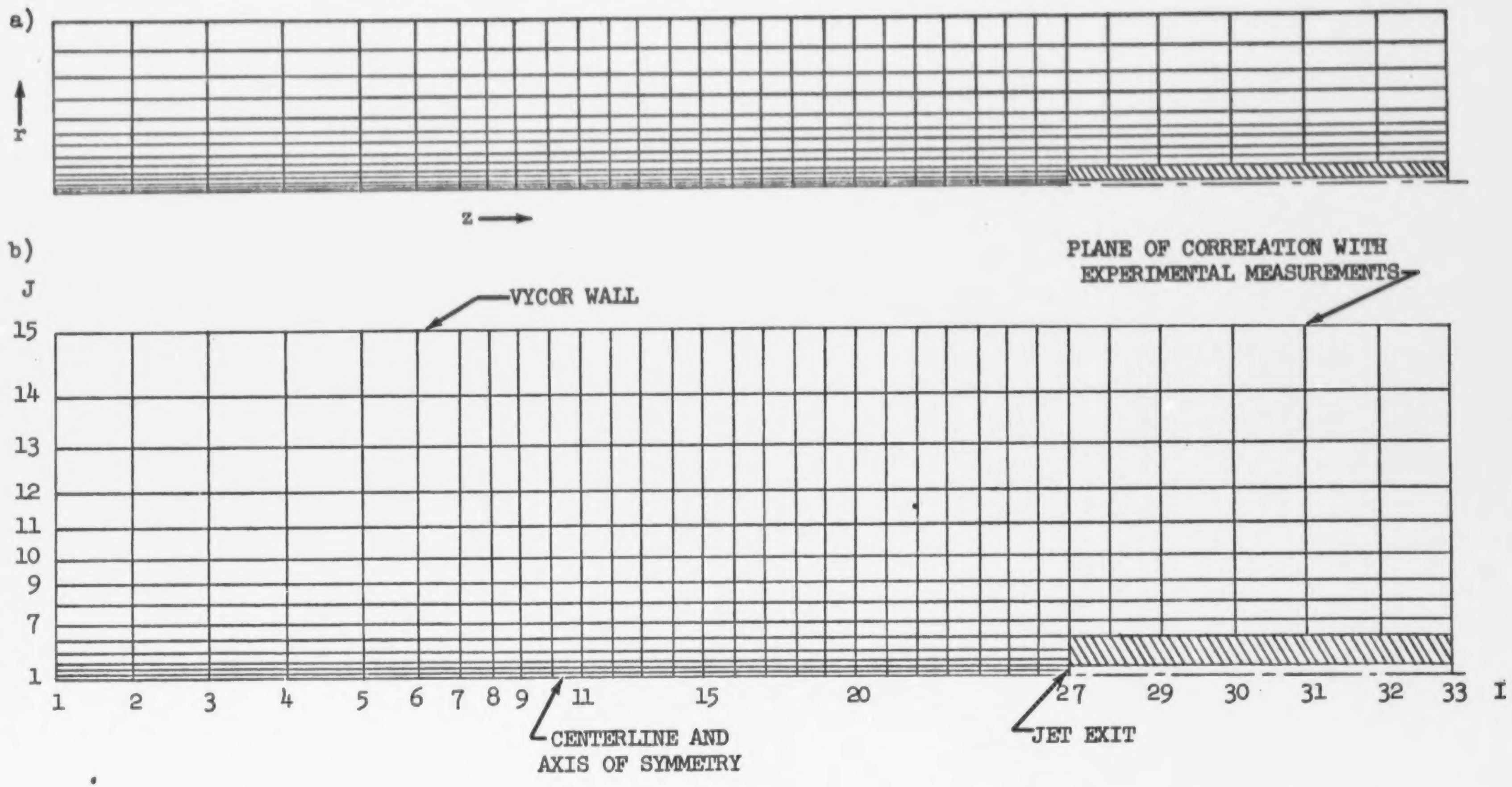
a)
r
z
b)
J
15
14
13
12
11
10
9
7
1
VYCOR WALL
PLANE OF CORRELATION WITH EXPERIMENTAL MEASUREMENTS
1
2
3
4
5
6
7
8
9
11
15
20
27
29
30
31
32
33
I
CENTERLINE AND AXIS OF SYMMETRY
JET EXIT

FIGURE 4.4 GRID SCHEMATIC
a) ACTUAL SIZE (IDENTICAL TO EXPERIMENT)
b) J-DIRECTION EXPANDED 2X

formula (Equation 4.12) shows that the value of the dependent variable is determined by the value assumed at the adjacent nodes. The updated value is determined by values at two adjacent nodes evaluated during the previous iteration, and values at the remaining two adjacent nodes evaluated during the current iteration. This is the Gauss-Seidel method. An obvious advantage of the method is that additional memory is not required to store all the values from the prior iteration.

Convergence is accelerated by under-relaxing the vorticity variable and the fuel mass fraction. The expression used for this purpose is:

$$\underset{\text{value stored}}{\phi_N} = RP_\phi \cdot \overset{\text{value calculated in current iteration}}{\phi_N} + [1 - RP_\phi]\,\underset{\text{value calculated during previous iteration}}{\phi_{N-1}} \tag{4.32}$$

where RP_ϕ is the relaxation parameter. If $RP_\phi < 1.0$, the variable, ϕ, is under-relaxed. If $RP_\phi > 1.0$, the variable is over-relaxed. When relaxation is not employed (as for the other dependent variables), $RP_\phi = 1.0$. A value of 0.75 for RP_ϕ is used to under-relax both the vorticity and the fuel mass fraction.

Convergence Criterion: The convergence criterion is based on the following expression

$$\frac{|\phi_N - \phi_{N-1}|}{\phi_N} < CC \tag{4.33}$$

Simply stated, the fractional change in the value of each dependent variable from one iteration (N-1) to the next (N) must be less than CC. The solution in the current study is taken to be converged if the net change of each dependent variable is less than 0.5 percent. This gives a value for CC of 0.005.

The cold-flow solutions take about 160 iterations to converge (6-minutes on a CDC 6400). Using the cold-flow solutions for initial values, the hot-flow solutions take about 400 iterations to converge (28-minutes on a CDC 6400). For a small perturbation (change in the approach velocity, kinetic constants, etc.), the hot-flow solutions usually converge within 50 iterations (4-minutes CDC 6400 time).

4.2.5 Analytical Results

Results are obtained for three cases!

Case 1: Cold flow at point A in Figure 4.1

Case 2: Cold flow at point B in Figure 4.1

Case 3: Hot flow at point B

The constants A and E in the chemical rate expression (Equation 4.24) are refined by comparing the numerical predictions to the experimental results. This procedure is described in Section 6. The values for A and E and the reaction rate used for the results described in this section are:

$$A = 22.0 \times 10^{10}$$

$$E = 6.00 \times 10^{4} \text{ Btu/lbm-mole}$$

$$R_{fu} = 22.0 \times 10^{10} m_{fu}^{0.75} m_{ox}^{1.20} \rho^{1.95} e^{-6.00\times10^{4}/RT} \tag{4.34}$$

Stream Function Distribution: The stream function distributions for the three cases considered are presented in Figure 4.5. In Figure 4.5a, the stagnation point is located 1-3/4 inches upstream of the jet exit for Case 1 (cold flow at the blowout velocity). For Case 2, the

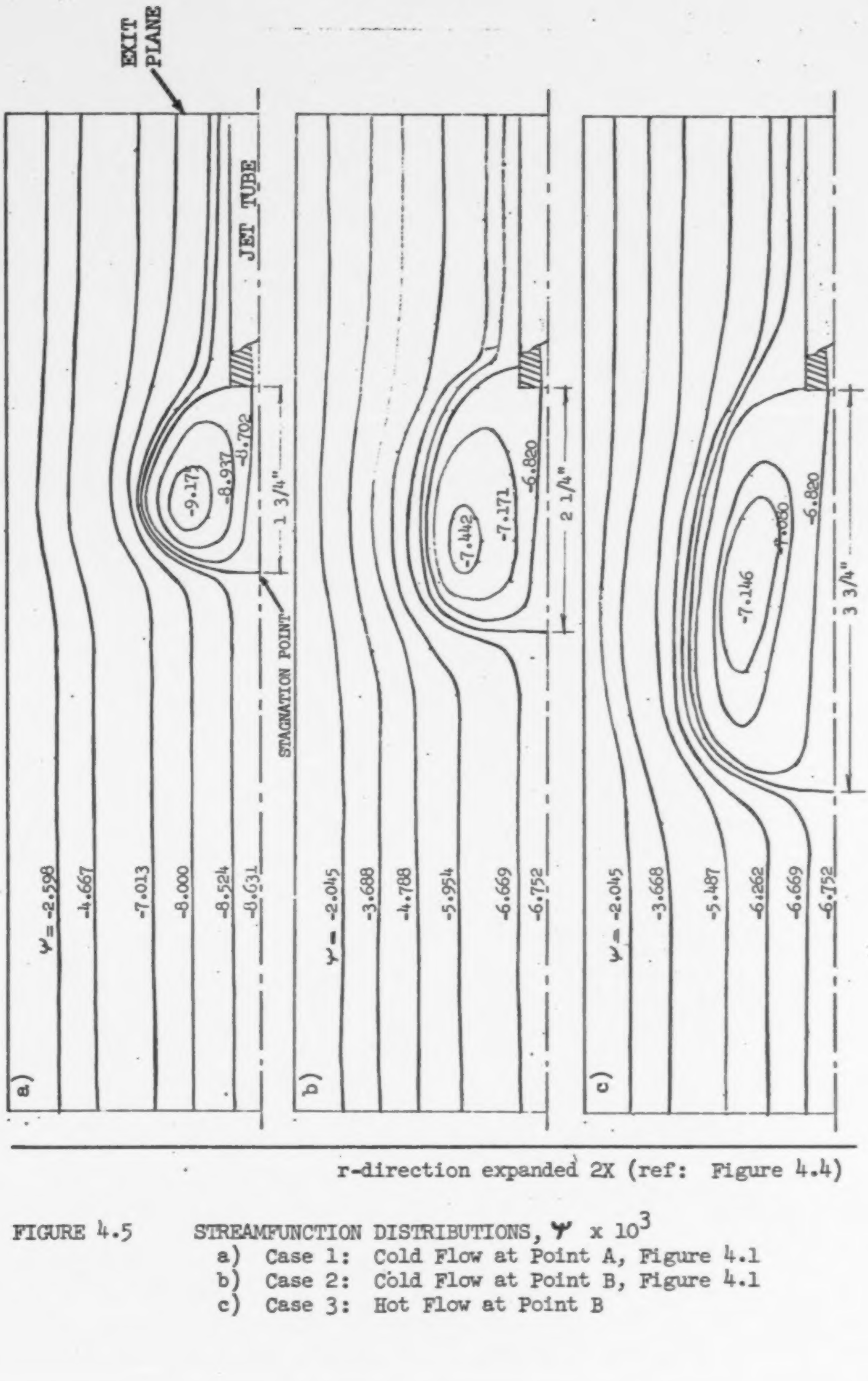

r-direction expanded 2X (ref: Figure 4.4)

FIGURE 4.5 STREAMFUNCTION DISTRIBUTIONS, $\Psi \times 10^3$
a) Case 1: Cold Flow at Point A, Figure 4.1
b) Case 2: Cold Flow at Point B, Figure 4.1
c) Case 3: Hot Flow at Point B

stagnation point is located further upstream (2-1/4 inches) than in the previous case. The difference in the location of the stagnation point is attributed to the lower approach velocity in Case 2.

The stream function distribution for hot flow is given in Figure 4.5c. The approach stream velocity corresponds to point B in Figure 4.1. The location of the stagnation point has moved upstream to a point 3-3/4 inches from the jet exit. The difference of the location of the stagnation point in the case of the reacting flow is attributed to the higher jet velocity. Although the jet mass flow rate is identical for both the hot and cold flow cases, the heating of the jet in the presence of combustion produces a jet velocity of 715 fps (ref: Section 5.4) compared to a jet velocity of 294 fps in the case of cold flow.

Temperature and Composition Distributions: Temperature and fuel mole fraction distributions are plotted in Figure 4.6 for Case 3. A region of highly reacted (fuel mole fraction = .004) and uniform temperature (3300°R) is located upstream of the stagnation point. The nose of the flame front is situated 3-7/8 inches upstream of the jet exit. This compares favorably to the actual flame front shown in Figure 1.1 for the approach conditions corresponding to point B.

Temperature and Composition Profiles: The predicted temperature and composition profiles for Case 3 are given in Figure 4.7. The mixture is almost completely reacted at the wall of the jet. At the Vycor wall the mixture is only slightly reacted. At a radius of 0.6-inch, a sharp increase in temperature occurs and the fuel mole fraction drops accordingly.

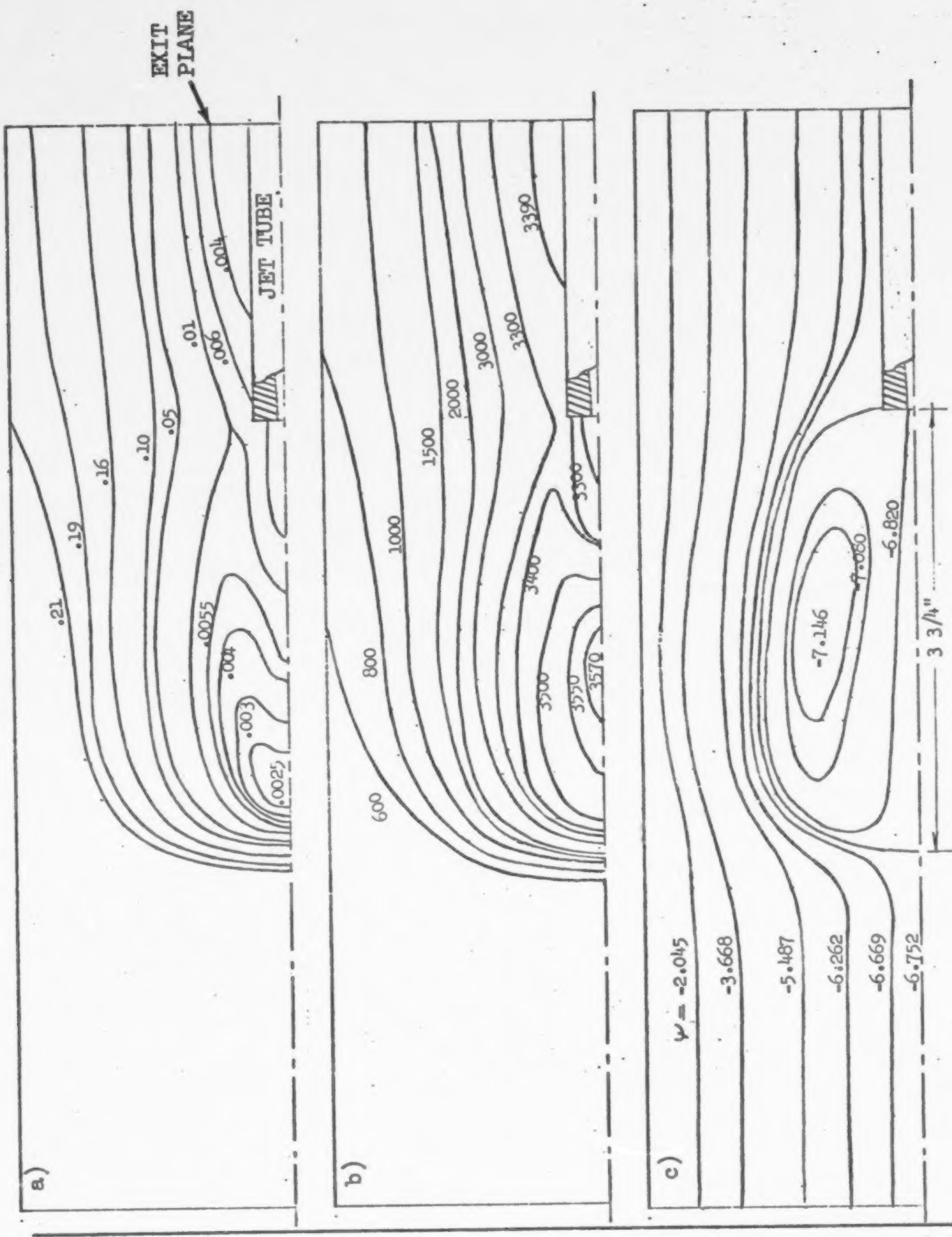

r-direction expanded 2X (ref: Figure 4.4)

FIGURE 4.6 DISTRIBUTIONS FOR CASE 3 (Hot Flow at Point B, Figure 4.1)
a) FUEL MOLE FRACTION
b) TEMPERATURE, °R
c) STREAMFUNCTION, $\psi \times 10^3$ (Ref: Figure 4.5c)

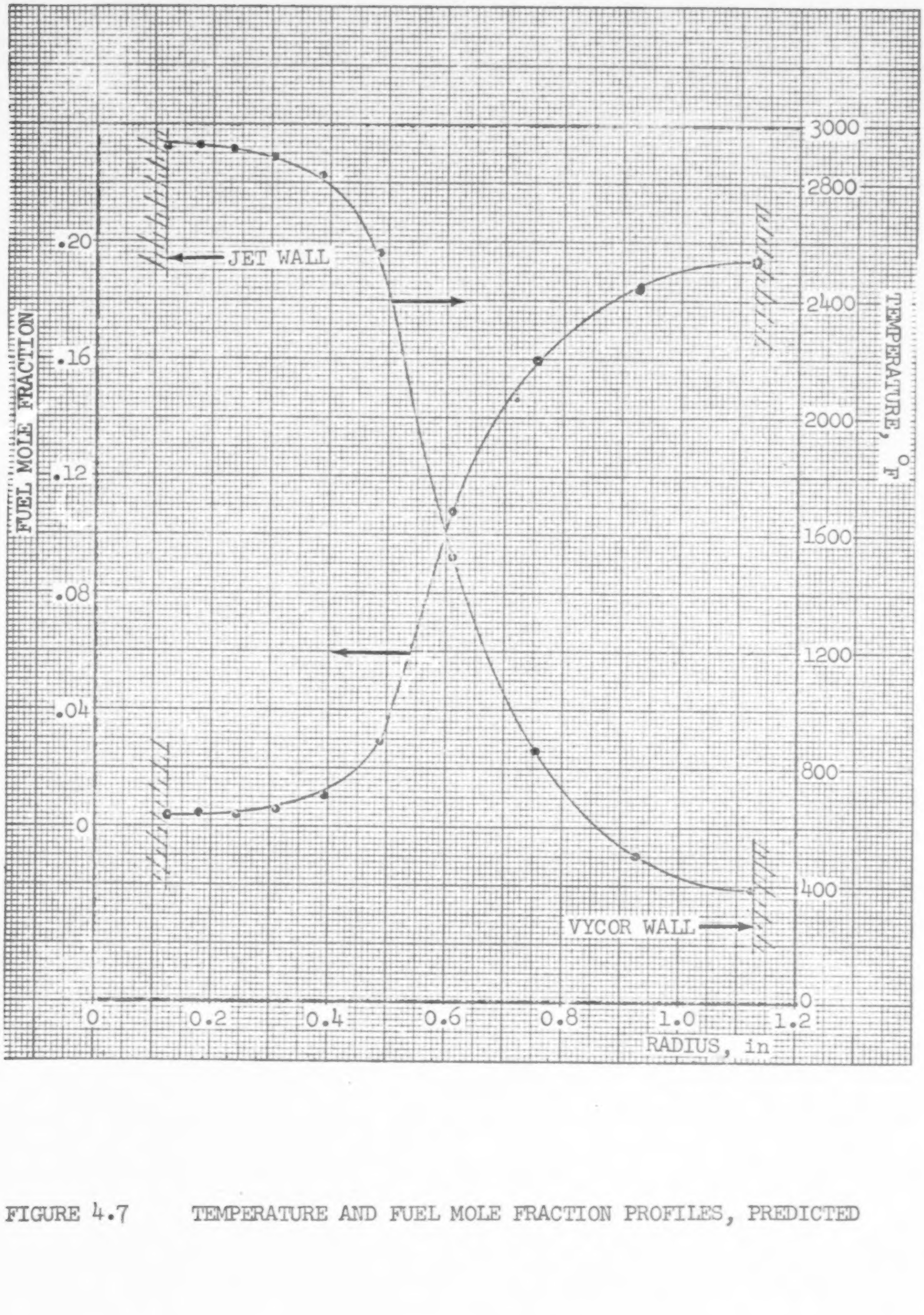

FIGURE 4.7 TEMPERATURE AND FUEL MOLE FRACTION PROFILES, PREDICTED

SECTION 5

Experimental Investigation

5.1 Experimental Facility
5.2 Inlet Velocity and Composition Profiles
5.3 Blowout Map
5.4 Jet Exit Temperature and Velocity
5.5 Composition and Temperature Measurements

An opposed-reacting-jet experimental facility was built so that radial profiles of composition and temperature could be measured and compared to those values predicted numerically. Below are presented:

1. a description of the experimental facility,
2. measurements of velocity and composition at the inlet of the combustor, used to specify the initial conditions in the numerical calculations,
3. a blowout map for a stoichiometric ammonia/air jet
4. measurements of the jet exit temperature and velocity, also used for initial conditions in the numerical program, and
5. measurements of temperature and composition in the reacting flow field obtained for comparison to the numerical calculations.

5.1 Experimental Facility

The combustion chamber is shown in Figure 1.1. The chamber itself is Vycor,* a high-temperature glass. The Vycor section is 14 inches in length, with an inner diameter of 57 millimeters (2-1/4 inches) and an outer diameter of 64 millimeters (2-1/2 inches).

---

*Product of Corning Glass Works, Corning, New York

The opposed-jet protrudes 2-1/2 inches into the Vycor. A cross section of the jet is shown in Figure 5.1. The jet is machined from 1/4-inch tantalum rod. Throughout most of its length, the inner diameter is bored to 5/32-inch. At the exit, a nozzle is shrink-fitted to the main section. The nozzle has a bell contour, converging from 5/32-inch to 0.063-inch exit diameter. The thermocouple shown has a 1/16-inch O.D. sheath and is used to determine the temperature and velocity of the exiting jet stream as described below.

Tantalum is used for the opposed-jet because of the apparent success in an earlier use of the high-temperature metal (Bohrer-1967). However, tantalum oxidizes at high temperatures in the presence of water and oxygen (Shaffer-1964).* The oxide builds up on the jet over a period of time and eventually begins to flake off. More critical, the oxide eventually accumulates in the jet exit, changing the geometry and consequently modifying the jet exit velocity. The experimental runs reported here are of sufficiently short duration to control the oxide build-up.

Another high-temperature metal (e.g., Inconel) might be satisfactory for the jet material without having the shortcoming experienced with tantalum. Another possibility is a water-cooled stainless-steel jet (e.g., Agoston, et al-1958). The water-cooled jet has the additional advantage of enabling control of the jet temperature. A water-cooled jet is not used here because of the desirability for the numerical calculations to make the walls

---

*The formation of tantalum oxide is a potential problem in many reacting flows where oxygen (as an oxidizer) and water (as a product of combustion) are present.

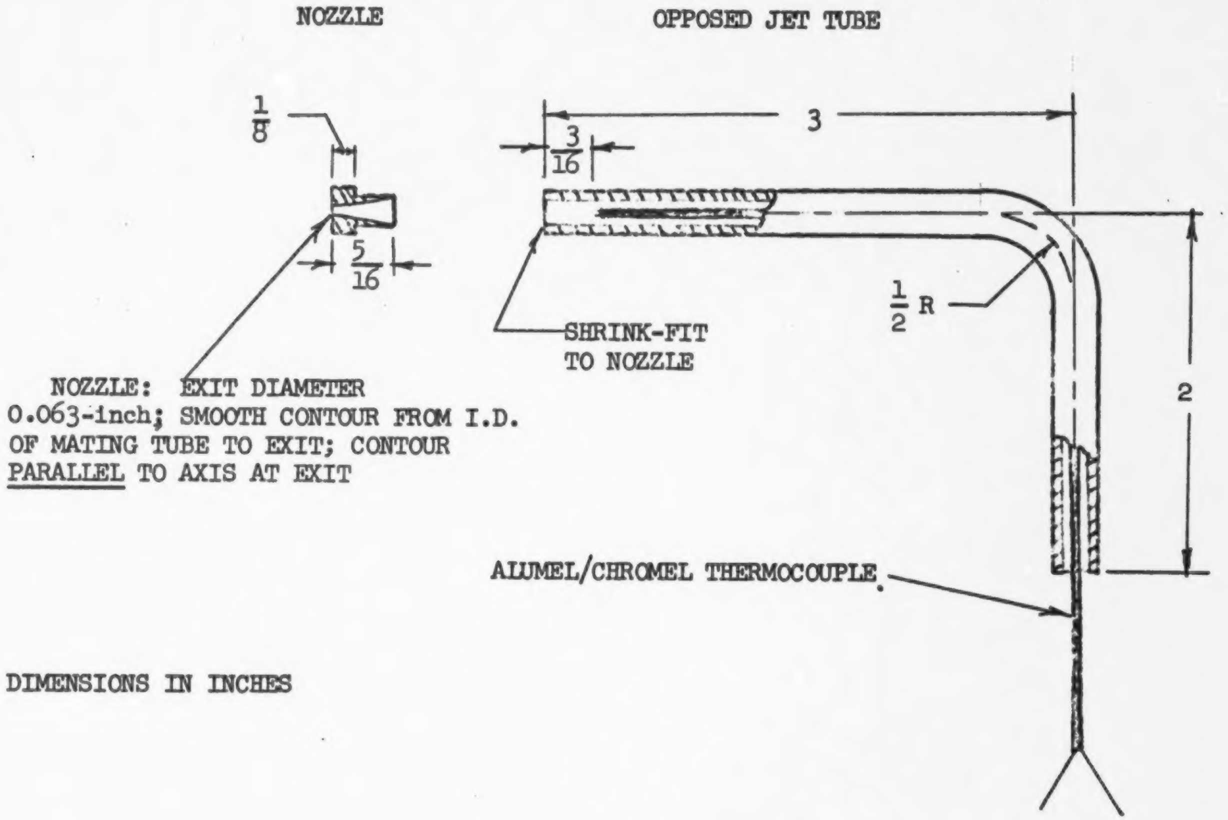
NOZZLE
OPPOSED JET TUBE
1/8
5/16
3/16
3
2
1/2 R
SHRINK-FIT TO NOZZLE
ALUMEL/CHROMEL THERMOCOUPLE

NOZZLE: EXIT DIAMETER 0.063-inch; SMOOTH CONTOUR FROM I.D. OF MATING TUBE TO EXIT; CONTOUR PARALLEL TO AXIS AT EXIT

DIMENSIONS IN INCHES

FIGURE 5.1 OPPOSED REACTING JET: CROSS-SECTION

as nearly adiabatic as possible, including the outer surface of the jet tube.* In a water-cooled jet, substantial energy is extracted from the wall of the jet creating a non-adiabatic wall. The non-cooled, tantalum jet approaches the main flow temperature and makes the jet wall more nearly adiabatic. Heat is transferred to the flow inside the jet, but the transfer of energy is considerably less than for a water-cooled jet.

To make the Vycor combustion chamber near-adiabatic, the Vycor cylinder is wrapped with 1-inch-thick asbestos lagging, commonly used to insulate steam lines. The lagging is shown fitted to the Vycor in Figure 5.2. Thermocouples are buried in the lagging to determine the effectiveness of the lagging in creating an adiabatic wall condition. The thermocouple measurements and the calculated heat loss through the lagging are presented in Appendix C.

The experimental facility is discussed in more detail in Appendix A.

5.2 Inlet Velocity and Composition Profiles

The radial distribution of the velocity at the inlet plane is needed to specify the velocity inlet condition in the numerical program.

The radial distribution of composition at the inlet is also needed. The experiment is designed to give a uniform profile of fuel and air at the inlet. The uniformity is verified by experimentally measuring the composition profile.

Both the velocity and composition measurements are made 2-inches upstream of the Vycor inlet, in the 3-foot stainless-steel straightening section described in Appendix A. The velocity profile is measured using

---

*An adiabatic boundary condition is relatively simple to specify.

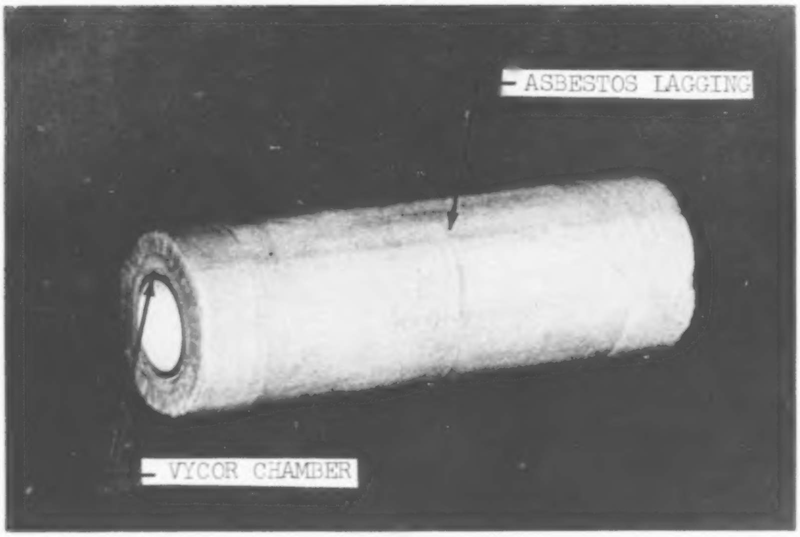
ASBESTOS LAGGING
VYCOR CHAMBER

FIGURE 5.2 VYCOR COMBUSTION CHAMBER WITH LAGGING

a stagnation pressure probe in conjunction with a static pressure tap at the wall. The stagnation pressure probe is made from hypodermic tubing with a 0.028-inch outer diameter and a 0.004-inch wall. A diagram of the probe is shown in Figure 5.3. The static pressure tap is located at the same axial position as the tip of the probe.

The stagnation pressure probe is moved radially across the chamber in 1/8-inch intervals (1/16-inch near the wall). At each radial point, the difference between the stagnation and static pressures, Δp, is measured in inches-of-water on an inclined manometer, the total range of which is 2 inches-of-water. The velocity is calculated from the relation

$$v^2 = \frac{2\Delta p}{\rho} \tag{5.1}$$

The density, ρ, is determined from the measured static pressure and the temperature, measured by a thermocouple.

The velocity profiles are given in Figure 5.4. Profiles for select approach velocities are given in Figure 5.4a. The approach velocities correspond to points A and B in Figure 4.1, the two velocities for which numerical calculations are made. The profiles show that the flow is turbulent at the inlet. (The velocity distribution for laminar flow is parabolic.) In Figure 5.4b, the velocity profiles are presented in non-dimensional form. The Reynolds number based on the diameter of the combustor is about 10^4 for both points A and B.

The stagnation pressure probe described above was also used to sample composition at the inlet of the main stream. Samples are withdrawn at various radial locations using a diaphram pump. The composition

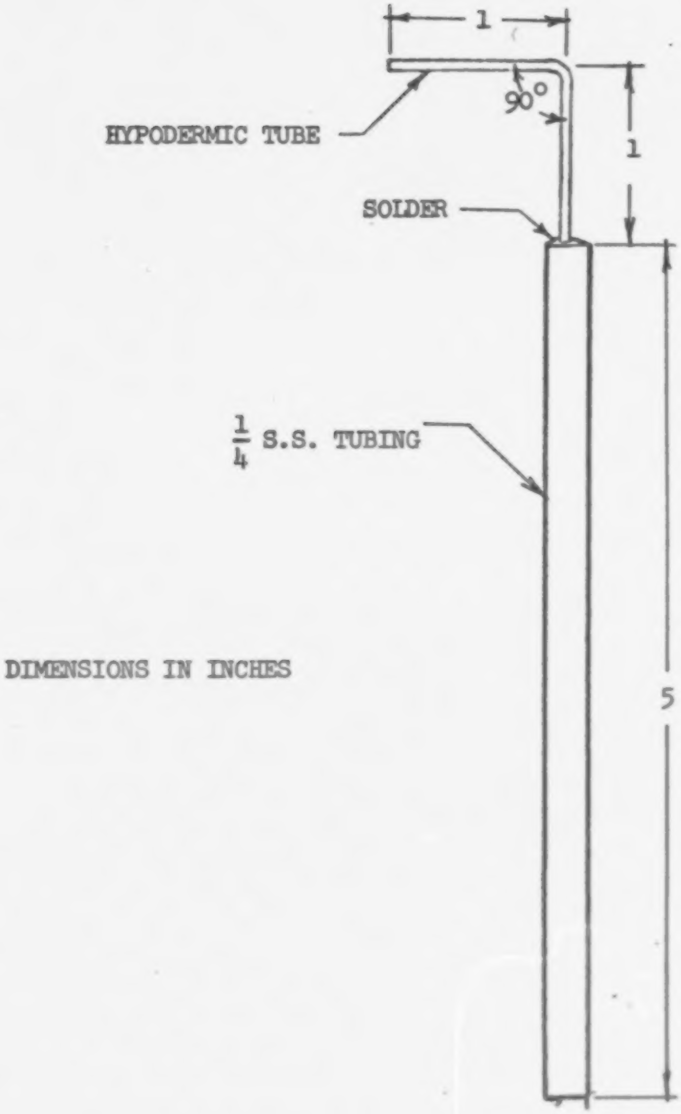
1
90°
HYPODERMIC TUBE
1
SOLDER
$\frac{1}{4}$ S.S. TUBING
5

DIMENSIONS IN INCHES

FIGURE 5.3 STAGNATION PROBE

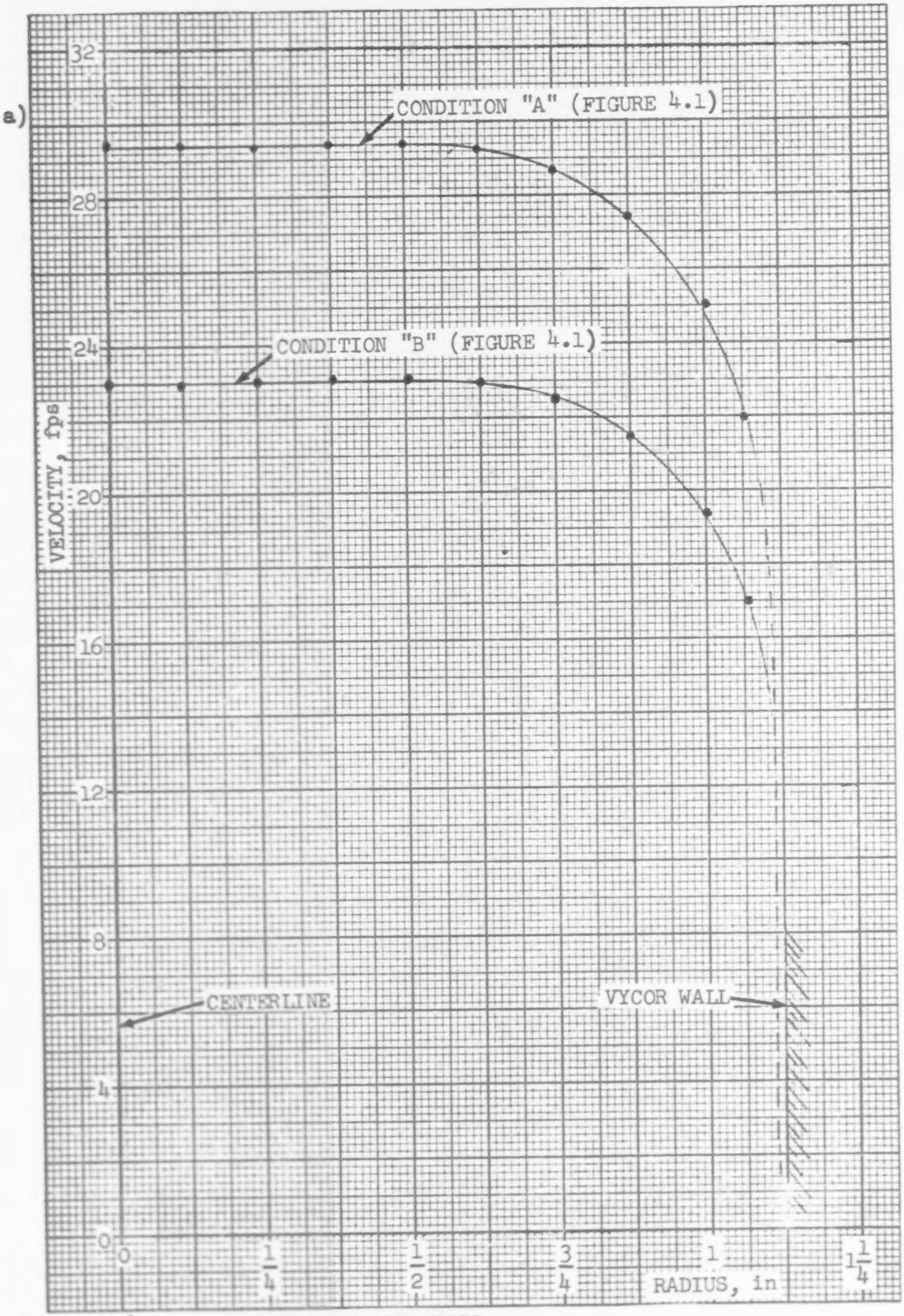

FIGURE 5.4 INLET VELOCITY PROFILES
a) ACTUAL INLET PROFILES
b) NONDIMENSIONAL PROFILE

b)

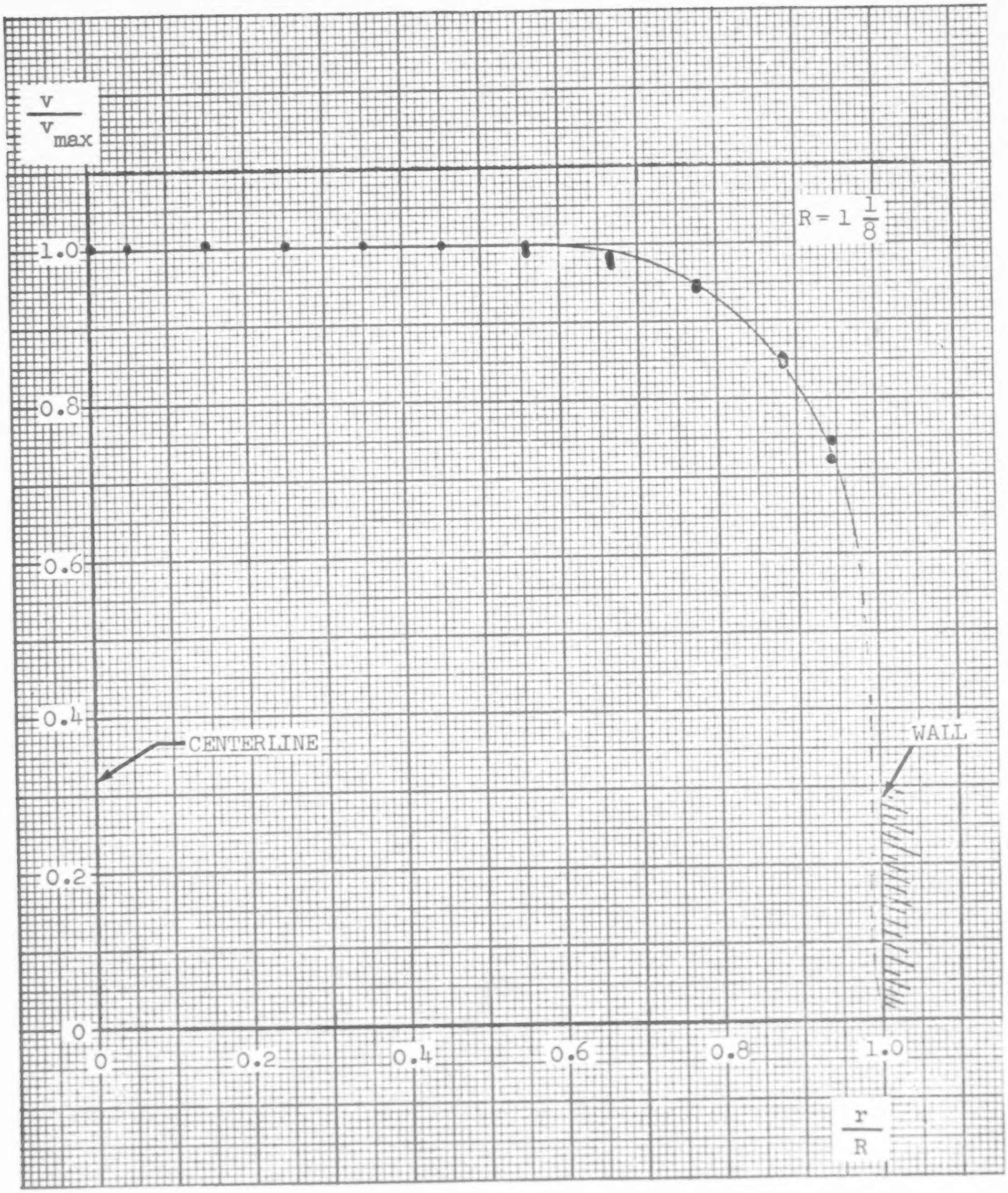

is monitored continuously by passing the samples from the diaphram pump through an Oxygen Process Analyzer (Beckman Instruments Model 716), which records the concentration of oxygen in percent volume. Measurements indicate that the oxygen concentration across the inlet is uniform and equal (within ± 1 percent) to the value expected of oxygen in air in a stoichiometric mixture with ammonia (16.4 percent).

The results show that the fuel/air mixing in the Venturi section, described in Appendix A, is effective in producing a uniform composition profile at the inlet.

5.3 Blowout Map

The blowout map is described in Section 2.1. The blowout map generated for the ammonia/air ORJ is given in Figure 5.5.* The jet is stoichiometric.

Comparison of the blowout map for ammonia/air to that of propane-air (Figure 2.3) shows that the flameholding capacity is substantially lower for the present experimental configuration and ammonia as a fuel. The peak approach velocity for propane is 300 fps, whereas the peak approach velocity for ammonia is only 27 fps. The difference is attributed to the lower reaction rate of ammonia and the lower jet pressure used in the ammonia study. For a reactant temperature of 150°C, the burning velocities of ammonia and propane in air are 0.49 fps (Cohen-1955) and 2.3 fps (Dugger and Heimel-1952) respectively.

Point A in Figure 5.5 lies on the blowout curve at the peak approach velocity. Point B is at a lower velocity, about 80 percent of the peak

---

*The blowout map is also given in Figure 4.1.

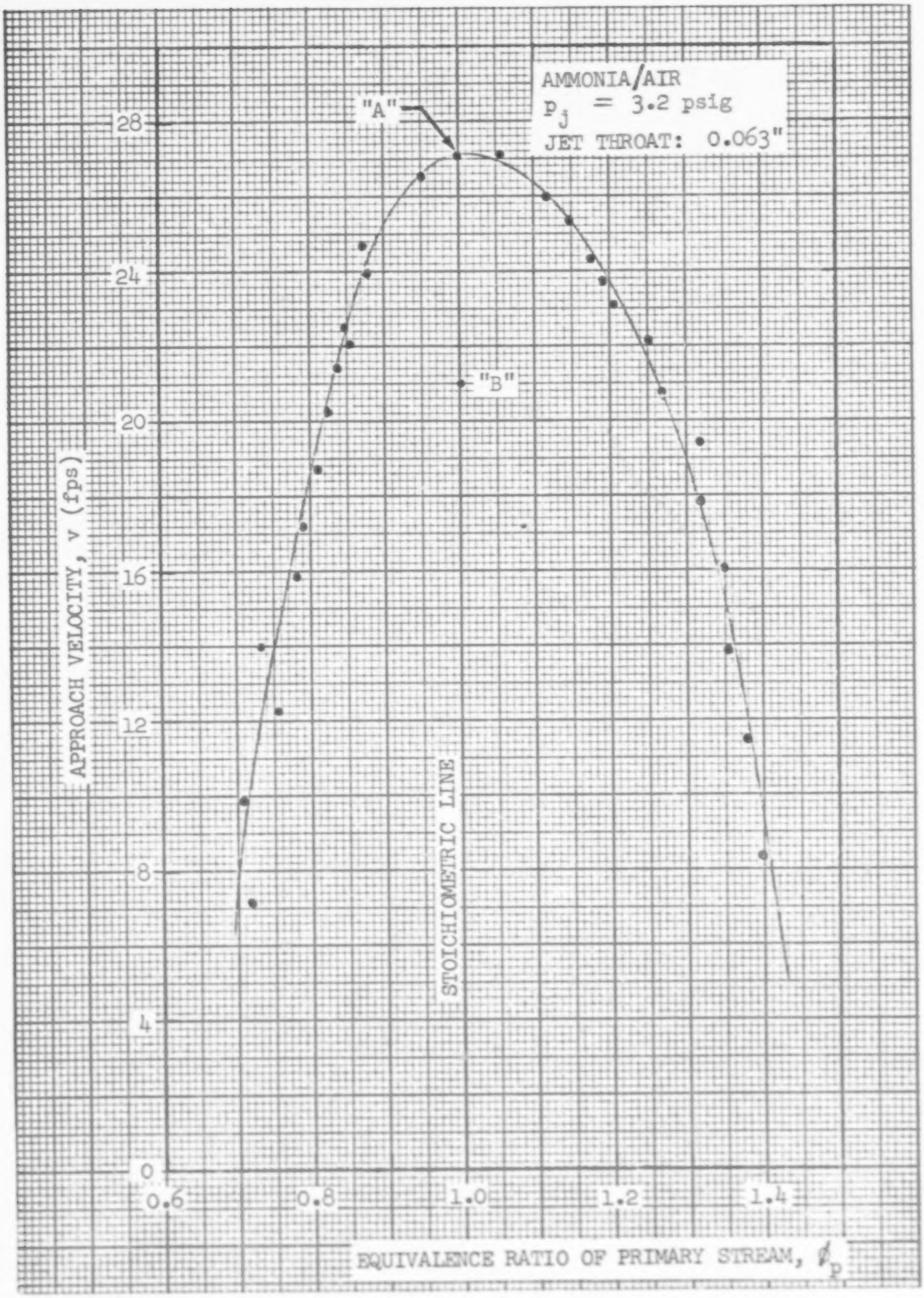

FIGURE 5.5 BLOWOUT MAP: AMMONIA/AIR OPPOSED REACTING JET

velocity. Points A and B correspond to a stoichiometric main stream composition. Hence, both the jet and the main stream are stoichiometric for A and B. Points A and B are the two points for which numerical solutions are obtained. Point A is used to refine the chemical kinetics in the numerical program to predict blowout. The refined kinetics are then used to predict composition and temperature throughout the flow field for the conditions represented by point B. Point B is chosen arbitrarily.

For the flow conditions represented by point B, composition and temperature are measured experimentally, as described in Section 5.5. The results of these measurements are compared to those numerically predicted, as described in Section 6.

5.4 Jet Exit Temperature and Velocity

For the numerical calculations, it is necessary to specify the inlet velocity and temperature of the jet stream. The velocity and temperature are required to evaluate the stream function and enthalpy of the entering jet stream.

The temperature is measured at the entrance to the jet nozzle by a thermocouple, as shown in Figure 5.1. The temperature and velocity of the jet stream at the nozzle exit are calculated assuming isentropic flow.

For the hot flow condition, the temperature is relatively invariant between the two points considered, points A and B in Figure 5.5. As a result, the calculated jet velocity is essentially identical for both conditions. The inlet temperature and velocity of the jet stream for points A and B are

condition	jet temperature (°R)	jet velocity (fps)	N_{Re} (based on jet exit I.D.)
cold flow	513	294	4×10^3
hot flow	1383	715	4×10^3

5.5 Composition and Temperature Measurements

Composition and temperature measurements are taken in the reacting flow for the flow conditions represented by point B in order to compare experimental results to those predicted by the numerical program. The axial plane in which the composition and temperature measurements are made is illustrated schematically in Figure 5.6. Measurements are taken 1-1/2 inches downstream of the jet exit (1-inch upstream of the exit plane of the Vycor). Radial traverses are made at 0.1-inch intervals. Measurements are also made as close to the jet and Vycor wall as possible, approximately .07 inches.

A water-cooled probe, 1/8-inch in diameter is used for the composition measurements. The probe is shown mounted on the traverse mechanism in Figure 5.7a; a cross-section of the probe is shown in Figure 5.7b. With a vacuum (2.5 torr) on the sample line, the sample is drawn into the probe through the small converging-diverging nozzle shown. This has the effect of rapidly quenching the reaction by aerodynamic cooling. The sample is maintained cool and the probe itself protected by circulation of cooling water through the concentric inner tubes. The 2.5 torr pressure in the probe is sufficiently low to prevent condensation of water.

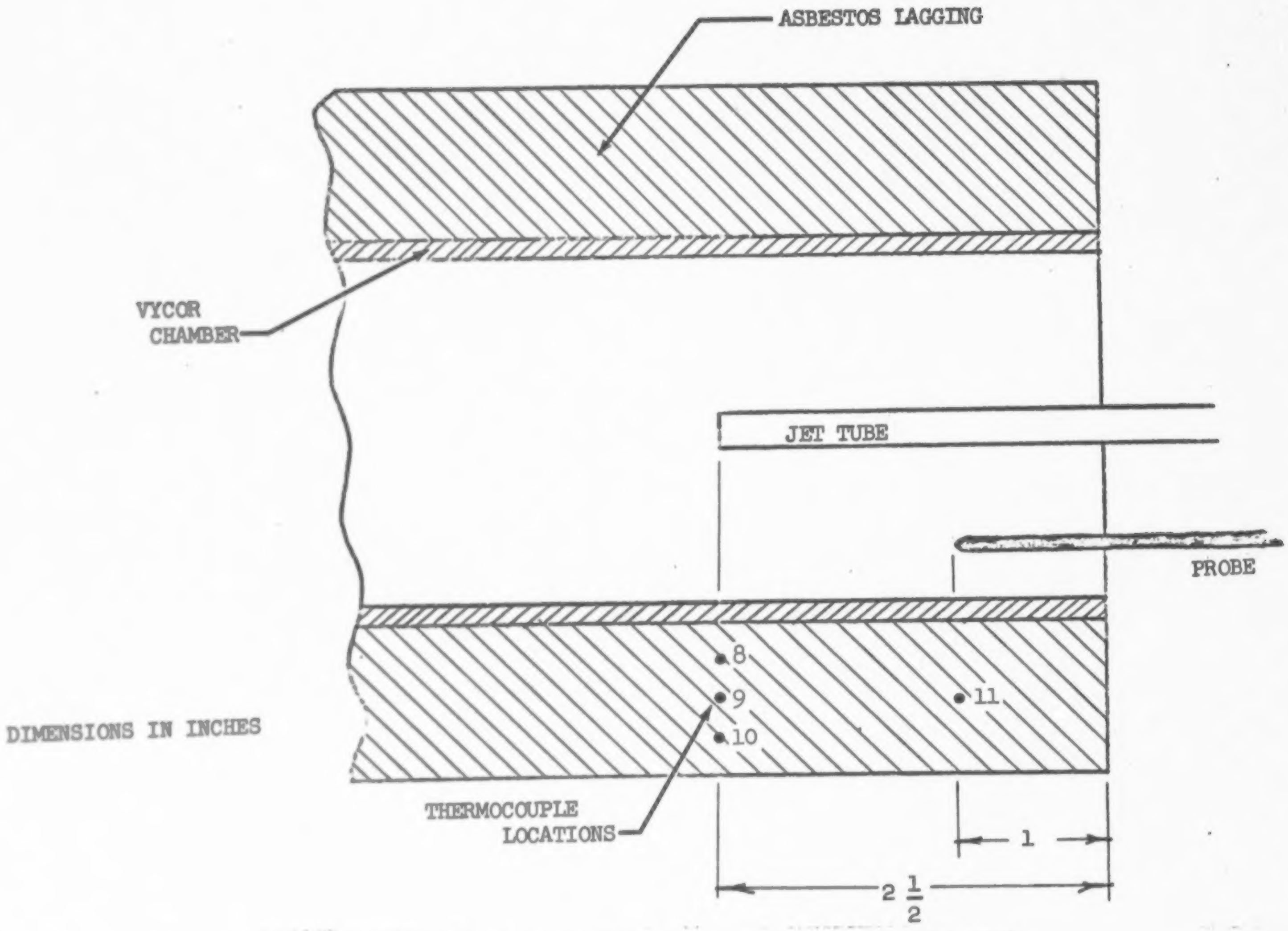
ASBESTOS LAGGING
VYCOR CHAMBER
JET TUBE
PROBE
8
9
10
11
THERMOCOUPLE LOCATIONS
1
2 1/2

DIMENSIONS IN INCHES

FIGURE 5.6 LOCATION OF COMPOSITION AND TEMPERATURE MEASUREMENTS

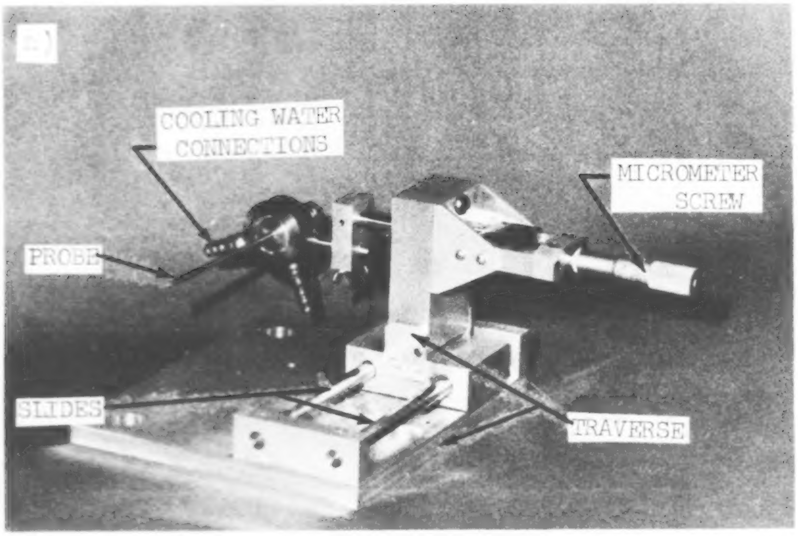
a)
COOLING WATER CONNECTIONS
MICROMETER SCREW
PROBE
SLIDES
TRAVERSE

FIGURE 5.7 COMPOSITION PROBE
a) MOUNTED IN TRAVERSE
b) CROSS-SECTION
c) POSITIONED DURING MEASUREMENT

Reproduced from best available copy.

b)

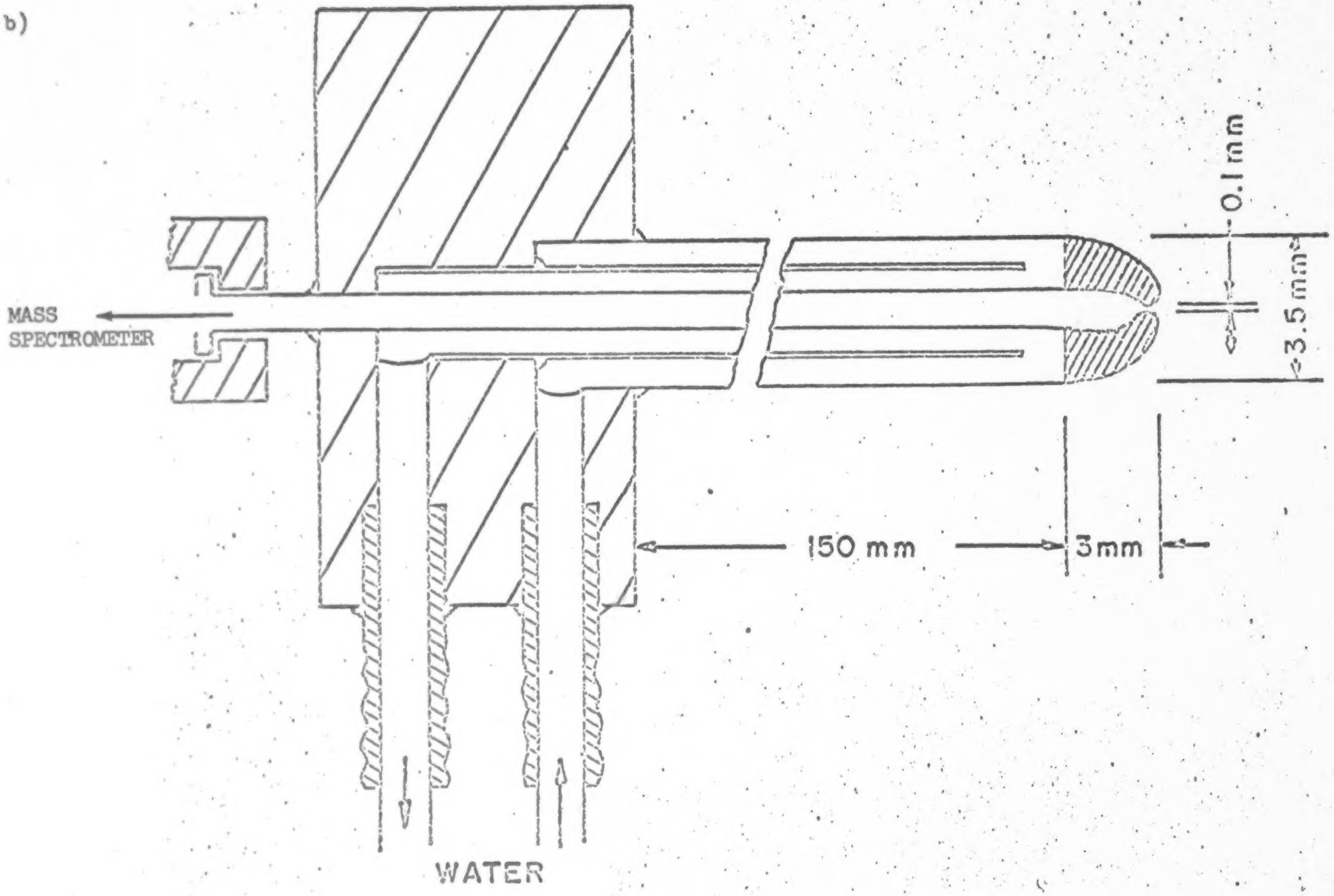
MASS SPECTROMETER
0.1 mm
3.5 mm
150 mm
3mm
WATER

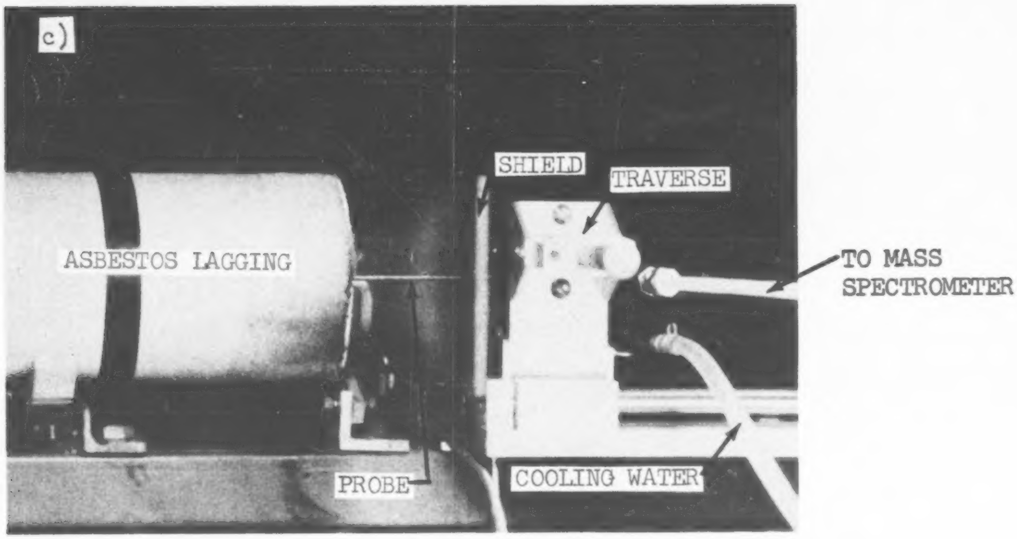
c)
SHIELD
TRAVERSE
ASBESTOS LAGGING
TO MASS SPECTROMETER
PROBE
COOLING WATER

The probe enters the Vycor chamber from the downstream end, protruding to a plane 1-1/2 inches downstream of the jet exit. The movement of the probe is controlled by a specially designed traverse which has two degrees of freedom. The two stainless steel slides, shown in Figure 5.7a, enable the probe to be located at the desired axial location, or removed from the reaction zone at will. Once located, the probe is moved radially to obtain composition profiles. The radial traverse is controlled by a micrometer screw.

The composition probe is shown during experimental measurements in Figure 5.7c. To protect the base of the probe, it is necessary to shield the base with a 1/8-inch-thick steel plate. The probe protrudes through an oblong slot in the shield. The slot is sized to allow the probe to traverse the flow field radially without obstruction.

The composition samples, drawn from the probe, are analyzed using a time-of-flight mass spectrometer (Bendix Model 17-210). The experimental facility including the mass spectrometer is shown in Figure A.1. The data from the mass spectrometer are reduced by a computer program developed by McLean and Sawyer (1967). The radial profile of the fuel mole fraction is given in Figure 5.8.

The temperature is measured with a Pt/Pt-13 percent Rh thermocouple mounted on a 1/8-inch diameter ceramic probe, shown in Figure 5.9a. The thermocouple probe is held by the same traverse used for the composition measurements. Identical to the positioning of the composition probe, the thermocouple probe extends 1-inch into the Vycor chamber to an axial location 1-1/2 inches downstream of the jet exit.

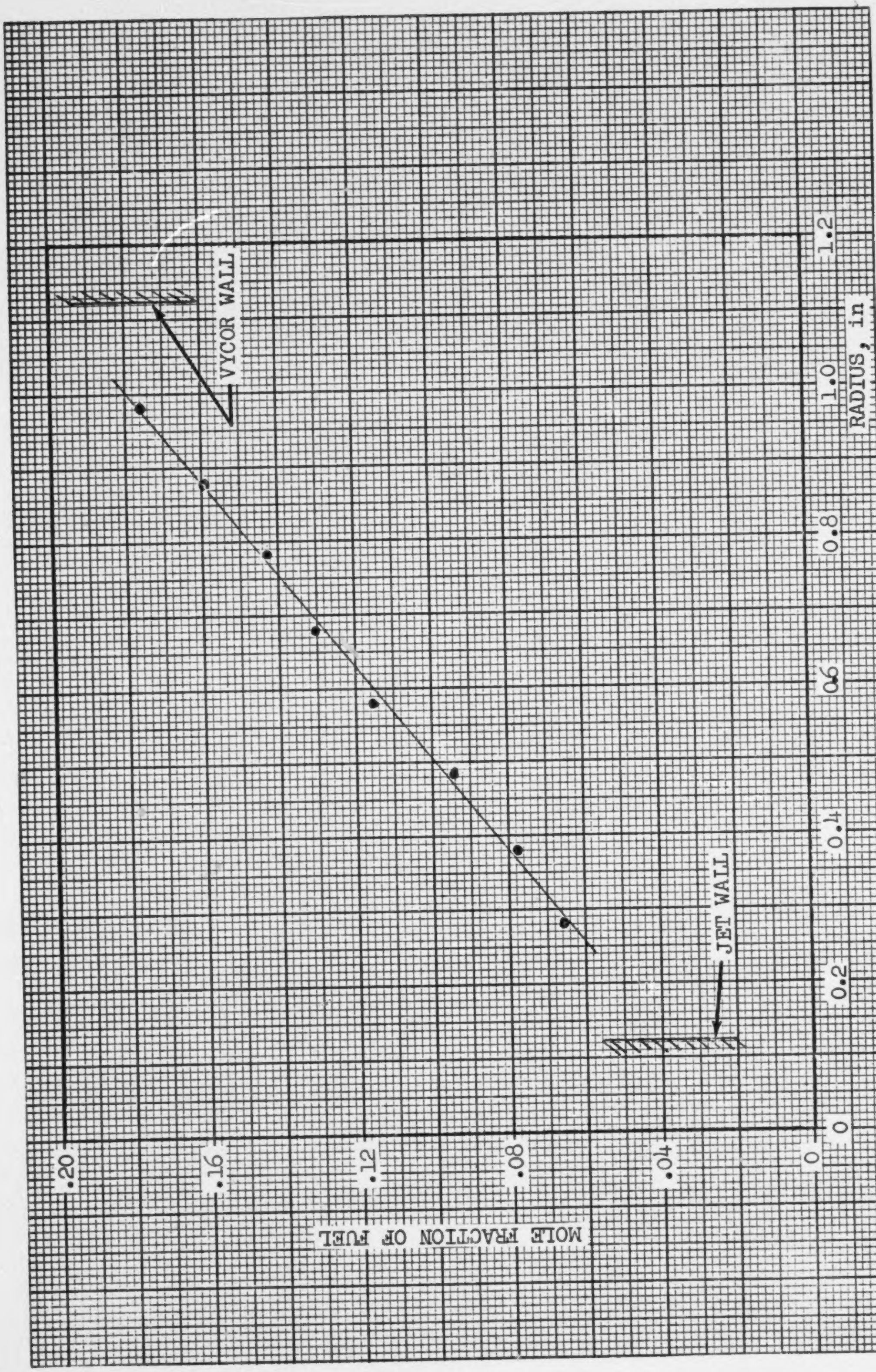

FIGURE 5.8 COMPOSITION PROFILE, EXPERIMENTALLY MEASURED

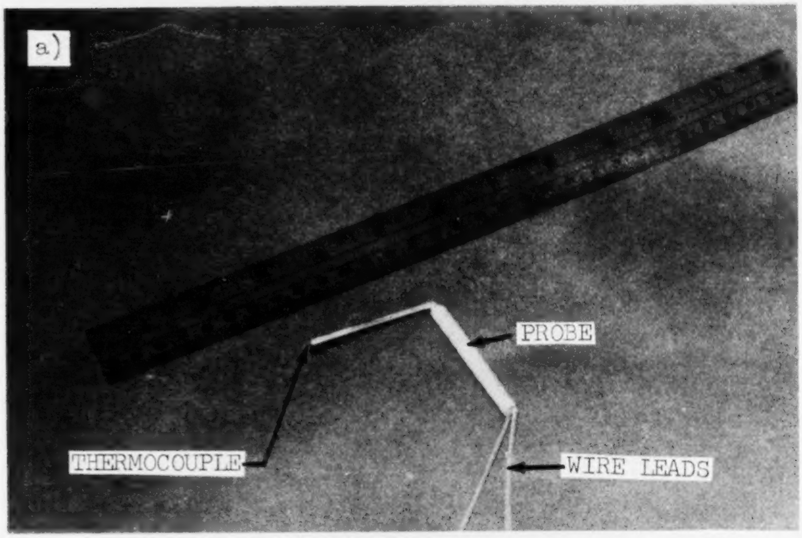
a)
PROBE
THERMOCOUPLE
WIRE LEADS

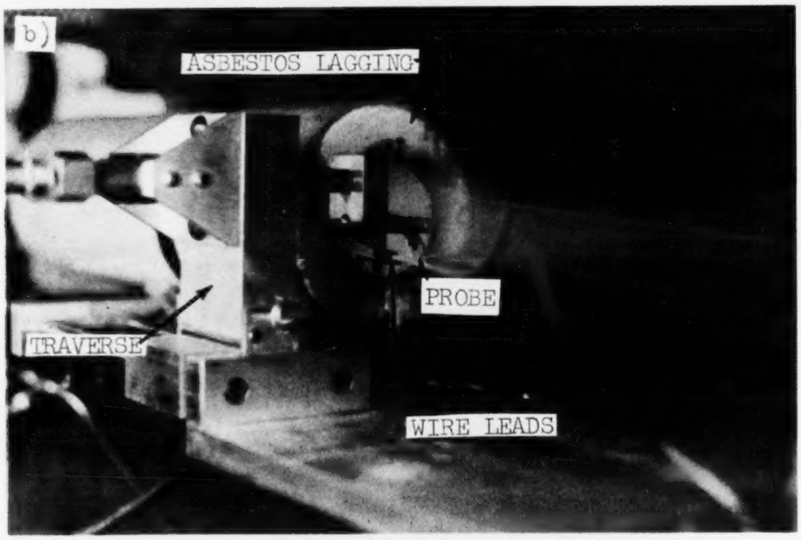
b)
ASBESTOS LAGGING
PROBE
TRAVERSE
WIRE LEADS

FIGURE 5.9 THERMOCOUPLE PROBE
a) PROBE
b) POSITIONED DURING MEASUREMENT

The probe is shown in Figure 5.9b positioned during a hot flow measurement. Readings are taken on a Leeds-Northrup (Model 8662) potentiometer and referenced to a cold junction ice-water bath. Errors associated with the thermocouple readings are discussed in Appendix B.

The measured temperature profile is plotted in Figure 5.10. Shown also is the fuel mole fraction profile from Figure 5.8. The profiles of these two variables are compared to the numerical predictions in Section 6.

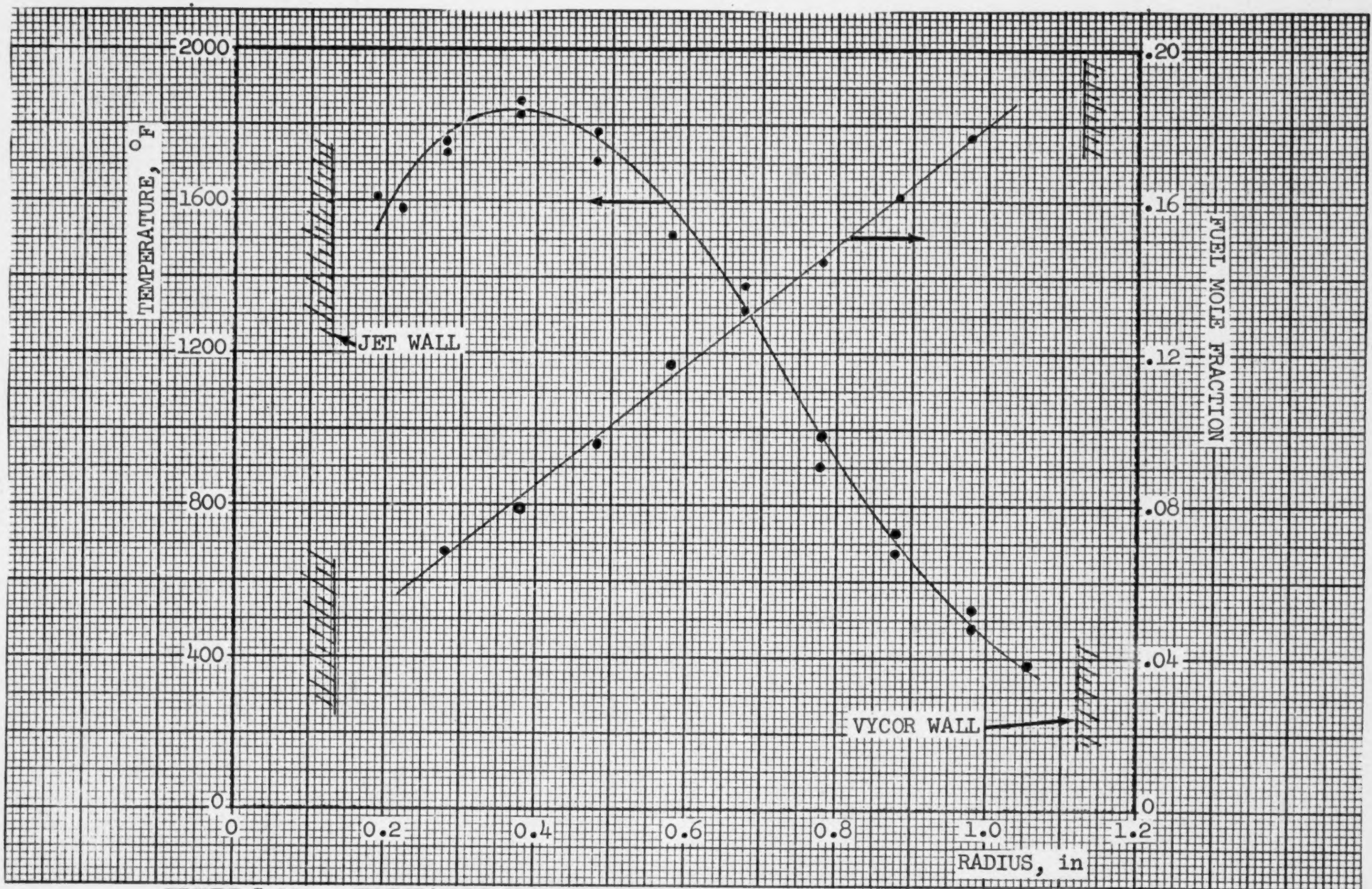

FIGURE 5.10 TEMPERATURE PROFILE, EXPERIMENTALLY MEASURED

SECTION 6

Analytical and Experimental Results Compared

The results of the analytical and experimental investigations are presented separately in Sections 4 and 5. The numerically predicted profiles of composition and temperature are presented in Figure 4.7 and the experimentally measured profiles are given in Figure 5.10. In this section, the analytical and experimental results are combined and compared.

The constants A and E in the chemical rate expression (Equation 4.24) are evaluated by making use of the experimental results at points A and B in Figure 4.1. In the first step, the pre-exponential factor, A, is varied to determine that value for which blowout is predicted at the conditions represented by point A (Case 1). This procedure gives a value for A of 36×10^{10}. The value of A is more than an order of magnitude higher than the value of A from the stirred reactor study of Pratt and Starkman (1969; Equation 4.24).

The experimentally measured profile of temperature is compared to the temperature profile predicted numerically in Figure 6.1 for the inlet conditions of point B and the value of 36×10^{10} for A in the chemical rate expression.

The next step is to refine the value of E, the activation energy. E is modified to predict temperature and composition profiles with reasonable agreement to the experimentally measured profiles. As the activation energy is reduced, the pre-exponential factor A must be also reduced. The reduction in A is necessary to satisfy the blowout condition at point A. The procedure of systematically reducing A and E

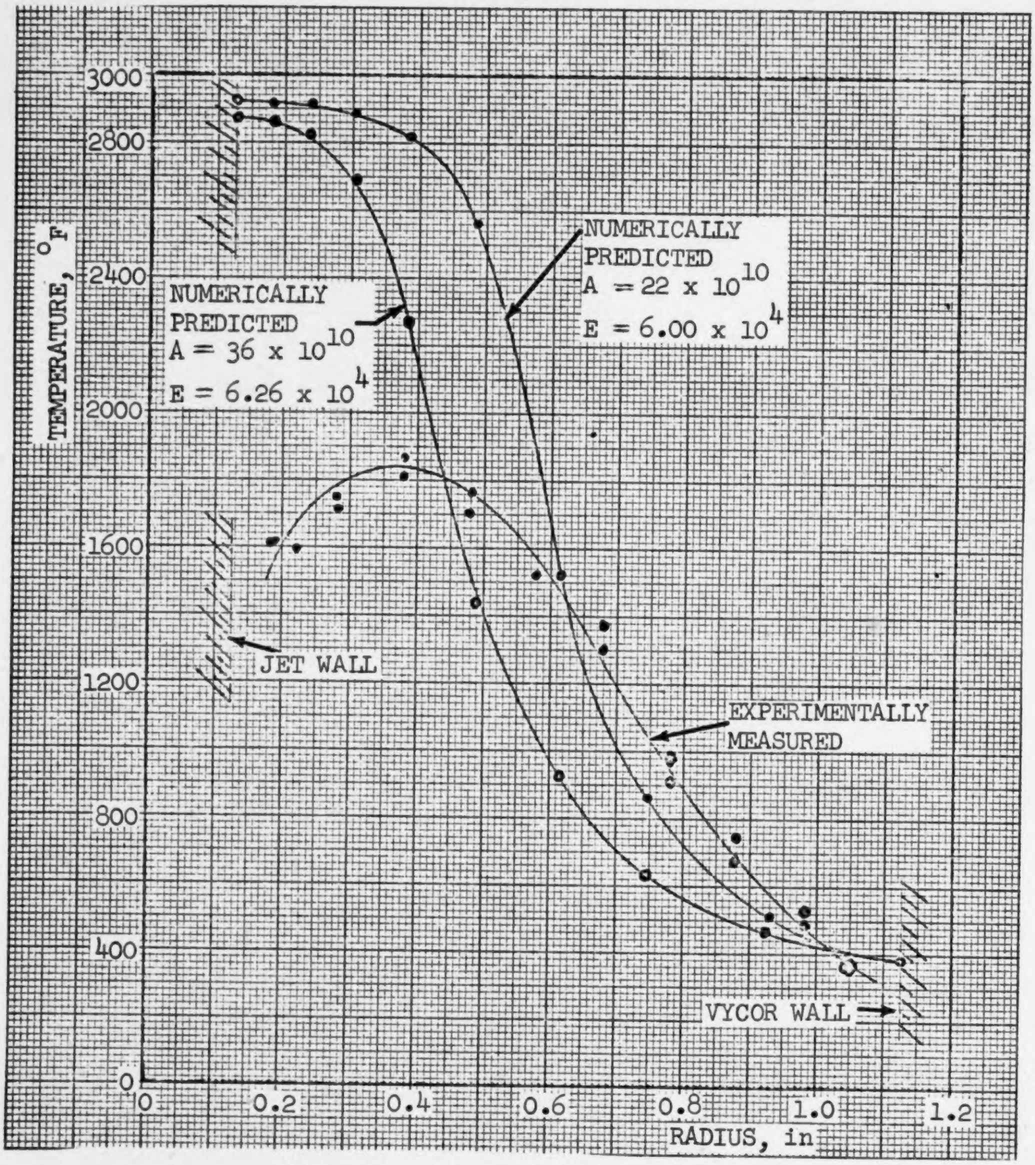

FIGURE 6.1 TEMPERATURE PROFILES, ADIABATIC JET WALL

is facilitated by adopting the guideline of maintaining a constant value for the product of the pre-exponential factor A and the exponential $e^{-E/RT}$ at the adiabatic flame temperature of 3460°R,

$$A\ e^{-E/R(3460)} = 36 \times 10^{10}\ e^{-6.26\times10^{4}/R(3460)}$$

The refinement of A and E is limited to obtaining reasonable agreement with the experiment because of 1) the excessive computer time involved and 2) the assumptions do not justify obtaining absolute agreement.

The numerically predicted profile of temperature is plotted in Figure 6.1 for the following values of A and E,

$$A = 22 \times 10^{10}$$

$$E = 6.00 \times 10^{4} \text{ Btu/lbm-mole}$$

$$R = 22 \times 10^{10}\ m_{fu}^{0.75}\ m_{ox}^{1.20}\ \rho^{1.95}\ e^{-6.00\times10^{4}/RT} \tag{6.1}$$

The chemical reaction rate given by Equation 6.1 is used to predict the distributions of stream function, fuel mole fraction, and temperature presented in Section 4.2.5 for the case of hot flow at point B. The numerically predicted and experimentally measured profiles of fuel mole fraction and temperature are compared in Figure 6.2. The agreement is satisfactory from the Vycor wall to a radius of 0.6-inch. The lower temperature and higher fuel mole fraction predicted numerically near the Vycor is attributed to the assumption of a constant and uniform specific heat. For temperatures below the adiabatic flame temperature, the value taken for the specific heat is higher than the actual specific heat of the mixture (ref: Section 4.2.3). The wide spacing of the grid near the Vycor wall is also a contributing factor. The boundary condition for the fuel mole fraction at the wall assumes that the gradient is

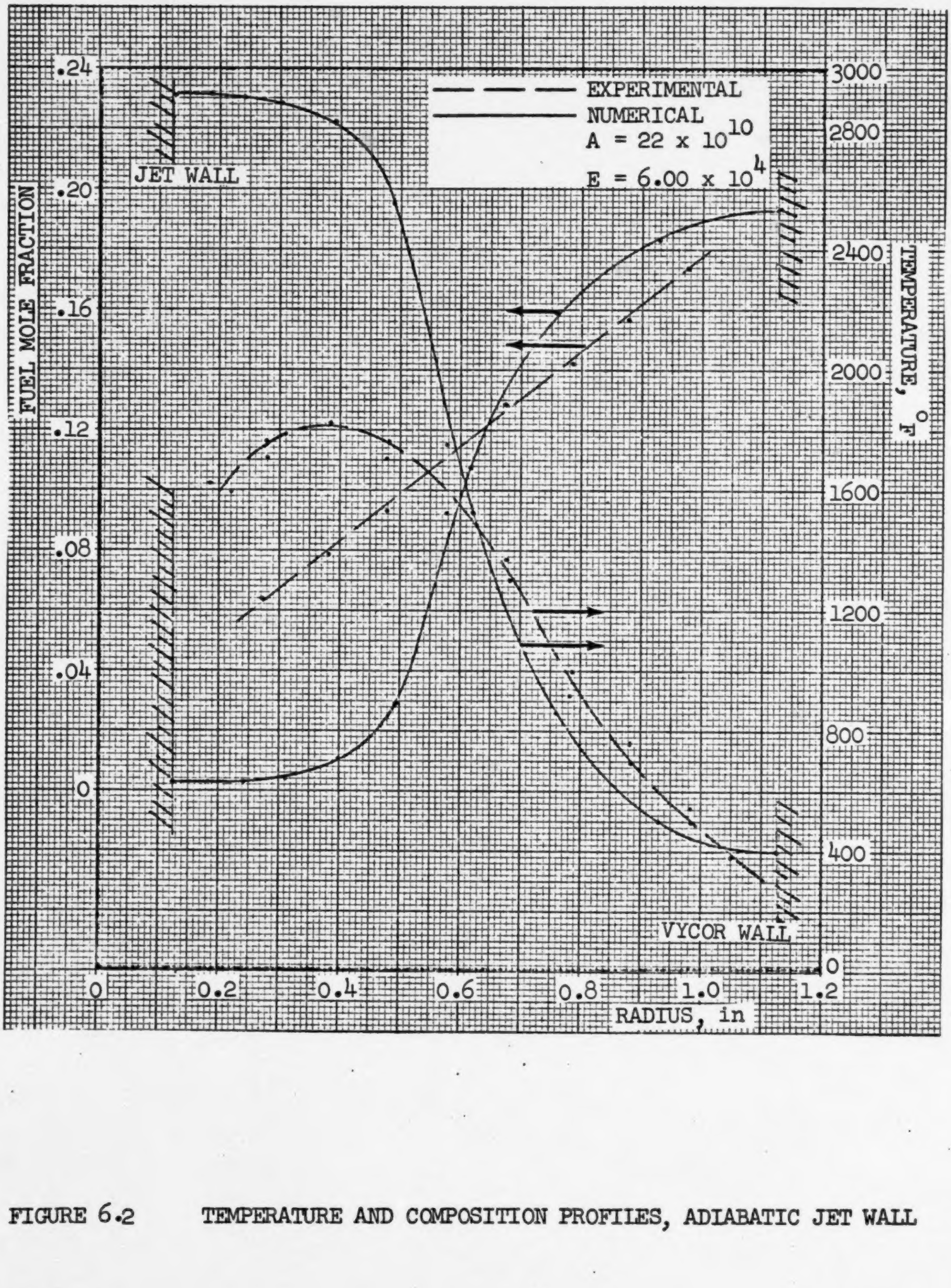

FIGURE 6.2 TEMPERATURE AND COMPOSITION PROFILES, ADIABATIC JET WALL

normal to the wall and the distribution is parabolic near the wall. This boundary condition in conjunction with the few grid points near the wall serves to exaggerate the curvature of the profile adjacent to the wall.

The effect of the jet cooling is indicated by the experimental measurements of temperature near the jet. The numerical calculations assume an adiabatic jet wall. The experimental measurements show that this assumption is not accurate. The results of the numerical program and experiment indicate that the heat-sink effect of the jet occurs at a critical point in the temperature history of the mixture. For an actual mixture temperature slightly greater than that limited by the jet cooling (1800°F), the results imply that the reaction would increase sharply due to the exponential dependence of the reaction on temperature.

To assess the effect on the numerical solution of assuming an adiabatic jet wall, a calculation is made with an isothermal jet wall. The choice of temperature for the jet wall is based on the experimental profile of temperature. An extrapolation of the temperature profile (Figure 6.1) to the jet wall gives a value of about 1000°F.

The profiles of temperature and composition for an isothermal jet wall at 1000°F are given in Figure 6.3.* The results show the strong influence of heat transfer on the predicted flow field near the jet when compared to the profiles of Figure 6.2 and the importance of accurately prescribing the boundary conditions. The predicted temperature

---

*The distributions of temperature and fuel mole fraction upstream of the jet presented in Figure 4.6 are unaffected when the jet wall is made diabatic. Only the distributions near the jet wall are affected by the modified jet boundary condition.

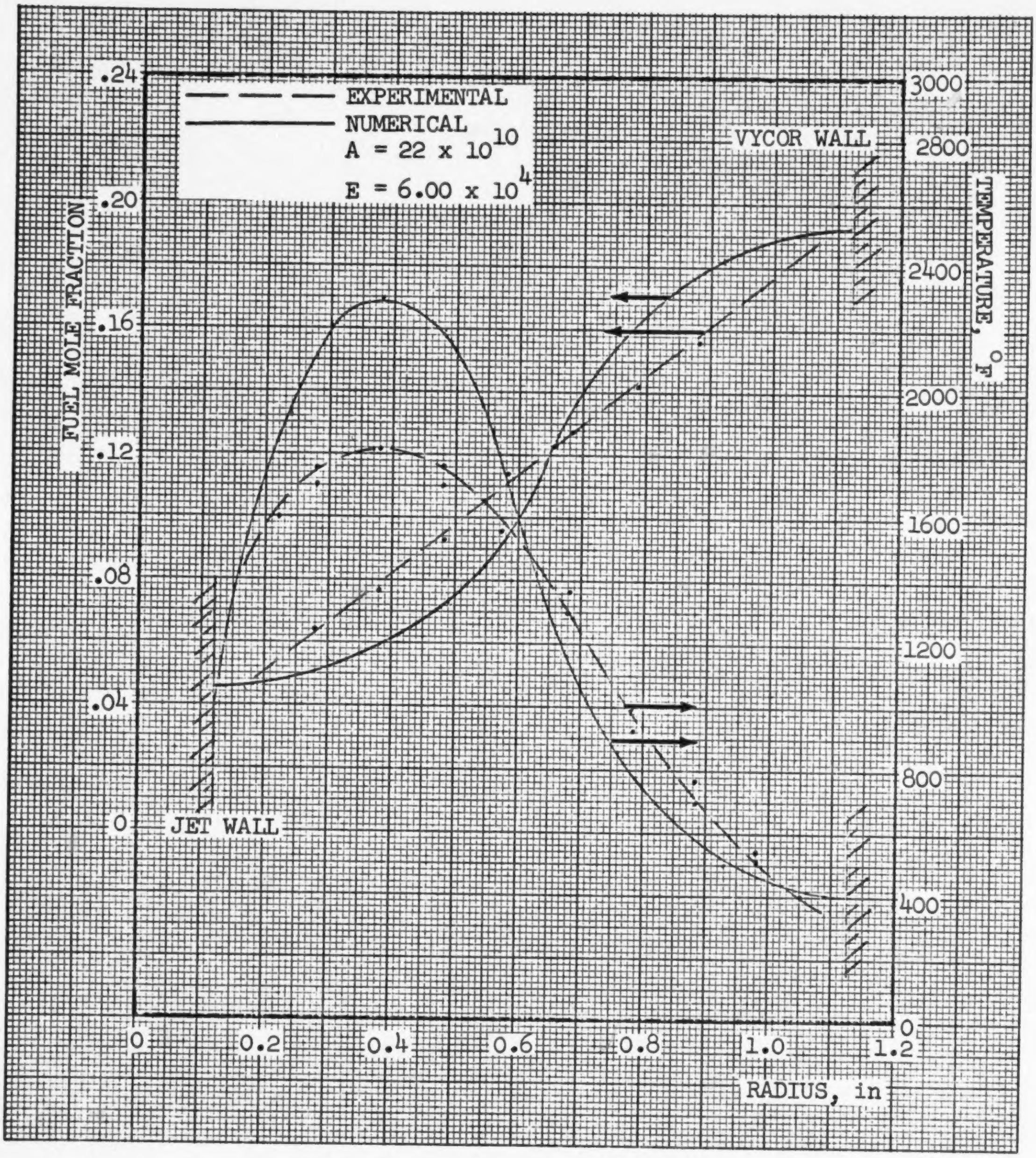

FIGURE 6.3 TEMPERATURE AND COMPOSITION PROFILES, DIABATIC JET WALL

drops near the jet wall, consistent with the experimental profile. The predicted fuel mole fraction near the jet wall shows that the degree of reaction is less than that indicated in Figure 6.2 for an adiabatic jet wall. This result is consistent with the experimental observation.

The difference between the predicted and experimentally measured temperature near the wall is attributed in part to the radiation heat loss from the thermocouple. The temperature loss due to radiation is on the order of a few hundred degrees at the measured temperature of 1800°F (ref: Appendix B). The difference between the predicted and experimentally measured fuel mole fraction is attributed to the simplified models of turbulence and chemical kinetics.

The assumption of an isothermal jet wall also contributes to the difference between the experimental and numerical results. The temperature most likely varies along the jet wall, though probably not appreciably.

It should be emphasized that the present study is exploratory in nature. Very little correlation has been previously attempted between numerical predictions and experimental measurements in turbulent, reacting flows with recirculation. The agreement between the numerical program and experimental work reported here is remarkedly good considering the simple models used and the adoption of a constant and uniform specific heat. The results of this work demonstrate the potential of numerical calculation to predict the point-by-point properties of a reacting, turbulent flow and suggest that more extensive correlation to experiment should be conducted to develop and refine the numerical models used.

SECTION 7

Conclusions

1. The governing equations for a reacting turbulent flow with recirculation can be solved with results consistent with experimental measurements.

2. Before the full utility of the solution procedure can be realized, more refined models of kinetics and turbulence must be developed and more extensive correlation to controlled experiment must be conducted.

3. The opposed-reacting-jet is attractive as a research tool for the study of reacting mixing flows. For example, the opposed-reacting-jet is valuable for,

a) the evaluation of turbulent and kinetic models,

b) the investigation of interactions between chemical kinetics, mass diffusion, and heat transfer, and

c) the study of air-pollution emissions in continuous combustion systems.

4. Analytical results indicate a zone of near-homogeneous mixture and uniform temperature located downstream of the stagnation region of the opposed-reacting-jet.

5. Boundary conditions must be controlled and monitored experimentally to provide accurate inputs to the numerical model.

REFERENCES

1. Agoston, G. A., Eustis, R. H., Noon, A. W., and Witherly, T. D. (1958). "Investigation of Jet Flameholders, Part III," WADC TN 56-316.
2. Agoston, G. A., Noon, A. W., and Witherly, T. D. (1958). "Experimental Study of a Reverse Jet Flameholder," Combustion and Flame, Vol. 2, No. 4, pp. 333-347.
3. ASME (1961). "Flowmeter Computation Handbook," American Society of Mechanical Engineers, New York.
4. Bellamy, L. (1966). "A Critical Zone Analysis of Reverse Jet Flame Stabilization," Ph.D. Dissertation, Tulane University, New Orleans, Louisiana.
5. Bellamy, L., Barron, C. H. and O'Loughlin, J. R. (1968). "The Influence of Chemical Inhibitor Addition on Reverse-Jet Flame Stabilization," ASME Paper No. 68-GT-39.
6. Bellamy, L., Barron, C. H., and O'Loughlin, J. R. (1968). "A Critical Zone Analysis of Reverse Jet Flame Stabilization," Combustion and Flame, Vol. 12, pp. 107-114.
7. Bertin, J., and Salmon, B. (1958). "Aerodynamic Combustion Ups Afterburner Performance," Aviation Age, Vol. 29, pp. 46-57.
8. Bird, R. B., Stewart, W. E., and Lightfoot, E. N. (1960). "Transport Phenomena," John Wiley and Sons, Inc., New York.
9. Bohrer, L. C. (1957). "Some Performance Characteristics and Data Correlation for the Opposed Jet Flameholder," M.S. Thesis, Northwestern University, Evanston, Illinois.
10. Boussinesq, T. V. (1877). Mém. prés. Acad. Sci., 3rd ed., Paris, XXIII, p. 46.

11. Bradshaw, W. G., and Mathews, C. O. (1958). "Properties of Refractory Materials: Collected Data and References," LMSD-2466.

12. Butze, H. F., and Metzler, A. J. (1959). "Exploratory Investigation of Aerodynamic Flameholders for Afterburner Application," NASA MEMO 4-9-59E.

13. Cambel, A. B. (1958). "A Review of Flame Stabilization by Means of Gaseous Jets," Combustion and Propulsion, Third AGARD Colloquium, Pergamon Press, London, pp. 541-554.

14. Choudhury, P. R., and Cambel, A. B. (1960). "Use of Inert Gases in Flame Stabilization," ARS Journal, Vol. 30, No. 1, p. 131.

15. Cohen, L. (1955). "Burning Velocities of Ammonia in Air and in Oxygen," Fuel, Vol. 34 (Supplement), p. 5123-5127.

16. Cunningham, R. G. (1951). "Orifice Meters with Supercritical Compressible Flow," Trans. Am. Soc. Mech. Engr., Vol. 73, pp. 625-638.

17. Douglas, G. W. (1966). "An Investigation of the Relation Between Flame Shape and Chamber Combustion Efficiency for a Flame Stabilized by an Opposed-Jet Flameholder," Ph.D. Dissertation, Tulane University, New Orleans, Louisiana.

18. Douglas, G. W., and O'Loughlin, J. R. (1968). "Studies of Combustion Efficiency and Flame Shape for Opposed-Jet Flameholders," AIAA Journal, Vol. 6, No. 4, pp. 672-678.

19. Duclos, D. P., Schaffer, A. B., and Cambel, A. B. (1957). "Flame-Stabilizing Effects of Inclined Air Jets," Industrial and Engineering Chemistry, Vol. 49, No. 12, pp. 2063-2066.

20. Dugger, G. L. and Heimel, S. (1952). "Flame Speeds of Methane-Air, Propane-Air, and Ethylene-Air Mixtures at Low Initial Temperatures," NACA-TN-2624, p. 13.

21. Eustis, R. H., and Mraz, C. L. (1956). "Investigation of Jet Flameholders," WADC TN 56-316.

22. Fluker, B. J. (1968). "An Investigation of the Effects of Unsteady Flow on Flame Stabilization by a Reverse Jet Flame Holder," Ph.D. Dissertation, Tulane University, New Orleans, Louisiana.

23. Fristrom, R. M., and Westenberg, A. A. (1965). "Flame Structure," McGraw-Hill, New York.

24. Fuhs, A. E. (1960). "Spectroscopic Studies of Reverse Jet Flame Stabilization," ARS Journal, Vol. 30, No. 3, pp. 238-243.

25. Gosman, A. D., Pun, W. M., Runchal, A. K., Spalding, D. B., and Wolfshtein, M. (1969). "Heat and Mass Transfer in Recirculating Flows," Academic Press, London.

26. Hammond, D. C. and Mellor, A. M. (1970). "An Investigation of Gas Turbine Combustors with High Inlet Air Temperatures, First Annual Report, Part 1: Analytical Developments," TM-70-2, Purdue University, Lafayette, Indiana.

27. Hill, P. G. and Peterson, C. R. (1967). "Mechanics and Thermodynamics of Propulsion," Addison-Wesley, Massachusetts, p. 219.

28. JANAF Thermochemical Data (1960). The Dow Chemical Company, Midland, Michigan.

29. Kreith, F. (1964). "Principles of Heat Transfer," International Textbook Company, Scranton, Pennsylvania, p. 26.

30. Kushida, Raymond (1968). "Theory of Laminar Flames in Stagnation Flows," Technical Report 32-1261, Jet Propulsion Laboratory, Pasadena, California.

31. Lewis, B., and Von Elbe, G. (1961). "Combustion, Flames, and Explosions of Gases," Second Ed., Academic Press, N.Y., p. 389.

32. Longwell, J. P., Frost, E. E., and Weiss, M. A. (1953). "Flame Stability in Bluff Body Recirculation Zones," Industrial and Engineering Chemistry, Vol. 45, No. 8, pp. 1629-1633.

33. McLean, W. J. and Sawyer, R. F. (1967). "Mass Spectrometer Data Reduction and Error Analysis," Univ. of Calif., College of Engineering Rept. No. TS-67-4.

34. McLean, W. J. and Sawyer, R. F. (1967). "Nitric Oxide in One-Atmosphere Ammonia Flames," unpublished.

35. Massaro, D. J. (1966). "Flame Stabilization by Convergent Annular Jets," M.S. Thesis, Northwestern University, Evanston, Illinois.

36. Massaro, D. J., and Trezek, G. J. (1967). "On Flame Stabilization by Convergent Annular Jets," Combustion and Flame, Vol. 11, No. 5, pp. 434-437.

37. Newhall, H. K. (1964). "Chemical Equilibrium Properties of Ammonia-Air Combustion Products," Univ. of Calif. Office of Research Services Technical Report No. 1, Ammonia Fuel Studies.

38. Noon, A. W. (1957). "Investigation of Jet Flameholders, Part II," WADC TN 56-316.

39. Noreen, A. E., and Martin, W. T. (1957). "Opposed Jet Flameholding," American Rocket Society, Paper 515-57.

40. Odlozinski, G. (1968). "A Procedure for Predicting the Distributions of Velocity and Temperature in a Flame Stabilized Behind a Bluff Body," Imperial College, Dept. of Mechanical Engr., EF/R/G/2.

41. O'Loughlin, J. R. (1968). "Final Report on Various Studies of Jet Flameholders," Tulane University, New Orleans, Louisiana.

42. Penner, S. S., and Williams, F. (1957). "Recent Studies on Flame Stabilization of Premixed Turbulent Gases," Applied Mechanics Reviews, Vol. 10, No. 6, pp. 229-237.

43. Pohlmann, E. (1954). "Stabilizing Effects of an Opposing Jet of Air-Propane Mixtures in High Velocity Combustion," M.S. Thesis, Northwestern University, Evanston, Illinois.

44. Pratt, D. T., and Starkman, E. S. (1969). "High-Temperature Kinetics of Ammonia-Air Combustion," Twelfth Symposium (International) on Combustion, The Combustion Institute, pp. 891-899.

45. Pun, W. M., and Spalding, D. B. (1967). "A Procedure for Predicting the Velocity and Temperature Distributions in a Confined, Steady, Turbulent, Gaseous, Diffusion Flame," Imperial College, Mechanical Engineering Department, SF/TN/11.

46. Putnam, A. A. (1957). "Comparison of Reverse Jet and Obstacle-Type Flameholders," Jet Propulsion, Vol. 27, No. 2, pp. 177-178.

47. Runchal, A. K., and Wolfshtein, M. (1966). "A Finite Difference Procedure for the Integration of the Navier-Stokes Equations," Imperial College, Mechanical Engineering Dept., SF/TN/1.

48. Sawyer, R. F. (1969). "Fundamental Processes Controlling the Air Pollution Emissions from Gas Turbine Engines," AIAA Paper 69-1040.

49. Sawyer, R. F., Teixeira, D. P., Starkman, E. S. (1969). "Air Pollution Characteristics of Gas Turbine Engines," Journal of Engineering for Power, pp. 290-296.

50. Schaffer, A. B. (1954). "Stabilizing Effects of an Opposing Jet in High-Velocity Combustion," M.S. Thesis, Northwestern University, Evanston, Illinois.

51. Schaffer, A. B., and Cambel, A. B. (1955). "The Effect of an Opposing Jet on Flame Stability," Jet Propulsion, Vol. 25, No. 6, pp. 284-287.

52. Schaffer, A. B., and Cambel, A. B. (1956). "Continued Investigations of the Opposing Jet Flameholder," Jet Propulsion, Vol. 26, No. 7, pp. 516-518.

53. Schaffer, A. B. (1957). "Phenomenological Analysis of the Opposed Jet Flameholder," Ph.D. Dissertation, Northwestern University, Evanston, Illinois.

54. Schlichting, H. (1968). "Boundary-Layer Theory," 6th Edition, McGraw-Hill Book Company, New York, p. 563.

55. Shaffer, P. T. B. (1964). "Plenum Press Handbooks of High-Temperature Materials: No. 1, Materials Index," Plenum Press, New York, p. 238.

56. Shapiro, A. H. (1954). "The Dynamics and Thermodynamics of Compressible Fluid Flow," The Ronald Press, New York, p. 1088.

57. Smith, D. S., Sawyer, R. F., and Starkman, E. S. (1968). "Oxides of Nitrogen from Gas Turbines," Journal of the Air Control Association, Vol. 18, No. 1, pp. 30-35.

58. Snyder, W. T. (1956). "Preliminary Photographic Study of the Flow Pattern of the Opposing Jet Flameholder," Progress Report to the Aircraft Gas Turbine Division, General Electric Company, Gas Dynamics Laboratory, Northwestern University.

59. Spalding, D. B. (1966). "Notes on the Solution of the Navier-Stokes Equations for Steady Two-Dimensional Turbulent Flow by Finite-Difference Techniques," Northern Research and Engineering Corporation, Cambridge, Massachusetts.

60. Spalding, D. B. (1970). "Mixing and Chemical Reaction in Steady Confined Turbulent Flames," presented at the Thirteenth Symposium (International) on Combustion, Salt Lake City, Utah, August 23-29.

61. Starkman, E. S., Newhall, H. K., Sutton, R., Maguire, T., and Farbar, L. (1966). "Ammonia as a Spark Ignition Engine Fuel: Theory and Application," SAE Paper No. 660155, Detroit, Michigan.

SYMBOLS

A	pre-exponential factor, Equation 4.24
CC	convergence criteria
c_p	specific heat, Btu/lbm-°R
D	combustor diameter, in
d	effective thermocouple diameter, in
$\mathcal{D}$	mass diffusivity
E	activation energy, Btu/lbm-mole
f	reaction order with respect to ammonia
HC	heat of combustion, Btu/lbm_{fu}
$\tilde{h}$	stagnation enthalpy, Btu/lbm
K	constant in effective viscosity expression
k	thermal conductivity, Btu/hr-ft-°F
L	length of flow field, ft
m	mass fraction
$\dot{m}$	mass flow rate, lbm/sec
$\mathcal{M}$	molecular weight
N	number of iterations
n	overall reaction order
n_i	normal distance from wall to adjacent node i
p	pressure, psig
$\bar{p}$	time-smoothed pressure, psig
p'	$p - \bar{p}$
R	radius of combustor, in
R_{fu}	reaction rate, $\text{lbm}_{fu}/\text{lbm-ft}^3\text{-sec}$
Ru	universal gas constant, 1545 ft-lbf/lbm-mole-°R
r	radius, in

S	constant in velocity profile expression
T	temperature, °F or °R
t	time, sec
v	velocity, fps
$\bar{v}_z$	time-smoothed velocity, fps
v'_z	$v_z - \bar{v}_z$
Γ	exchange coefficient
ε	emissivity
μ	viscosity
ρ	density, lbm/ft^3
σ	Stefan-Boltzmann constant, 0.1714 Btu/hr-ft^2-°R^4
σ_{fu}	Schmidt Number
σ_h	Prandtl Number
$\underline{\underline{\tau}}$	stress tensor
Φ	equivalence ratio
ϕ	dependent variable
ψ	stream function

Subscripts

a	air
eff	effective
fu	fuel
h	enthalpy
j	jet stream
mix	mixture
ox	oxidizer
p	primary stream

prod	product
r	radial direction
stoich	stoichiometric
x	x direction
y	y direction
z	z direction
ϕ	dependent variable ϕ

Superscripts

t	turbulent
ℓ	laminar

APPENDIX A

Experimental Facility

A.1 Introduction

A few details concerning the experimental facility are given in Section 5.1. Specifically, the combustion chamber and opposed-jet are discussed. The fuel and air supply systems, the metering of the fuel and air, and all other aspects essential to an experimental facility are not discussed. The purpose of this appendix is to describe the support system.

A schematic of the experimental facility is shown in Figure A.la, and a picture of the facility is given in Figure A.lb. The discussion below is divided between the subsystems that comprise the facility. A few components of the facility have features common to all the subsystems. These components are the metering valves and the thermocouples.

The four metering values (main air, main ammonia, jet air, jet ammonia) were selected with orifices sized such that the flow would be choked across the valves. This has the advantage of preventing perturbations, produced by fluctuations in the combustor, from propagating to the supply. Choking is effective in stabilizing the flow in the supply lines.

The thermocouples used are alumel/chromel. The thermocouple emf is read on a Leeds and Northrup Potentiometer (Model 8662) using an ice bath for a reference junction.

A.2 Main Air and Fuel

The main air is supplied from the house compressed air system which is maintained at a nominal pressure of 200 psig. A 2-inch line is used

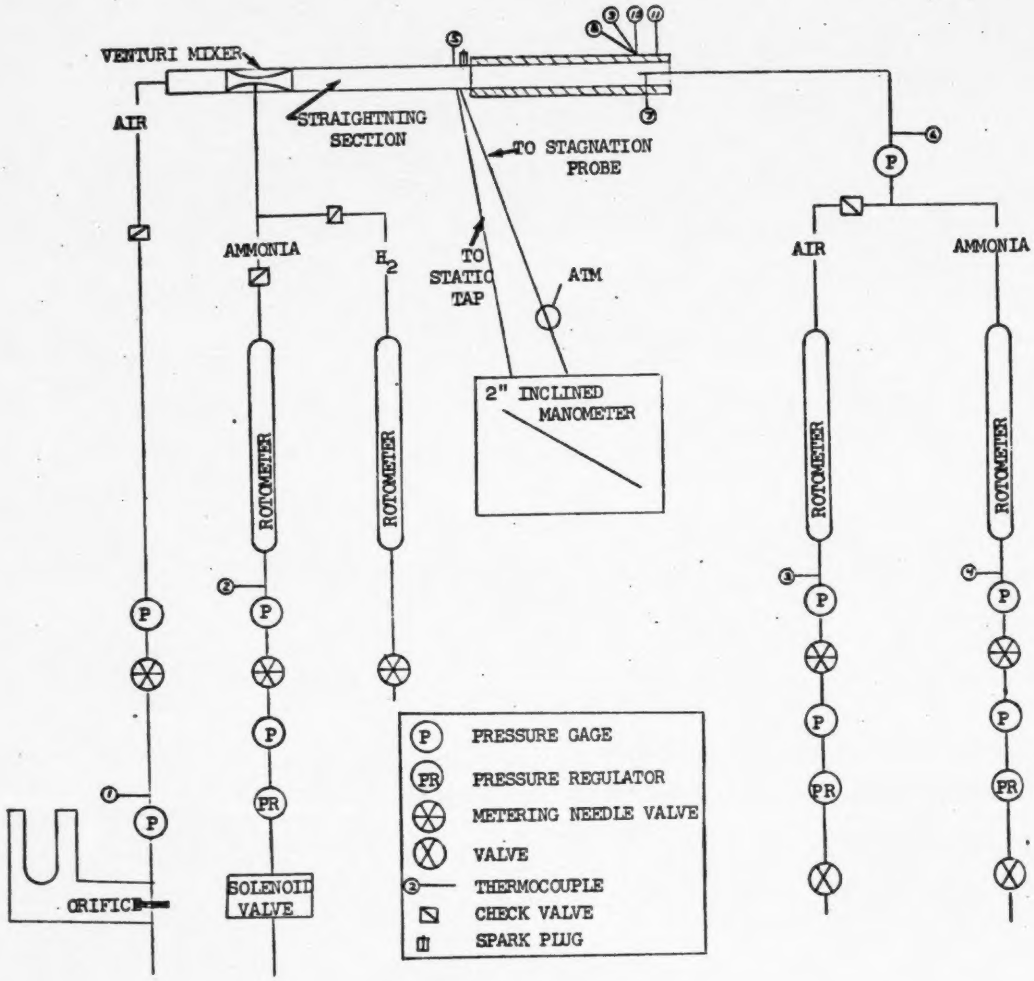
VENTURI MIXER
AIR
STRAIGHTNING SECTION
TO STAGNATION PROBE
⑤
⑧ ⑨ ⑩ ⑪
⑦
④
AMMONIA
H2
TO STATIC TAP
ATM
2" INCLINED MANOMETER
ROTOMETER
ROTOMETER
ROTOMETER
ROTOMETER
AIR
AMMONIA
②
①
③
ORIFICE
SOLENOID VALVE
P PRESSURE GAGE
PR PRESSURE REGULATOR
METERING NEEDLE VALVE
VALVE
THERMOCOUPLE
CHECK VALVE
SPARK PLUG

FIGURE A.1 EXPERIMENTAL FACILITY
a) SCHEMATIC
b) PHOTOGRAPH

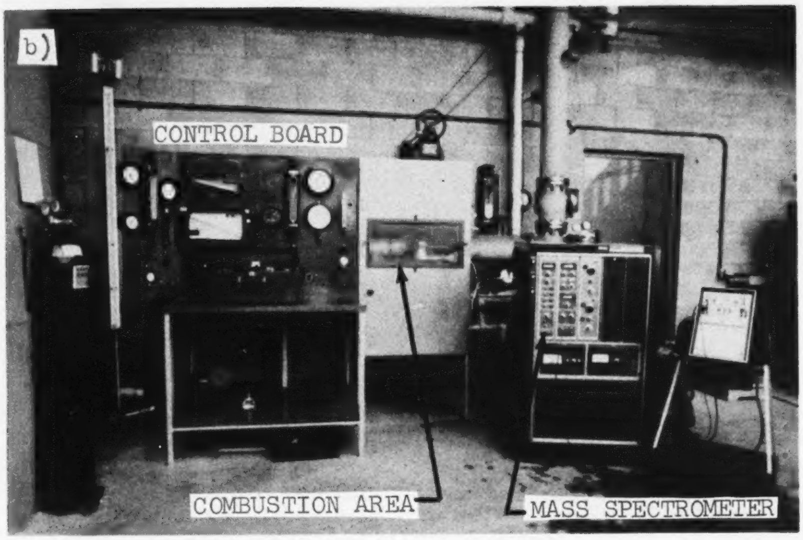
b)
CONTROL BOARD
COMBUSTION AREA
MASS SPECTROMETER

to supply the experimental facility. The pressure is reduced to 50 psig prior to metering. The main air is metered with a standard ASME orifice (with flange pressure taps) in accordance with ASME Codes (ASME-1961; Cunningham-1951). The diameter of the orifice is 0.600-inch. The pressure ratio across the orifice is read in inches-of-water on a manometer with a total range of 50-inches. The upstream static pressure is measured by a Bourdon gage, and the temperature of the flow is measured by a thermocouple.

Control of the main air flow is maintained by a 1/2-inch needle metering valve. The 2-inch line is reduced to a 1/2-inch line downstream of the orifice-metering section to accomodate the valve.

The ammonia supply consists of two pressure tanks, cross coupled, immersed in a water bath equipped with stream coils. The purpose of the bath is to provide sufficient heat to vaporize the liquid ammonia. The ambient environment is not sufficient to meet the flow requirements. The gaseous ammonia, drawn from the top of the tanks, passes through 30-feet of 3/8-inch O.D. stainless steel tubing prior to metering. The tube allows the gas to regain the temperature loss during expansion across the regulator just downstream of the tank, and insures that the ammonia will be super-heated at the rotometer. There is a fast-response solenoid shut-off valve in the ammonia supply line for positive and rapid shut-off of the main fuel.

The main fuel is metered in a Fisher-Porter Stable-Vis Rotometer (tube B-4N25-A, float BSX-41-A-SS). Pressure and temperature of the stream is measured at the rotometer to enable calculation of the mass flow rate. The rotometer had been calibrated against a critical flow orifice and two different size subcritical orifices. A hydrogen line is coupled to the main fuel line as noted in Figure A.1a. Ammonia/air mixtures are not readily ignited, and the hydrogen is used to prime the stream. Consistent with previous experience (Starkman, et al-1966), 5-percent by weight of hydrogen is sufficient to facilitate ignition of the main stream.

The ammonia fuel (and hydrogen during priming) is mixed with the main air in a venturi section. The main air enters the Venturi section at an entrance diameter of 2-inches. The fuel is injected radially into the air stream at a 0.9-inch-diameter throat through four nozzles evenly spaced about the circumference. The nozzles are interchangeable and have an orifice size of 1/16-inch. The mixture of fuel and air then diverges to the 2-1/4 inch inner diameter of the straightening section. The length of the straightening section is 3-feet. At the end of the section, the 14-inch long Vycor combustion chamber is attached. Just prior to entrance of the Vycor combustion chamber, the pressure and temperature of the main stream are measured through taps in the straightening section.

The spark plug (Champion H-14Y), used to ignite the flow, is located diametrically opposite the pressure and temperature taps at the end of the straightening section. The spark is energized by a 120/120,000 volt ac transformer.

Jet Fuel and Air

The jet ammonia is tapped off the main ammonia line just downstream of the fast response solenoid shut-off valve. The jet fuel is metered in a Matheson ball rotometer (tube 605), which had been calibrated with a wet test meter.

The jet air is tapped off the main air line well upstream of the orifice meter. The jet air is metered in a Fisher-Porter "Stable-Vis" rotometer (tube B3A-25, float BSX-33-SS) which had also been calibrated with a wet test meter.

The jet fuel and air are mixed in a 1/4-inch Swedgelok Tee, about 4-feet upstream of the jet exit. The temperature and pressure of the combined jet stream are measured downstream of the mixing-tee. The temperature of the jet flow is also measured in the opposed jet as described in Section 5.4.

APPENDIX B

Thermocouple Corrections

B.1 Introduction

Temperature profiles were measured in the reaction zone using a Pt-Pt/13 percent Rh thermocouple as described in Section 5.5. Thermocouple measurements of high temperature reactive gases are subject to several potential sources of error. The more important sources are radiation heat loss from the probe to the wall, heat conduction loss along the thermocouple lead wires, and catalytic promotion of reaction on the thermocouple surface.

B.2 Radiation Heat Loss from Probe to Wall

The radiation loss is the most important source of error. As shown in Appendix C, the walls of the Vycor tube are about 300°F. The radiation loss will be greatest for the highest temperature recorded by the thermocouple probe, about 1800°F (see Figure 5.10).

The effect of radiation loss on the measured gas temperature is estimated by equating the heat transferred to the probe from the gas to that lost by radiation. Following Fristrom and Westenberg (1965), the difference between the gas temperature and the thermocouple temperature is

$$\Delta T = \frac{\sigma\ \varepsilon\ d(T_{probe}^4 - T_{wall}^4)}{2\ k} \tag{B.1}$$

σ = Stefan-Boltzman constant = 0.1714×10^{-8} Btu/hr-ft^2-°R^4

ε = emissivity of the probe

d = diameter of radiating surface

k = thermal conductivity of the gas

It remains to specify the emissivity, the thermal conductivity, and the effective thermocouple diameter.

The emissivity may attain a maximum value of unity. Because this presents the worse condition so far as radiation loss is concerned, $\epsilon = 1$ is used here.

The thermal conductivities for the gases present (N_2, O_2, NH_3, etc.), are all about 0.04 Btu/hr-ft-°F at 1500°F.

The diameter, d, in Equation B.1 is the diameter of a spherical radiation source. For a spot-welded thermocouple, it is reasonable to approximate the effective diameter as the sum of the diameter of the separate wires. For the 3-mil wire used here, the diameter is 0.006-inch.

Incorporating these values into Equation B.1, the maximum temperature difference is

$$\Delta T_{max} = 280°F$$

In terms of percent of the maximum temperature,

$$\% \Delta T_{max} = \frac{280}{1800} \times 100 = 15.4\%$$

B.3 Heat-Conduction Loss

The length of the probe is 3-inches. Because the probe is bathed with the hot combustion gases along a near-isothermal path, the losses due to heat conduction are small and are considered to be negligible for the purpose of this investigation.

B.4 Catalytic Reaction on Thermocouple Surface

Platinum is a strong catalyst, particularly in the oxidation of ammonia. To eliminate this source of error the thermocouple was coated with a thin layer of silica.

APPENDIX C

Heat Loss

Asbestos lagging is placed over the Vycor combustion chamber to minimize the heat loss through the wall and simulate adiabatic wall boundary conditions (ref: Section 5.1). Adiabatic wall conditions are convenient to describe in the numerical calculations. The assumption of an adiabatic wall is used to specify the boundary conditions for the enthalpy, as outlined in Section 4.2.2. The purpose of this appendix is to evaluate the effectiveness of the asbestos lagging in minimizing the heat loss from the walls to a negligible value.

To determine the heat loss through the asbestos lagging, thermocouples were placed in the wall of the lagging. Three thermocouples were placed 2-1/2 inches upstream of the exit, at the same axial position of the jet exit. The three thermocouples were buried at different depths in the lagging: 1/4-inch, 1/2-inch, and 3/4-inch from the outer wall of the 1-inch thick lagging. These positions are illustrated schematically in Figure 5.6. A fourth thermocouple was placed 1-inch upstream of the exit, at the same axial position at which the composition and temperature measurements were made.

The temperatures measured in the lagging are given in Figure C.1. These measurements are for the conditions represented by point B in Figure 4.1, the conditions for which the composition and temperature measurements were taken. The temperature profile, T(r), shown in Figure C.1 and the temperatures at the walls were calculated from principles of heat conduction in cylindrical symmetry (Kreith-1964) for the measured temperatures by applying the relation

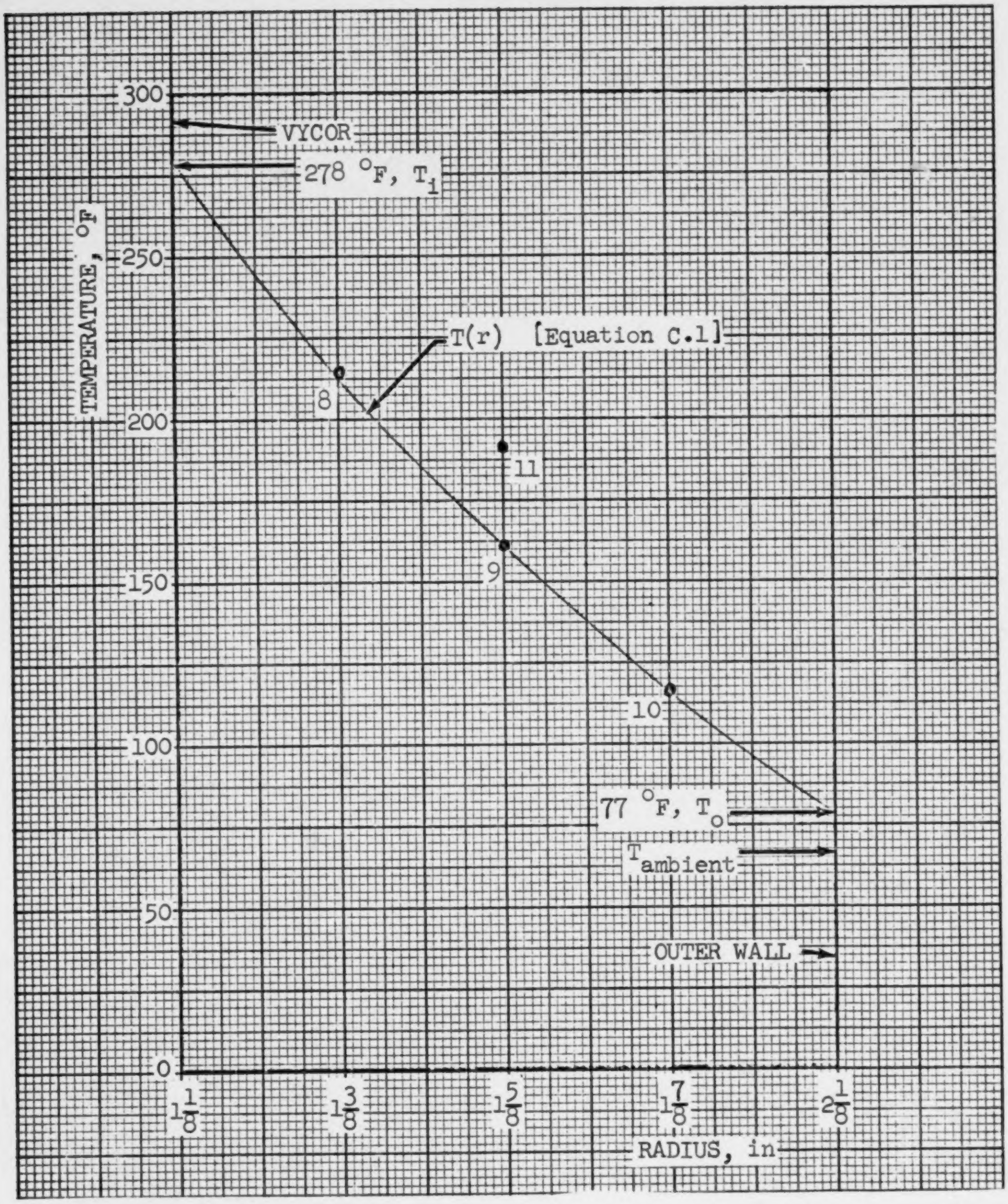

FIGURE C.1 LAGGING WALL TEMPERATURES

$$T(r) = T_i - \frac{T_i - T_o}{\ln\left(\frac{r_o}{r_i}\right)} \ln \frac{r}{r_i} \tag{C.1}$$

The heat loss is calculated from the relation

$$q = \frac{T_i - T_o}{\ln\left(\frac{r_o}{r_i}\right)} (2\pi k) \qquad \left[\frac{\text{Btu}}{\text{hr-ft}}\right] \tag{C.2}$$

where, from Kreith for asbestos

$$k = 0.12 \frac{\text{Btu}}{\text{hr-ft-°F}}$$

Using the data of Figure C.1 and a liberal estimate that the heat is lost along a 1-foot length (the flame protrudes only about 6-inches inside the Vycor) the heat loss through the lagging wall is

$$q = \frac{(278 - 77)}{\ln\left(\frac{2.125}{1.125}\right)} (2\pi) \; (0.12) \; (1)$$

$$q = 238 \frac{\text{Btu}}{\text{hr}} \tag{C.3}$$

To determine the significance of this loss, the sensible enthalpy release is estimated. The sensible enthalpy release can be estimated by multiplying the heat of combustion, HC, by the fuel mass flow rate with some estimate of the total amount of fuel reacted. The fuel mass flow rate for the conditions represented by point B is

$$\dot{m}_{fu} = 0.578 \times 10^{-2} \text{ lbm/sec} \tag{C.4}$$

Assuming that 50-percent of the fuel reacts, the sensible enthalpy release, Q, is approximately

$$Q = (.5)8050\ \frac{\text{Btu}}{\text{lbm}_{\text{fu}}} \times 0.578\times10^{-2}\ \frac{\text{lbm}_{\text{fu}}}{\text{sec}} \times 3600\ \frac{\text{sec}}{\text{hr}}$$

$$Q = 84{,}000\ \frac{\text{Btu}}{\text{hr}} \qquad \text{(C.4)}$$

The percent of heat loss compared to the sensible enthalpy release, then, is

$$\frac{238}{84{,}000} \times 100 = 0.29\ \%$$

Even should the estimates noted above be low by an order of magnitude, the heat loss through the asbestos is negligible. This result shows that the asbestos lagging was effective in producing an "adiabatic" boundary condition.

APPENDIX D

Description of Numerical Computer Program

This appendix is divided into three parts: 1) a description of the subroutines, 2) a list of the FORTRAN names, and 3) a listing of the computer program. The subroutines follow the general format of and are adapted from Gosman et al (1969). Subroutine INIT is wholly unique to this investigation.

D.1 Description of the Subroutines

1. BLOCK DATA: All numerical data and control indices are specified here.

2. Program "MAIN": The program actually begins here. Alphanumeric information is read and if appropriate, initial values of the dependent variables are read. The grid spacings are calculated. Control is transferred to start and administer the iteration procedure. When the program has converged, control is returned to MAIN for final print-out and program termination.

3. Subroutine INIT: This subroutine calculates the initial values of the fuel mass fraction, enthalpy, density, mass velocities along the inlet planes. Initial guesses are also specified at the remaining nodes.

4. Subroutine HEADCT: This subroutine prints out heading information and some of the input data including that specified in BLOCK DATA.

5. Subroutine SOLVCT: This subroutine controls the overall iteration process and is called by the MAIN program. It calls the subroutines that do the bulk of the calculations for the dependent variables

to be solved. This subroutine also tests for convergence. Upon convergence, control is transferred back to MAIN.

SOLVCT prints out information to document the progress of the iterative procedure. Fractional and absolute differences from one iteration to the next of each dependent variable are printed. At select intervals all the values of the dependent variables are printed.

6. Subroutine MVBCCT: In this subroutine, the mass velocities G1 and G2 are calculated at every grid point on the boundary.

7. Subroutine MVELCT: This subroutine calculates the mass velocities, G1 and G2, at nodes other than those on the boundaries using the stream function distribution.

8. Subroutine FDEQCT: This subroutine is the finite-difference component of the program and is called by SOLVCT for each dependent variable at every iteration. Here the new values of the dependent variables at all the grid points are calculated using Equation 4.12. FDEQCT itself calls various subroutines to evaluate the variables of Equation 4.12.

9. Subroutine SORCCT: This subroutine evaluates the D term of Equation 4.12. For example, the source term for the fuel mass fraction is evaluated here.

10. Subroutine COEFCT: This subroutine evaluates the diffusion terms of Equation 4.12.

11. Subroutine CONVEC: This subroutine calculates the convection terms of Equation 4.12.

12. Subroutine BOUNCT: This subroutine calculates the values of the dependent variables on the boundary using the boundary conditions prescribed in Section 4.2.2.

13. Subroutine PRINCT: This subroutine prints out the values of the dependent variables and also temperature values in the case of combustion and values of pressure if calculated (by specifying INDE(NP) = 1).

This subroutine is called if the program has converged or a specified maximum number of iterations (NMAX) has been reached without convergence. It is also called at regular intervals (specified by NPRIN) to document the progress of the iterative process.

14. Subroutine TABUCT: This subroutine prints out most of the results in tabulated form for every grid point. Included in the printout are values of the velocity in the r and z directions, the density, the effective viscosity, and the dependent variables. TABUCT is called when the program has converged.

15. Subroutine DENSCT: This subroutine calculates the mixture density, ρ, for the entire field of integration using equation 4.21.

16. Subroutine VISCCT: This subroutine calculates the effective viscosity for the entire field of integration using equation 4.23.

17. Function T(I,J): This is a FUNCTION subprogram which calculates the temperature at the node specified by (I,J) according to the Equation 4.28.

18. Function VS2 (I,J): This is a FUNCTION subprogram which calculates the quantity $(v_r^2 + v_z^2)$ at the point specified by (I,J).

19. Subroutine PLOTCT: This subroutine plots contours of the dependent variables and of temperature in the case of combustion. It is called only when the iterative process has converged. The subroutine does not use a plotter. As a result, only approximate and not-to-scale

plots are printed, particularly in the case of a nonuniform grid. Linear interpolation is used to calculate values between the nodes.

20. Function ADF: This is a FUNCTION subprogram, designed to evaluate the first derivative of a given variable at a point anywhere in the field of integration. The first derivative is calculated from a three-point quadratic approximation.

21. Subroutine PRESCT: This subroutine calculates the static pressure at every point in the field by integrating the momentum-conservation equations. Use is made of a reference point on the inlet plane at which the static pressure is specified.

D.2 List of FORTRAN Symbols

FORTRAN Symbols	Meaning
A (I,J, 1 to 9), also AQ(I,J, 1 to 9)	Dependent variables
ACTE	Activation energy; E in Equation 4.24
AGLOB	See GLOB
ANAME	Full names for dependent variables; for use in print-out
AQ (I,J, 1 to 13)	For convenience, some variables are assigned two variable-names, through an EQUIVALENCE statement, one of the two is AQ
AQ (I,J, 14)	Temporary storage locations
ASYMBL	Symbol array for dependent variables, e.g. STRM for stream function; for use in print-out
ATITLE	Title of problem to be input through this array
AU	The finite-difference approximation for the convection terms for the dependent variable ϕ is: ZU $\cdot$ ϕ_P-AU
BB	Coefficient in the quadratic representation of a ϕ-profile near an adiabatic boundary, i.e. $n_3^2/(n_3^2 - n_2^2)$ in Equation 4.20

FORTRAN Symbols	Meaning
BGLOB	See GLOB
CC	"Convergence criterion"
CN, CS, CE, CW	These are related to the B's of Equation 4.12 through: $CN = B_N/V_P$; $CS = B_S/V_P$; etc.
CPJ (1 to 3)	Specific heats of mixture components
CPREF	Reference specific heat
DCN, DN	Chamber dimensions
DC	"Divergence criterion"
DELX 1 (I)	Length of control volume in the z direction for nodes on grid-line I
DELX 2 (J)	Length of control volume in the r direction for nodes on grid-line J
G1(I,J), also AQ(I,J,10) G2(I,J), also AQ(I,J,11)	Mass velocities in directions z and r respectively
GC	Gravitational constant
GCPM	Universal gas constant
GM1E, GM1W, GM2N, GM2S	Quantities used for evaluation of the convection terms
GLOB	Preexponential factor in Equation 4.24; $GLOB = AGLOB \cdot 10^{BGLOB}$
HC	Heat of combustion
IC, IN	Grid-line designations
IE	Number of partial differential equations to be solved
IN	Number of z = constant grid lines
INM	= IN - 1
IMIN(J),IMAX(J)	Respectively, value of I on Jth grid-line at left-hand boundary and right-hand boundary
INDG	Control index for geometry of flow: 1 for Cartesian coordinates, 2 for cylindrical coordinates

FORTRAN Symbols	Meaning
INDRO	Control index for density: 2 for non-uniform density, 1 for constant density
INDE(K)	Only when this index is put equal to 1 will the equation for the dependent variable having the ordering index, e.g. NF, in place of K be solved
INDZMU	Control index for viscosity: 2 for variable viscosity, 1 for constant viscosity
JN	Number of r constant grid lines
JC1, JC2, JC, JN	Grid-line designations
JJC2	JC2 + 1
JC2M	JC2 - 1
JC1M	JC1 - 1
JNM	JN - 1
KVORT	A control index used during calculation of vorticities on boundaries: when KVORT = 0, wall vorticities are not calculated; when KVORT = 1, wall values calculated as well
NW	Dependent-variable ordering and identifying index, respectively for: vorticity/radius
NF	stream function
NZML	fuel mass fraction
NZMH	stagnation enthalpy
NZMF	mixture fraction
NVT	swirl velocity
NP	static pressure
NMAX	Maximum number of iterations to be performed
NPRIN	Results to be printed out, in display form, at intervals of NPRIN iterations
NHOT	NHOT = 0, cold flow and HC = 0; NHOT = 1, hot flow
NPRES	NPRES = 0 static pressure not obtained; NPRES = 1 static pressure is obtained

FORTRAN Symbols	Meaning
PR (1 to 9)	Prandtl or Schmidt numbers, i.e., $\sigma_{h,eff}$ or $\sigma_{fu,eff}$
PREF	Reference static pressure
R(J)	Value of r at the constant r grid-line J
RADC1, RADC2, RADN	Chamber radii
RO(I,J),also AQ(I,J,12)	Mixture density, ρ
ROP	Mixture density at primary or fuel inlet
ROREF	Reference density
ROJ	Mixture density at jet inlet
ROWF	Weighting factor (or under-relaxation factor) for density
RP (1 to 9)	Relaxation parameters for dependent variables
STC	Stoichiometric air/fuel ratio
STOX	Stoichiometric oxygen/fuel ratio
SOURCE	The source term for the dependent variable ψ is approximated by: source term $\approx$ SOURCE + ZQ × ϕ_P
T (I,J)	Absolute temperature
TREF	Reference temperature
VINP	Axial velocity at primary inlet
VINJ	Axial velocity at jet inlet
WC1H	Equation 4.17 for constant r walls
WC1V	Similar to Equation 4.17 for constant z walls
X1(I)	Spatial length to grid-line I
X2(J)	Spatial length to grid-line J
ZEX	Exponential factor, Equation 4.24
ZJC	Joule's constant
ZMU(I,J), also AQ(I,J,13)	Effective viscosity, μ_{eff}

FORTRAN Symbols	Meaning
ZMUK	Constant K in the effective-viscosity law
ZMUREF	Reference viscosity
ZMW (1 to 3)	Molecular weights
ZU	See AU
ZQ	See SOURCE

D.3 FORTRAN Listing of Program OPJET

```
      BLOCK DATA
C    OPJET8H
      COMMON/CVP/A(33,15,9),G1(33,15),G2(33,15),RO(33,15),ZMU(33,15)
      COMMON/CGRID/IMIN(33),IMAX(33),IN,JN,INM,JNM,IE
      COMMON/CNUMBR/NW,NF,NZML,NZMH,NZMF,NVT,NP
      COMMON/CINDEX/INDE(9),INDG,INDRO,INDZMU
      COMMON/CCHECK/RSDJ(9),RP(9),CC,DC,NMAX,NPRIN
      COMMON/CREFER/ROREF,PREF,ZMUREF,TREF,CPREF
      COMMON/CCONST/PR(9),ZMW(3),CPJ(3),GCPM,GC,ZJC
      COMMON/CYLI/JC1,JC2,IC,RADC1,RADC2,RADN,DCN,DN,JJC2,ICM,JC2M,JC1M
      COMMON/CHEM/STC,STOX,HC,GLOB,ZEX
      COMMON/CX1X2/X1(33),X2(15),DELX1(33),DELX2(15)
      COMMON/CVARY/NHOT,NPUNCH,NREAD,NPRES
      COMMON/CIGNIT/ISTAG1,ISTAG2,JSTAG
      COMMON/CROWF/ROWF
      COMMON/CZMUK/ZMUK
      COMMON/CPARAM/VINJ,VINP(15),TP,PP,TJ,PJ,PHIP,PHIJ
      COMMON/CGLOB/AGLOB,BGLOB,ACTE
      COMMON/CTIME/TMAX
      COMMON/CENTHL/NENTHL,NSTRM
      DIMENSION AQ(33,15,14)
      EQUIVALENCE (A(1,1,1),AQ(1,1,1))
C*******************************************************************
C
C
C*******************************************************************
      DATA  NHOT,NPUNCH,NREAD,NPRES,NENTHL,NSTRM  /
     1         1,     1,    2,    0,     1,    1   /
C
      DATA  ISTAG1, ISTAG2, JSTAG /
     1            7,     23,     6  /
C
      DATA  ROWF,  ZMUK,  AGLOB,  BGLOB,  ACTE  /
     1    1.00,  .012,  55.00,   9.63,  6.00E04 /
C
      DATA  (VINP(J),J=1,15),  PHIP,  VINJ,  PHIJ,  TJ  /
     1            12*29.4,28.6,26.8,0.0,
     2                               1.0, -715.,   1.0, 1383.  /
C
      DATA NMAX,NPRIN,INDG,INDRO,INDZMU,TMAX /
     1      49,   20,   2,    2,     2,420. /
C
      DATA JN,IN,JC1,JC2,IC/
     1     15,33,  3,  6,27 /
C
      DATA  ROREF,PREF,ZMUREF,TREF,CPREF/
     1     .075,2116.,.01333,530.,.395 /
C
      DATA (RP(L1),L1=1,9),(PR(L2),L2=1,9),(ZMW(L3),L3=1,3)/
     1  .75,1.,.75,6*1.,9*1.,17.03,32.0,28.0 /
C
      DATA (CPJ(L1),L1=1,3),CC,DC,GCPM,GC,ZJC/
     1      3*0.29,0.0050,1000.00,1545.,32.2,778./
```

```
C
      DATA    NW,NF,NZML,NZMH,NZMF,NVT,NP,IE/
     1         1, 2,   3,   4,   5,  6, 7, 4/
C
      DATA STC,HC / 0.165.8050.0 /
      END
      PROGRAM OPJET8H (INPUT,PUNCH,OUTPUT)
      COMMON/CVP/A(33,15,9),G1(33,15),G2(33,15),RO(33,15),ZMU(33,15)
      COMMON/CPARAM/VINJ,VINP(15),TP,PP,TJ,PJ,PHIP,PHIJ
      COMMON/CX1X2/X1(33),X2(15),DELX1(33),DELX2(15)
      COMMON/CNAME/ATITLE(12),ASYMBL(12),ANAME(6,15)
      COMMON/CGRID/IMIN(33),IMAX(33),IN,JN,INM,JNM,IE
      COMMON/CINDEX/INDE(9),INDG,INDRO,INDZMU
      COMMON/CNUMBR/NW,NF,NZML,NZMH,NZMF,NVT,NP
      COMMON/CYLI/JC1,JC2,IC,RADC1,RADC2,RADN,DCN,DN,JJC2,ICM,JC2M,JC1M
      COMMON/CRAD/R(15)
      COMMON/CCONST/PR(9),ZMW(3),CPJ(3),GCPM,GC,ZJC
      COMMON/CHEM/STC,STOX,HC,GLOB,ZEX
      COMMON/CREFER/KOREF,PREF,ZMUREF,TREF,CPREF
      COMMON/CNITER/NITER
      COMMON/CVARY/NHOT,NPUNCH,NREAD,NPRES
      COMMON/CCHECK/PSDU(9),RP(9),CC,DC,NMAX,NPRIN
      COMMON/CGLOB/AGLOB,BGLOB,ACTE
      DIMENSION AQ(33,15,14)
      EQUIVALENCE (A(1,1,1),AQ(1,1,1))
C***********************************************************************
C
C
C***********************************************************************
      READ 101, ATITLE, ASYMBL, ANAME
      IF (NHOT.EQ.0)  GO TO 60
      GO TO 61
60    IE=2
      INDRO=1
      HC=0.0
61    CONTINUE
      GLOB=AGLOB*10.0**BGLOB
      ZEX=ACTE*ZJC/GCPM
      INM=IN-1
      JNM=JN-1
      JJC2=JC2+1
      ICM=IC-1
      JC2M=JC2-1
      JC1M=JC1-1
      IF (INDE(NVT).EQ.1)  GO TO 20
      DO 84 L=1,4
84    ANAME(L,6) =ANAME(L,7)
      ASYMBL(6) =ASYMBL(7)
      DO 51  L=1,4
51    ANAME(L,7) =ANAME(L,8)
      ASYMBL(7) =ASYMBL(8)
20    CONTINUE
      IF  (NHOT.NE.0)  GO TO 22
      DO 23 L=1,4
23    ANAME(L,3)=ANAME(L,8)
      ASYMBL(3)=ASYMBL(8)
22    CONTINUE
      FCT=1.27
      X2(1)=0.0
      X2(2)=0.016/12.
      X2(3)=0.032/12.
      DO 900  J=4,JN
      IF  (J.GE.7)  FCT=1.195
 900  X2(J)=X2(J-1)+(X2(J-1)-X2(J-2))*FCT
      FCT=1.0
      X1(1)=0.0
      X1(2)=0.500/12.
      DO 910 I=3,IN
      IF (I.GE.6) FCT=1./1.36
      IF (I.GE.9) FCT=1.0
      IF (I.GE.28) FCT=1.33
      IF (I.GE.31) FCT=1.00
 910  X1(I)=X1(I-1)+(X1(I-1)-X1(I-2))*FCT
      DO 3 I=2,INM
 3    DELX1(I)=0.5*(X1(I+1)-X1(I-1))
      DO 4 J=2,JNM
 4    DELX2(J)=0.5*(X2(J+1)-X2(J-1))
      DO 5 J=1,JN
      IF(INDG.EQ.1) R(J)=1.0
      IF(INDG.EQ.2) R(J)=X2(J)
 5    CONTINUE
      IF(INDG.NE.1) GO TO 6
 C    FOR PLANE FLOWS PUT THE CHAMBER RADII EQUAL UNITY
      RADC1=1.0
      RADC2=1.0
      RADN=1.0
      GO TO 7
 C**** SPECIFYING CHAMBER DIMENSIONS
    6 RADC1=X2(JC1)
      RADC2=X2(JC2)
      RADN=X2(JN)
    7 DCN=X1(IC)
      DN=X1(IN)
 C**** SPECIFYING INDE≠S
      DO 8 L=1,IE
 8    INDE(L)=1
      IE1=IE+1
      DO 9 L=IE1,9
 9    INDE(L)=9
      IF  (NPRES.EQ.1)  INDE(NP)=1
 C**** SPECIFYING IMIN≠S AND IMAX≠S
      DO 30 L=1,JN
 30   IMIN(L)=1
      DO 32 L=1,JC2M
 32   IMAX(L)=IC
      DO 33 L=JC2,JN
 C****      SETTING INITIAL VALUES
 33   IMAX(L)=IN
      DO 2  J=1,JN
      DO 2  I=1,IN
      DO 13   K=1,IE
      A(I,J,K)=-1.0E-100
 13   CONTINUE
```

```
      A(I,J,NF)=-5.0E-03
      G1(I,J)=0.
      G2(I,J)=0.
      AQ(I,J,14)=0.0
 2    CONTINUE
      IF  (NREAD.EQ.0)  GO TO 12
      IZ=2
      IF  (NREAD.EQ.2)  IZ=IE
      READ 100, (((A(I,J,K), I=1,IN), J=1,JN), K=1,IZ)
      NITER=1
      CALL PRINCT (IZ)
 12   CONTINUE
 C
      TP=TREF
      PP=PREF
      IF  (NHOT.EQ.0)  TJ=TP
      PJ=PREF
      VT=0.0
      IF(INDE(NVT).NE.1) GO TO 46
      DO 45 J=1,JC1
 45   A(IC,J,NVT)=VT*R(J)
 46   CONTINUE
      CALL INIT
      CALL HEADCT
      ITAB=IE+1
      IF((INDE(NZML).EQ.1).AND.(INDE(NZMH).NE.1))  ITAB=IE+3
      IF((INDE(NZMH).EQ.1).AND.(INDE(NZMF).NE.1))  ITAB=IE+2
      IF(INDE(NVT).EQ.1) ITAB=ITAB+1
      IF  (NHOT.EQ.0)  ITAB=ITAB-1
      CALL SOLVCT (ITAB)
      IF(INDE(NP).EQ.1) CALL PRESCT
      IF  (NHOT.EQ.0)  GO TO 92
C******CALCULATING MOLE FRACTION
      NZ=IE+3
      IF  (INDE(NP).EQ.1)  NZ=NZ+1
      ITAB=ITAB+1
      DO 90  L=1,4
 90   ANAME(L,NZ)=ANAME(L,9)
      ASYMBL(NZ)=ASYMBL(9)
      DO 91  J=1,JN
      IL=IMIN(J)
      IH=IMAX(J)
      DO 91  I=IL,IH
      TEMP=T(I,J)
      ZMEAN=RO(I,J)*GCPM*TEMP/PREF
 91   A(I,J,NZ)=A(I,J,NZML)*ZMEAN/ZMW(1)
 92   CONTINUE
      CALL PRINCT (ITAB)
      IF  (NPUNCH.EQ.0)  GO TO 16
      PUNCH 100, (((A(I,J,K), I=1,IN), J=1,JN), K=1,IZ)
 16   CONTINUE
      IF (NITER.GT.NMAX)  STOP
      CALL TABUCT (ITAB)
      CALL PLOTCT (ITAB)
```

```
1       CONTINUE
100     FORMAT (5(E16.9))
101     FORMAT(12A5)
        STOP
        END
```

```
      SUBROUTINE INIT
      COMMON/CPARAM/VINJ,VINP(15),TP,PP,TJ,PJ,PHIP,PHIJ
      COMMON/CVP/A(33,15,9),G1(33,15),G2(33,15),RO(33,15),ZMU(33,15)
      COMMON/CNUMBR/NW,NF,NZML,NZMH,NZMF,NVT,NP
      COMMON/CGRID/IMIN(33),IMAX(33),IN,JN,INM,JNM,IE
      COMMON/CHEM/STC,STOX,HC,GLOB,ZEX
      COMMON/CYLI/JC1,JC2,IC,RADC1,RADC2,RADN,DCN,DN,JJC2,ICM,JC2M,JC1M
      COMMON/CCONST/PR(9),ZMW(3),CPJ(3),GCPM,GC,ZJC
      COMMON/CREFER/ROREF,PREF,ZMUREF,TREF,CPREF
      COMMON/CIGNIT/ISTAG1,ISTAG2,JSTAG
      COMMON/CVARY/NHOT,NPUNCH,NREAD,NPRES
      COMMON/CRAD/R(15)
      COMMON/CINDEX/INDE(9),INDG,INDRO,INDZMU
C***********************************************************************
C CALCULATES DENSITY, ENTHALPY, FUEL MASS FRACTION, AND MIXTURE FRACTION
C MASS FLOW RATE AT INLET PLANE OF APPROACH AND JET
C***********************************************************************
      AFUSTC=STC/(1.+STC)
      FIPSTC=AFUSTC/((1.+1./3.77)*STC)
      FOXSTC=1.0-AFUSTC-FIPSTC
      STOX=AFUSTC/FOXSTC
C
C FUEL MASS FRACTION A(I,J,NZML)
C
      XX=PHIP*STC
      AFUP=XX/(1.+XX)
      FIPP=AFUP/((1.+1./3.77)*XX)
      XX=PHIJ*STC
      AFUJ=XX/(1.+XX)
      FIPJ=AFUJ/((1.+1./3.77)*XX)
      IF  (NREAD.EQ.2)  GO TO 22
      DO 2  J=1,JN
      II1=IMIN(J)
      II2=IMAX(J)
      DO 2  I=II1,II2
2     A(I,J,NZML)=AFUP
      DO 3  J=1,JC1
3     A(IC,J,NZML)=AFUJ
      IF  (NHOT.EQ.0)  GO TO 22
      DO 14  J=1,JSTAG
      DO 14  I=ISTAG1,ISTAG2
14    A(I,J,NZML)=1.0E-05
22    CONTINUE
C
C DENSITY RO(I,J)
C
      FOXP=1.0-AFUP-FIPP
      ZMEAN=1.0/(AFUP/ZMW(1)+FOXP/ZMW(2)+FIPP/28.0)
      RO(1.1)=(PP*ZMEAN)/(TP*GCPM)
      DO 5  J=1,JN
      II1=IMIN(J)
      II2=IMAX(J)
      DO 5  I=II1,II2
```

```
5      RO(I,J)=RO(1,1)
       FOXJ=1.0-AFUJ-FIPJ
       ZMEAN=1.0/(AFUJ/ZMW(1)+FOXJ/ZMW(2)+FIPJ/28.0)
       RO(IC,1)=(PJ*ZMEAN)/(TJ*GCPM)
       DO 7 J=1,JC1
7      RO(IC,J)=RO(IC,1)
       IF  (NHOT.EQ.0)  GO TO 21
       IF  (NREAD.EQ.2)  GO TO 23
C
C ENTHALPY     A(I,J,NZMH)
C
       A(1,1,NZMH)=CPREF*TP+AFUP*HC
       DO 9 J=1,JN
       II1=IMIN(J)
       II2=IMAX(J)
       DO 9  I=II1,II2
9      A(I,J,NZMH)=A(1,1,NZMH)
       A(IC,1,NZMH)=CPREF*TJ+AFUJ*HC
       DO 11 J=1,JC1
11     A(IC,J,NZMH)=A(IC,1,NZMH)
C
C MIXTURE FRACTION      A(I,J,NZMF)
C
23     CONTINUE
       IF  ((NREAD.EQ.2).AND.(INDE(NZMF).EQ.1))  GO TO 21
       A(1,1,NZMF)=AFUP-FOXP*STOX
       IF (PHIP.EQ.1.0)  A(1,1,NZMF)=0.0
       DO 13 J=1,JN
       II1=IMIN(J)
       II2=IMAX(J)
       DO 13 I=II1,II2
13     A(I,J,NZMF)=A(1,1,NZMF)
       A(IC,1,NZMF)=AFUJ-FOXJ*STOX
       IF (PHIJ.EQ.1.0)  A(IC,1,NZMF)=0.0
       DO 15 J=1,JC1
15     A(IC,J,NZMF)=A(IC,1,NZMF)
C
C MASS VELOCITY     G1(I,J)
C
21     CONTINUE
       IF  (NREAD.EQ.2)  CALL DENSCT
       DO 17 J=1,JN
17     G1(1,J)=RO(1,J)*VINP(J)
       DO 19 J=1,JC14
19     G1(IC,J)=RO(IC,J)*VINJ
       IF  (NREAD.EQ.2)  RETURN
C
C INLET VORTICITY
C
       JJ=J+1
       DO 30 J=JJ,JNM
       A(1,J,NW)=-ADF(1,J,2,15)/R(J)
30     IF  (ABS(A(I,J,NW)).LT.1.0)  A(I,J,NW)=0.0
C
```

```
C   SWIRL VELOCITY  A(I,J,NVT)
C
      RETURN
      END
      SUBROUTINE HEADCT
      COMMON/CINDEX/INDE(9),INDG,INDRO,INDZMU
      COMMON/CCHECK/RSDU(9),RP(9),CC,DC,NMAX,NPRIN
      COMMON/CREFER/ROREF,PREF,ZMUREF,TREF,CPREF
      COMMON/CGRID/IMIN(33),IMAX(33),IN,JN,INM,JNM,IE
      COMMON/CCONST/PR(9),ZMW(3),CPJ(3),GCPM,GC,ZJC
      COMMON/CNAME/ATITLE(12),ASYMBL(12),ANAME(6,10)
      COMMON/CNUMBR/NW,NF,NZML,NZMH,NZMF,NVT,NP
      COMMON/CYLI/JC1,JC2,IC,RADC1,RADC2,RADN,DCN,DN,JJC2,ICM,JC2M,JC1M
      COMMON/CHEM/STC,STOX,HC,GLOB,ZEX
      COMMON/CX1X2/X1(33),X2(15),DELX1(33),DELX2(15)
      COMMON/CPARAM/VINJ,VINP(15),TP,PP,TJ,PJ,PHIP,PHIJ
C**********************************************************************
C    **HEADING** SUBROUTINE
C   THIS SUBR. PRINTS OUT SOME OF THE INFORMATION FED IN
C**********************************************************************
      PRINT 101, ATITLE
      IF(INDG.EQ.2) GO TO 3
      PRINT 401
      GO TO 4
3     PRINT 402
4     IF(INDZMU.EQ.2) GO TO 5
      PRINT 105
      GO TO 6
5     PRINT 106
6     IF(INDRO.EQ.2) GO TO 7
      PRINT 107
      GO TO 8
7     PRINT 108
8     PRINT 109
      DO 10 K=1,IE
   10 IF(INDE(K).EQ.1) PRINT 110, (ANAME(L, K),L=1, 6)
      PRINT 111, JN, IN, (J,IMIN(J), IMAX(J), J = 1, JN)
      PRINT 201, JC1,JC2,IC,RADC1,RADC2,RADN,DCN,DN
      DO 20 I=1,IN
20    X1(I)=X1(I)*12.
      DO 21 J=1,JN
21    X2(J)=X2(J)*12.
      PRINT 202, (I,I = 1, 11)
      PRINT 203, (X1(I), I = 1, 11 )
      PRINT 204, (X2(J), J = 1, 11)
      IF (IN.GT.21) GO TO 50
      PRINT 205, (I,I=12,21)
      PRINT 203, (X1(I), I=12,21)
      GO TO 51
50    PRINT 205, (I, I = 12, 22)
      PRINT 203, (X1(I), I=12,22)
51    IF (JN.GT.11) PRINT 204, (X2(J), J = 12, JN)
      IF (IN.GT.22)  PRINT 205, (I,I=23,IN)
      IF (IN.GT.22) PRINT 203, (X1(I), I=23,IN)
      DO 22 I=1,IN
22    X1(I)=X1(I)/12.
      DO 23 J=1,JN
```

```
23     X2(J)=Y2(J)/12.
       PRINT 112, (VINP(J),J=1,JN)
       PRINT 113,                      VINJ, TP, PP, TJ, PJ, ROREF, PREF,
      1 ZMUREF, TREF, CPREF, GC, ZJC
       PRINT 301, STC, STOX, HC
       IF (INDE(NZMH).EQ.1) PRINT 114, CPJ(I)
       IM=NZMH-NZML+1
       IF (INDE(NZML).EQ.1) PRINT 115, IM, ZMW, CPJ, (PR(L),L=NZML, NZMH)
       PRINT 116, CC, DC, NMAX
101    FORMAT(1H1,35X,43HFINITE-DIFFERENCE  ITERATION  SOLUTION  FOR/
      236X,43H-------------------------------------------//
      320X,12A6)
105    FORMAT(1H050X,15HFOR LAMINAR AND)
106    FORMAT(1H050X,17HFOR TURBULENT AND)
107    FORMAT(1H050X,20HINCOMPRESSIBLE FLOW )
108    FORMAT(1H050X,24HNON-UNIFORM-DENSITY FLOW)
109    FORMAT(1H0//46H THE DEPENDENT VARIABLES BEING CONSIDERED ARE,/
      246H --- --------- --------- ----- ---------- --- )
110    FORMAT(1H040X,6A6)
111    FORMAT(1H024HTHE GEOMETRICAL DATA ARE/
      225H --- ----------- ---- ---/
      341X,44HJN,     THE NUMBER OF ROWS    (DIRECTION-2) =,I3/
      441X,44HIN,     THE NUMBER OF COLUMNS (DIRECTION-1) =,I3//
      441X,1HJ,11X,4HIMIN,10X,4HIMAX//(1H 39X,3(I2,11X)))
112    FORMAT(22H1THE PHYSICAL DATA ARE/
      222H --- -------- ---- ---/
      210X,50HVINP,   INLET VEL. OF THE PRIMARY STREAM,  FT/SEC=,15F5.1)
113    FORMAT (
      210X,50HVINJ,   INLET VEL. OF THE JET STREAM,      FT/SEC=,F10.2//
      210X,50HTP(R), PP(PSF), APPROACH INLET T AND P............=,2F10.2//
      210X,50HTJ(R), PJ(PSF), JET INLET T AND P.................=,2F10.2//
      310X,50HROREF,  REFERENCE DENSITY FOR THE FLUID..........=,F10.4/
      410X,50HPREF,   REFERENCE PRESSURE FOR THE FLUID.........=,F10.4/
      510X,50HZMUREF, REFERENCE VISCOSITY FOR THE FLUID........=,F10.8/
      610X,50HTREF,   REFERENCE TEMPRATURE FOR THE FLUID.......=,F10.4/
      710X,50HCPREF,  REFERENCE SPECIFIC-HEAT FOR THE FLUID....=,F10.4/
      610X,50HGC,     GRAVITATIONAL CONSTANT...................=,F10.4/
      710X,50HZJC,    JOULE≠S MECH.EQUIVALENT FOR HEAT.........=,F10.4/)
114    FORMAT(1H  9X,50HREFERENCE SP.HEAT FOR FIRST MASS COMPONENT.......
      1=,F10.4)
115    FORMAT(1H  9X,50HIM,     NUMBER OF MASS SPECIES BEING CONSIDERED..
      1=,I6/
      210X,50HZMW≠S   MOLECULAR WEIGHTS OF SPECIES 1,2,3 ......=,3F10.4/
      310X,50HCPJ≠S   REFERENCE SP.HEATS FOR SPECIES 1,2,3 ....=,3F10.4/
      410X,50HPR≠S    TURB.SCHMIDT NUMBERS FOR SPECIES 1,2,3 ..=,3F10.4)
116    FORMAT(1H0///24H OTHER DATA SUPPLIED ARE/
      224H ----- ---- -------- ---//
      310X,50HCC,     THE CONVERGENCY CRITERION................=,F13.7/
      410X,50HDC,     THE DIVERGENCY  CRITERION................=,F13.7/
      510X,50HNMAX,   THE MAXIMUM NUMBER OF ITERATIONS.........=,I6)
201    FORMAT(1H0,20X,22H           JC1,JC2,IC = ,3(I3,1H,),12HRESPECTIVELY
      1        /1H0,20X,28H           RADC1,RADC2,RADN = ,3(F6.3,1H,),5X,
      2        16HFT, RESPECTIVELY/
      3        1H0,20X,19H           DCN,DN = ,2(F6.3,1H,),5X,
     4        16HFT, RESPECTIVELY/)
 202  FORMAT(1H1,10X,10H  I OR J  ,5X,11(3X,I2,3X))
 203  FORMAT(1H ,10X,10H  X1(I)   ,5X,11(F8.4))
 204  FORMAT(1H ,10X,10H  X2(J)   ,5X,11(F8.4))
 205  FORMAT(1H0,10X,10H  I OR J  ,5X,11(3X,I2,3X))
 301  FORMAT(10X,
     1 50HSTC,     (STC LB OF FUEL REACTS WITH 1 LB OF AIR),=,F10.4/10X,
     2 50HSTOX,    (STOX LB OF FUEL REACTS WITH 1 LB OF OX),=,F10.4/10X,
     2 50HHC,      HEAT OF REACTION, BTU/LB OF FUEL         =,F10.4)
 401  FORMAT(1H050X,24HIN CARTESIAN COORDINATES)
 402  FORMAT(1H050X,26HIN CYLINDRICAL COORDINATES)
      RETURN
      END
      SUBROUTINE SOLVCT (ITAB)
      COMMON/CVP/A(33,15,9),G1(33,15),G2(33,15),RO(33,15),ZMU(33,15)
      COMMON/CINDEX/INDE(9),INDG,INDRO,INDZMU
      COMMON/CCHECK/RSDU(9),RP(9),CC,DC,NMAX,NPRIN
      COMMON/CGRID/IMIN(33),IMAX(33),IN,JN,INM,JNM,IE
      COMMON/CNAME/ATITLE(12),ASYMBL(12),ANAME(6,10)
      COMMON/CNUMBR/NW,NF,NZML,NZMH,NZMF,NVT,NP
      COMMON/CNITER/NITER
      COMMON/CPARAM/VINJ,VINP(15),TP,PP,TJ,PJ,PHIP,PHIJ
      COMMON/CDI/DIFMAX(9),IPT(9),JPT(9),IPTR(9),JPTR(9)
      COMMON/CKVORT/KVORT
      COMMON/CYLI/JC1,JC2,IC,RADC1,RADC2,RADN,DCN,DN,JJC2,ICM,JC2M,JC1M
      COMMON/CTIME/TMAX
      COMMON/CVARY/NHOT,NPUNCH,NREAD,NPRES
      COMMON/CIGNIT/ISTAG1,ISTAG2,JSTAG
      COMMON/CENTHL/NENTHL,NSTRM
C********************************************************** *********
C    ≠≠SOLVE≠≠ SUBROUTINE
C   THIS SUBR. CONTROLS THE ITERATION PROCEDURE
C********************************************************** *********
      PRINT 101
      DO 10 K=1,IE
10     IF(INDE(K).EQ.1) PRINT 102, K, (ANAME(L,K),L = 1, 6)
      PRINT 103, (ASYMBL(K),K=1, IE)
      NITER=1
      NNN=NPRIN
      KVORT=0
      CALL  BOUNCT(NW)
1     CALL MVELCT(NF)
      IF  ((NITER.EQ.(NMAX-9)).AND.(NHOT.EQ.1))  IE=4
      IF  ((NITER.EQ.(NMAX-1)).AND.(NHOT.EQ.1))  NSTRM=1
      IF((INDZMU.EQ.1).AND.(NITER.EQ.1))  CALL VISCCT
      IF(INDZMU.EQ.2) CALL VISCCT
      IF(INDRO.EQ.2) CALL DENSCT
      CALL MVBCCT
      DO 2 K=1,IE
      IF  ((NSTRM.EQ.2).AND.(K.EQ.2))  K=K+1
      DIFMAX(K)=0.
      RSDU(K)=0.
2     IF(INDE(K).EQ.1) CALL FDEQCT(K,INDG)
      PRINT 104, NITER, (RSDU(K),IPTR(K),JPTR(K),K=1,IE)
      IF  (NITER.LE.20)  GO TO 34
      IF ((NENTHL.GE.1).OR.(NHOT.EQ.0)) GO TO 30
      IF  (ABS(RSDU(NZMH)).GT..005)  GO TO 30
      IE=3
      NENTHL=2
30    CONTINUE
      IF  ((NSTRM.GE.1).OR.(NHOT.EQ.0))  GO TO 34
      IF  (ABS(RSDU(NF)).GT..005)  GO TO 34
      NSTRM=2
34    CONTINUE
      IPTRR=IPTR(NW)
      JPTRR=JPTR(NW)
```

```
       PRINT 109, A(IPTRR,JPTRR,NW)
       RES=RSDU(1)
       DO 3 K=2,IE
 3     IF(ABS(RSDU(K)).GT.ABS(RES)) RES=RSDU(K)
       CALL SECOND (TIME)
       IF  ((TMAX-5.0-TIME).LT.0.0)  GO TO 11
       IF(NITER.GT.NMAX) GO TO 5
       IF(NITER-NNN)6,7,7
 7     NNN=NNN+NPRIN
 8     CONTINUE
       KVORT=1
       CALL  BOUNCT(NW)
       IF(INDE(NP).EQ.1) CALL PRESCT
       CALL PRINCT (ITAB)
       PRINT 103, (ASYMBL(K),K=1, IE)
 6     CONTINUE
       IF  ((NITER.EQ.1).AND.(NREAD.NE.0))  CALL PRINCT (4)
       NITER=NITER+1
       IF((ABS(RES).GT.CC).OR.(NITER.LE.2))  GO TO 1
       IF  (NHOT.EQ.0)  GO TO 33       .
       IE=4
       IF ((NENTHL.EQ.2).OR.(NSTRM.EQ.2))  GO TO 32
       IF ((ABS(RSDU(NZMH)).GT..005).OR.(ABS(RSDU(NF)).GT..005)) GO TO 1
 33    CONTINUE
       KVORT=1
       CALL  BOUNCT(NW)
       RETURN
 32    NENTHL=1
       NSTRM=1
       PRINT 121,  NITER
       NITER=NMAX-25
       NNN=(NITER/NPRIN)*NPRIN + NPRIN
       GO TO 1
 11    PRINT 108, TIME
       KVORT=1
       CALL BOUNCT (NW)
       NITER=NMAX+1
       RETURN
 5     PRINT 106, NITER
       KVORT=1
       CALL BOUNCT (NW)
 100   FORMAT (8(E10.3))
 101   FORMAT(1H1///10X,45HTHE FOLLOWING ARE MAXIMUM RESIDUES IN THE FIE,
      141HLD OF INTEGRATION AT EACH ITERATION FOR..//)
 102   FORMAT(1H 40X,I2,3H.  ,6A6)
 103   FORMAT     (1H1,30X,35H..NOTE.. PREFIX *R* DENOTES RESIDUE//
      1117H0....NOTE.....LEFT-HAND-COLUMNS FOR FRACTIONAL DIFFERENCES, RI
      1GHT-HAND-COLUMNS FOR CORRESPONDING ABSOLUTE DIFFERENCES///
      26X,5HNITER,9(5X,1HR,A6)//)
 104   FORMAT(1H ,6X,I3,4(1PE12.3,2I3))
 106   FORMAT (32H0THE PROCESS DID NOT CONVERGE IN,I5,13H   ITERATIONS)
 107   FORMAT  (46X,4(1PE12.3,2I3))
 108   FORMAT (32H0THE PROCESS DID NOT CONVERGE IN,F8.3,9H  SECONDS)
 109   FORMAT  (1H+,85X,3(1PE12.3))
```

```
121    FORMAT  (35HOVORT, STRM, FUMF HAVE CONVERGED IN,I5,
      1  13H   ITERATIONS)
       RETURN
       END
      SUBROUTINE MVBCCT
      COMMON/CVP/A(33,15,9),G1(33,15),G2(33,15),RO(33,15),ZMU(33,15)
      COMMON/CGRID/IMIN(33),IMAX(33),IN,JN,INM,JNM,IE
      COMMON/CPARAM/VINJ,VINP(15),TP,PP,TJ,PJ,PHIP,PHIJ
      COMMON/CREFER/ROREF,PREF,ZMUREF,TREF,CPREF
      COMMON/CNUMBR/NW,NF,NZML,NZMH,NZMF,NVT,NP
      COMMON/CYLI/JC1,JC2,IC,RADC1,RADC2,RADN,DCN,DN,JJC2,ICM,JC2M,JC1M
      COMMON/CCONST/PR(9),ZMW(3),CPJ(3),GCPM,GC,ZJC
      COMMON/CX1X2/X1(33),X2(15),DELX1(33),DELX2(15)
      COMMON/CRAD/R(15)
      COMMON/CINDEX/INDE(9),INDG,INDRO,INDZMU
      DIMENSION AQ(33,15,14)
      EQUIVALENCE (A(1,1,1),AQ(1,1,1))
C*********************************************************** *********
C    ##MASS-VELOCITY-BOUNDARY-CONDITION## SUBROUTINE
C    THIS SUBR. CALCULATES G1, G2 ON THE BOUNDARIES
C*********************************************************** *********
C
C*********************************************************** *********
C    UNIFORM INLET-VELOCITY DISTRIBUTIONS...
C    ZERO AXIAL GRADIENTS OF STREAM FUNCTION AND VORTICITY AT EXIT
C    VEXIT IS THE MEAN VELOCITY AT EXIT
C*********************************************************** *********
      DO 31 J=JJC2,JNM
      G1(IN,J)=ADF(IN,J,2,NF)/R(J)
31    CONTINUE
      BB=1./(1.-((X2(2)-X2(1))/(X2(3)-X2(1)))**2)
      DO 10 I=2,ICM
   10 G1(I,1)=BB*G1(I,2)-(BB-1.)*G1(I,3)
      RETURN
      END
      SUBROUTINE MVELCT(NF)
      COMMON/CVP/A(33,15,9),G1(33,15),G2(33,15),RO(33,15),ZMU(33,15)
      COMMON/CRAD/R(15)
      COMMON/CGRID/IMIN(33),IMAX(33),IN,JN,INM,JNM,IE
      COMMON/CYLT/JC1,JC2,IC,RADC1,RADC2,RADN,DCN,DN,JJC2,ICM,JC2M,JC1M
      DIMENSION AQ(33,15,14)
      EQUIVALENCE (A(1,1,1),AQ(1,1,1))
C***********************************************************************
C    ≠≠MASS-VELOCITY≠≠ SUBROUTINE
C    THIS SUBR. CALCULATES G1 AND G2 AT ALL POINTS  NOT ON THE BCUND.
C***********************************************************************
      DO 10  J=2,JNM
      IL=IMIN(J)+1
      IH=IMAX(J)-1
      IF(J.EQ.JC2)  IH=IC-1
      DO 10  I=IL,IH
      G1(I,J)=ADF(I,J,2,NF)/R(J)
10    G2(I,J)=-(ADF(I,J,1,NF)/R(J))
      RETURN
      END
      SUBROUTINE FDEQCT(K,INDG)
      COMMON/CVP/A(33,15,9),G1(33,15),G2(33,15),RO(33,15),ZMU(33,15)
      COMMON/CCOEF/CE,CW,CN,CS,C(5)
      COMMON/CCHECK/RSDU(9),RP(9),CC,DC,NMAX,NPRIN
      COMMON/CGRID/IMIN(33),IMAX(33),IN,JN,INM,JNM,IE
      COMMON/CNUMBR/NW,NF,NZML,NZMH,NZMF,NVT,NP
      COMMON/CDI/DIFMAX(9),IPT(9),JPT(9),IPTR(9),JPTR(9)
      COMMON/CYLI/JC1,JC2,IC,RADC1,RADC2,RADN,DCN,DN,JJC2,ICM,JC2M,JC1M
      COMMON/CX1X2/X1(33),X2(15),DELX1(33),DELX2(15)
      COMMON/CZW/ZW,IL,IH
      COMMON/CRAD/R(15)
      COMMON/CPARAM/VINJ,VINP(15),TP,PP,TJ,PJ,PHIP,PHIJ
      WC1H(WK,DELF,ROP,DELRO,RAD)=   -DELF/(324.*DX2*DX2*(WK*DX2+RAD)*
     1   (ROP*(WK*DX2/37.+RAD/19.)+DELRO*(WK*DX2/55.+RAD/37.)))
      WC2H(WK,ROP,DELRO,RAD)=-(RAD+WK*DX2)*
     2                                   (ROP*(RAD/6.+WK*DX2/8.)
     3                                   +DELRO*(RAD/8.+WK*DX2/10.))
     4                            /(RAD*(ROP*(RAD/3.+5.*WK*DX2/24.)
     5                            +DELRO*(5.*RAD/24.+3.*WK*DX2/20.)))
      WC1V(DELF,ROP,DELRO,ETA2)=-DELF/(((ETA2*DX1)**2)*
     1                                 (ROP/3.+5.*DELRO/24.))
      WC2V(ROP,DELRO)=-(ROP/6.+DELRO/8.)/(ROP/3.+5.*DELRO/24.)
C*****************************************************************************
C    ##FINITE-DIFFERENCE-EQUATION## SUBROUTINE
C*****************************************************************************
      IPTR(K)=2
      JPTR(K)=2
      IPT(K)=2
      JPT(K)=2
      DO 10 J=2,JNM
      IL=IMIN(J)+1
      IH=IMAX(J)-1
      IF(J.EQ.JC2)IH=IC-1
      DO 10 I=IL,IH
      IF((K.EQ.NW).AND.((J.EQ.JC1).AND.(I.EQ.(IC-1))))  GO TO 100
      GO TO 110
100   CALL COEFCT (I,J,NF,INDG)
      YY=A(I,J,NF)*(CE+CW+CN+CS)
      YY=YY-(CE*A(I+1,J,NF)+CW*A(I-1,J,NF)+CN*A(I,J+1,NF)
     1 +CS*A(I,J-1,NF))
      Z=A(I,J,NW)
      A(I,J,NW)=YY/R(J)
      GO TO 222
110   CONTINUE
      CALL SORCCT(I,J,K,SOURCE,ZQ)
      CALL COEFCT(I,J,K,INDG)
      IF(K.NE.NW) GO TO 999
C***  INCORPORATING B.C. FOR VORTICITY IN THE FINITE DIFF. FORMULATION
C***  UP TO STATEMENT NUMBER 999
      ZW=0.
      ZWMU=0.0
      IF((I.EQ.IH).AND.((J.GE.JC1).AND.(J.LE.JC2)))   GO TO 600
      GO TO 700
```

```
501   LJNS=J+1
      WKNS=FLOAT(1-INDG)
      RADNS=RADN
      CQNS=CN
      GO TO 666
502   LJNS=J-1
      WKNS=FLOAT(INDG-1)
      RADNS=RADC2
      CQNS=CS
      GO TO 666
600   LIEW=I+1
      CQEW=CE
      GO TO 555
700   IF(J.EQ.JNM) GO TO 501
      IF((J.EQ.(JC2+1)).AND.(I.GE.IC))  GO TO 502
      GO TO 999
555   DX1=ABS(X1(LIEW)-X1(I))
      A(LIEW,J,NW)=WC1V(A(I,J,NF)-A(LIEW,J,NF),RO(LIEW,J),
     1                   RO(I,J)-RO(LIEW,J), R(J))
      ZW=CQEW*WC2V(RO(LIEW,J),RO(I,J)-RO(LIEW,J))
      ZWMU=ZWMU+ZW*ZMU(LIEW,J)
      GO TO 999
666   DX2=ABS(X2(LJNS)-X2(J))
      A(I,LJNS,NW)=WC1H(WKNS,A(I,J,NF)-A(I,LJNS,NF),RO(I,LJNS),
     1                   RO(I,J)-RO(I,LJNS),RADNS)
      ZW=0.0
      ZWMU=ZWMU+ZW*ZMU(I,LJNS)
C***  END VORTICITY B.C. SPECIAL FORMULATION
999   CONTINUE
      IF(K.NE.NF) GO TO 1
      IF ((J.EQ.JC1).AND.(I.EQ.(IC-1)).AND.(VINJ.NE.0.0))  GO TO 223
      GO TO 1
223   A(I,J,NF)=A(IC,JC1,NF)
      GO TO 10
1     CONTINUE
      CALL  CONVEC(I,J,K,AU,ZU)
      IF(K.EQ.NW) AU=AU*R(J)*R(J)
      IF(K.EQ.NW) ZU=ZU*R(J)*R(J)
      ANUM=CE*C(2)*A(I+1,J,K)+CW*C(4)*A(I-1,J,K)
     1    +CN*C(3)*A(I,J+1,K)+CS*C(5)*A(I,J-1,K)+AU+SOURCE
      ADNM=(CE+CW+CN+CS)*C(1)+ZU+ZQ
      IF(K.EQ.NW) ADNM=ADNM-ZWMU
      IF((ADNM.EQ.0.0).OR.(ANUM.EQ.0.0)) GO TO 10
4     Z=A(I,J,K)
      A(I,J,K)=ANUM/ADNM
      IF  (ABS(A(I,J,NF)).GT.2.0E-02)  A(I,J,NF)=-3.0E-03
222   CONTINUE
      DIF=A(I,J,K)-Z
      A(I,J,K)=Z+RP(K)*DIF
      AB=0.25*(ABS(A(I+1,J,K))+ABS(A(I-1,J,K))+ABS(A(I,J+1,K))
     1  +ABS(A(I,J-1,K)))
      IF((A(I,J,K).EQ.0.0).OR.(AB.EQ.0.0))  GO TO 10
      RS=DIF/A(I,J,K)
      RSM=DIF/AB
      IF(ABS(RSM).LT.ABS(RS)) RS=RSM
      IF(ABS(RS).GT.ABS(RSDU(K)))   GO TO 55
      GO TO 54
 55   RSDU(K)=RS
      IPTR(K)=I
      JPTR(K)=J
 54   CONTINUE
      IF(ABS(DIF).GT.ABS(DIFMAX(K)))  GO TO 52
      GO TO 10
 52   DIFMAX(K)=DIF
      IPT(K)=I
      JPT(K)=J
 10   CONTINUE
      CALL BOUNCT(K)
      RETURN
      END
      SUBROUTINE SORCCT(I,J,K,SOURCE,ZQ)
      COMMON/CVP/A(33,15,9),G1(33,15),G2(33,15),RO(33,15),ZMU(33,15)
      COMMON/CNUMBR/NW,NF,NZML,NZMH,NZMF,NVT,NP
      COMMON/CX1X2/X1(33),X2(15),DELX1(33),DELX2(15)
      COMMON/CRAD/R(15)
      COMMON/CCONST/PR(9),ZMW(3),CPJ(3),GCPM,GC,ZJC
      COMMON/CHEM/STC,STOX,HC,GLOB,ZEX
      COMMON/CINDEX/INDE(9),INDG,INDRO,INDZMU
      COMMON/CREFER/ROREF,PREF,ZMUREF,TREF,CPREF
C*********************************************************** *********
C    **SOURCE** - TERMS SUBROUTINE
C    SOURCE TERMS IN FINITE DIFFERENCE FORM
C*********************************************************** *********
      GO TO (1,2,5,3,3,4,3),K
C*****  FOR VORTICITY
1     SOURCE=0.
      DEN=16.0*DELX1(I)*DELX2(J)/(R(J)**2)
      S1=RO(I,J+1)+RO(I,J)
      S1=S1*(VS2(I+1,J)-VS2(I-1,J)+VS2(I+1,J+1)-VS2(I-1,J+1))
      S2=RO(I,J-1)+RO(I,J)
      S2=S2*(VS2(I-1,J)-VS2(I+1,J)+VS2(I-1,J-1)-VS2(I+1,J-1))
      S3=RO(I+1,J)+RO(I,J)
      S3=S3*(VS2(I,J-1)-VS2(I,J+1)+VS2(I+1,J-1)-VS2(I+1,J+1))
      S4=RO(I-1,J)+RO(I,J)
      S4=S4*(VS2(I,J+1)-VS2(I,J-1)+VS2(I-1,J+1)-VS2(I-1,J-1))
      SOURCE=SOURCE+(S1+S2+S3+S4)/DEN
      IF(INDE(NVT).EQ.1) SOURCE=SOURCE+(RO(I+1,J)*(A(I+1,J,NVT)**2)
     1     -RO(I-1,J)*(A(I-1,J,NVT)**2))/((X1(I+1)-X1(I-1))*R(J))
      ZQ=0.
      RETURN
C*****  FOR STREAM FUNCTION
2     SOURCE=A(I,J,NW)*R(J)
      ZQ=0.
      RETURN
C*****  FOR MIXTURE FRACTION AND ENTHALPY
3     SOURCE=0.
      ZQ=0.
      RETURN
C*****  FOR SWIRL VELOCITY
4     ZQ=0.
      SOURCE=0.0
      RETURN
C*****  FOR FUEL MASS FRACTION
5     AMF=A(I,J,NZMF)
      AFU=A(I,J,NZML)
      AH=A(I,J,NZMH)
      IF (AFU.LE.0.0) GO TO 350
      FOX=(AFU-AMF)/STOX
      IF (FOX.LE.0.0) GO TO 350
      TEMP=(AH-AFU*HC)/CPREF
      IF (TEMP.LT.300.) TEMP=TREF
      FIP=1.0-FOX-AFU
      ZMW3=ZMW(3)-((0.1416-AFU)/0.1416)*3.2
      ZMEAN=1.0/(AFU/ZMW(1)+FOX/ZMW(2)+FIP/ZMW3)
      SORC=(PREF*ZMEAN)/(TEMP*GCPM)
      SORC=SORC**1.95
      SORC=SORC*GLUB*(AFU**0.75)*(FOX**1.20)
      SORC=-SORC/(EXP(ZEX/TEMP))
      ZQ=-(SORC/AFU)*R(J)
      IF (ZQ.LE.-.0001) PRINT 142
 142  FORMAT (1H 10X,16HZQ LESS THAN 0.0)
      GO TO 450
 350  ZQ=0.0
 450  SOURCE=0.0
      RETURN
      END
      SUBROUTINE COEFCT(I,J,K,INDG)
      COMMON/CX1X2/X1(33),X2(15),DELX1(33),DELX2(15)
      COMMON/CVP/A(33,15,9),G1(33,15),G2(33,15),RO(33,15),ZMU(33,15)
      COMMON/CCOEF/CE,CW,CN,CS,C(5)
      COMMON/CCONST/PR(9),ZMW(3),CPJ(3),GCPM,GC,ZJC
      COMMON/CRAD/R(15)
      COMMON/CNUMBR/NW,NF,NZML,NZMH,NZMF,NVT,NP
      COMMON/CYLI/JC1,JC2,IC,RADC1,RADC2,RADN,DCN,DN,JJC2,ICM,JC2M,JC1M
C*********************************************************************** *********
C    **COEFFICIENT** (FOR DIFFUSION TERMS) SUBROUTINE
C*********************************************************************** *********
C*****  SUBSCRIPTS 1,2,3,4,5  REFER TO POINTS P,E,N,W,S RESPECTIVELY
      DIMENSION B(5)
      DO 16 L=1,5
16    C(L)=1.0
      IF((K.NE.NW).AND.(K.NE.NP))  GO TO 2
C*****  FOR VORTICITY
      B(1)=R(J)**3
      B(2)=B(1)
      B(3)=R(J+1)**3
      B(4)=B(1)
      B(5)=R(J-1)**3
      C(1)=ZMU(I,J)
      C(2)=ZMU(I+1,J)
      C(3)=ZMU(I,J+1)
      C(4)=ZMU(I-1,J)
      C(5)=ZMU(I,J-1)
      GO TO 20
2     IF(K.NE.NF) GO TO 3
C*****  FOR STREAM FUNCTION
      B(1)=1./(R(J)*RO(I,J))
      B(2)=1./(R(J)*RO(I+1,J))
      B(3)=8.0/((R(J)+R(J+1))*(RO(I,J)+RO(I,J+1)))-B(1)
      B(4)=1./(R(J)*RO(I-1,J))
      B(5)=8.0/((R(J)+R(J-1))*(RO(I,J)+RO(I,J-1)))-B(1)
      GO TO 20
3     IF(K.NE.NVT) GO TO 15
C*****  FOR SWIRL VELOCITY
      B(1)=ZMU(I,J)*R(J)**3
      B(2)=ZMU(I+1,J)*R(J)**3
      B(3)=ZMU(I,J+1)*R(J+1)**3
      B(4)=ZMU(I-1,J)*R(J)**3
      B(5)=ZMU(I,J-1)*R(J-1)**3
      C(1)=1./(R(J)*R(J))
      C(2)=C(1)
      C(3)=1./(R(J+1)*R(J+1))
      C(4)=C(1)
      IF(R(J-1).GT.0.0) C(5)=1./(R(J-1)*R(J-1))
      IF(R(J-1).EQ.0.0) C(5)=0.0
      GO TO 20
C*****  FOR MIXTURE FRACTION AND ENTHALPY
15    B(1)=ZMU(I,J)*R(J)/PR(K)
      B(2)=ZMU(I+1,J)*R(J)/PR(K)
      B(3)=ZMU(I,J+1)*R(J+1)/PR(K)
      B(4)=ZMU(I-1,J)*R(J)/PR(K)
      B(5)=ZMU(I,J-1)*R(J-1)/PR(K)
   20 CONTINUE
C*****  FOR ALL DEPENDENT VARIABLES
      CE=(B(2)+B(1))/((X1(I+1)-X1(I))*2.*DELX1(I))
      CW=(B(1)+B(4))/((X1(I)-X1(I-1))*2.*DELX1(I))
      CN=(B(3)+B(1))/((X2(J+1)-X2(J))*2.*DELX2(J))
      CS=(B(1)+B(5))/((X2(J)-X2(J-1))*2.*DELX2(J))
      RETURN
      END
      SUBROUTINE CONVEC(I,J,K,AU,ZU)
      COMMON/CVP/A(33,15,9),G1(33,15),G2(33,15),RO(33,15),ZMU(33,15)
      COMMON/CX1X2/X1(33),X2(15),DELX1(33),DELX2(15)
      COMMON/CNUMBR/NW,NF,NZML,NZMH,NZMF,NVT,NP
      COMMON/CYLT/JC1,JC2,IC,RADC1,RADC2,RADN,DCN,DN,JJC2,ICM,JC2M,JC1M
      COMMON/CPAD/R(15)
      COMMON/CZW/ZW,IL,IH
      COMMON/CCOEF/CE,CW,CN,CS,C(5)
      COMMON/CGRID/IMIN(33),IMAX(33),IN,JN,INM,JNM,IE
C************************************************************** *********
C    **CONVECTION** - TERM  SUBROUTINE
C    TANK-AND-TUBE FORMULATION OF THE CONVECTION TERMS
C************************************************************** *********
      AU=0.
      ZU=0.
      IF(K.EQ.NF) GO TO 12
      DX12=1./(4.*DELX1(I)*DELX2(J))
      GM1E=DX12*(A(I,J+1,NF)-A(I,J-1,NF)+A(I+1,J+1,NF)-A(I+1,J-1,NF))
      GM1W=DX12*(A(I,J+1,NF)-A(I,J-1,NF)+A(I-1,J+1,NF)-A(I-1,J-1,NF))
      GM2S=-DX12*(A(I+1,J,NF)-A(I-1,J,NF)+A(I+1,J-1,NF)-A(I-1,J-1,NF))
      GM2N=-DX12*(A(I+1,J,NF)-A(I-1,J,NF)+A(I+1,J+1,NF)-A(I-1,J+1,NF))
C
      IF(GM1W)1,3,2
1     ZU=-GM1W
      GO TO 3
2     AU=GM1W*A(I-1,J,K)
3     IF(GM2S)4,6,5
4     ZU=ZU-GM2S
      GO TO 6
5     AU=AU+GM2S*A(I,J-1,K)
      IF((K.EQ.NW).AND.(J.EQ.(JC2+1)).AND.(I.GE.IC))  GO TO 501
6     IF(GM1E)7,9,8
7     AU=AU-GM1E*A(I+1,J,K)
      IF((K.EQ.NW).AND.((I.EQ.IH).AND.((J.GE.JC1).AND.(J.LE.JC2))))
     1  GO TO 502
      GO TO 9
8     ZU=ZU+GM1E
9     IF(GM2N)10,11,11
10    AU=AU-GM2N*A(I,J+1,K)
      IF((K.EQ.NW).AND.(J.EQ.JNM))  GO TO 504
      RETURN
11    ZU=ZU+GM2N
12    RETURN
C
  501 ZU=ZU-GM2S*ZW/CS
      GO TO 6
  502 ZU=ZU+GM1E*ZW/CE
      GO TO 9
504   ZU=ZU+GM2N*ZW/CN
      RETURN
      END
      SUBROUTINE BOUNCT(K)
      COMMON/CVP/A(33,15,9),G1(33,15),G2(33,15),RO(33,15),ZMU(33,15)
      COMMON/CGRID/IMIN(33),IMAX(33),IN,JN,INM,JNM,IE
      COMMON/CNUMBR/NW,NF,NZML,NZMH,NZMF,NVT,NP
      COMMON/CPARAM/VINJ,VINP(15),TP,PP,TJ,PJ,PHIP,PHIJ
      COMMON/CREFER/ROREF,PREF,ZMUREF,TREF,CPREF
      COMMON/CCONST/PP(9),ZMW(3),CPJ(3),GCPM,GC,ZJC
      COMMON/CYLI/JC1,JC2,IC,RADC1,RADC2,RADN,DCN,DN,JJC2,ICM,JC2M,JC1M
      COMMON/CX1X2/X1(33),X2(15),DELX1(33),DELX2(15)
      COMMON/CRAD/R(15)
      COMMON/CKVORT/KVORT
      COMMON/CNITER/NITER
      COMMON/CINDEX/INDE(9),INDG,INDRO,INDZMU
      FP(ROP,Y,XI2)= -ROP*VINP(J)*(Y-XI2)*((0.5*(Y+XI2))**(INDG-1))
      FJ(ROJ,Y,XI2)=FBASE+ROJ*VINJ*(Y-XI2)*((0.5*(Y+XI2))**(INDG-1))
      WP(XI2)=0.0*XI2
      WJ(XI2)=0.0*XI2
      WVW(    DELF,WQ,ROP,DELRO,ETA2)= -(    DELF/((ETA2*DX1)**2)
     1                                  +WQ*(ROP/6.+DELRO/8.))
     2                               /(ROP/3.+5.*DELRO/24.)
      WHW(WK,DELF,WQ,ROP,DELRO,RAD)=  -(    DELF/(DX2*DX2)
     1                              +WQ*(RAD+WK*DX2)*
     2                               (ROP*(RAD/6.+WK*DX2/8.)
     3                               +DELRO*(RAD/8.+WK*DX2/10.)))
     4                        /(RAD*(ROP*(RAD/3.+5.*WK*DX2/24.)
     5                        +DELRO*(5.*RAD/24.+3.*WK*DX2/20.)))
      YY(YN,YP)=1./(1.-(YP/YN)**2)
C*********************************************************************
C    ≠≠BOUNDARY≠≠ - CONDITIONS SUBROUTINE
C    BOUNDARY VALUES FOR ALL THE DEPENDENT VARIABLES
C*********************************************************************
C
C
C*********************************************************************
C    UNIFORM INLET-VELOCITY DISTRIBUTIONS...
C    ZERO AXIAL GRADIENTS FOR ALL DEPENDENT VARIABLES AT EXIT
C    QUADRATIC PROFILE NEAR ≠ADIABATIC≠ BOUNDARIES
C*********************************************************************
      GO TO (1,2,3,3,3,4,3),K
C*********************************************
C    FOR STREAM FUNCTION..... A(I,J,NF)
C*********************************************
2     CONTINUE
      IF(NITER.GE.2) GO TO 211
      DO 205 J=1,JN
      IF(INDG.EQ.2) A(1,J,NF)=FP(RO(1,J),RADN,R(J))
  205 IF(INDG.EQ.1)  A(1,J,NF)=FP(RO(1,J),X2(JN),X2(J))
      DO 204 I=1,IC
204   A(I,1,NF)=A(1,1,NF)
      FBASE=A(IC,1,NF)
      DO 207  J=2,JC1
      IF(INDG.EQ.2)  A(IC,J,NF)=FJ(RO(IC,J),R(J),R(1))
  207 IF(INDG.EQ.1)  A(IC,J,NF)=FJ(RO(IC,J),X2(J),X2(1))
```

```
      DO 201  I=1,IN
 201  A(I,JN,NF)=0.
      DO 208  J=JC1,JC2
  208 A(IC,J,NF)=A(IC,JC1,NF)
      DO 202  I=IC,IN
  202 A(I,JC2,NF)=A(IC,JC2,NF)
.211  CONTINUE
      BB=YY(2.*DELX1(IN-1),X1(IN)-X1(IN-1))
      DO 210  J=JJC2,JN
 210  A(IN,J,NF)=BB*A(IN-1,J,NF)-(BB-1.)*A(IN-2,J,NF)
 299  RETURN
C*******************************************************
C FOR MASS FRACTION, ENTHALPY, AND MIXTURE FRACTION
C*******************************************************
C
3     BB=YY(2.*DELX2(JNM),X2(JN)-X2(JNM))
      DO 816  I=2,INM
 816  A(I,JN,K)=BB*A(I,JNM,K)-(BB-1.)*A(I,JN-2,K)
      IF  ((JC2-JC1).EQ.1)  GO TO 51
      JJC1=JC1+1
      BB=YY(2.*DELX1(IC-1),X1(IC)-X1(IC-1))
      DO 817  J=JJC1,JC2M
 817  A(IC,J,K)=BB*A(IC-1,J,K)-(BB-1.)*A(IC-2,J,K)
 51   BB=YY(2.*DELX2(2),X2(2)-X2(1))
      DO 819 I=2,ICM
      A(I,1,K)=BB*A(I,2,K)-(BB-1.)*A(I,3,K)
      IF (K.EQ.NZMF) GO TO 819
      IF(A(I,J,K).LT.0.0) A(I,1,K)=0.5*(A(I,1,K)+A(I,2,K))
      IF(A(I,J,K).LT.0.0) A(I,1,K)=0.5*(A(I,1,K)+A(I,2,K))
      IF(A(I,J,K).LT.0.0) A(I,1,K)=A(I,2,K)
 819  CONTINUE
      BB=YY(2.*DELX2(JC2+1),X2(JC2+1)-X2(JC2))
      DO 843  I=IC,INM
 843  A(I,JC2,K)=BB*A(I,JC2+1,K)-(BB-1.)*A(I,JC2+2,K)
      BB=YY(2.*DELX1(IN-1),X1(IN)-X1(IN-1))
      DO 820 J=JC2,JN
 820  A(IN,J,K)=BB*A(IN-1,J,K)-(BB-1.)*A(IN-2,J,K)
      RETURN
C*******************************************************
C   FOR VORTICITY.... A(I,J,NW)
C*******************************************************
1     CONTINUE
      WK=FLOAT(INDG-1)
      IF(KVORT.NE.1) GO TO 111
      DX2=X2(JN)-X2(JN-1)
      DO 11  I=1,INM
 11   A(I,JN,NW)=WHW(-WK,A(I,JN-1,NF),A(I,JN-1,NW),RO(I,JN),
     1               RO(I,JN-1)-RO(I,JN),RADN)
      DX2=X2(JC2+1)-X2(JC2)
      DO 101  I=IC,INM
 101  A(I,JC2,NW)= WHW(WK,A(I,JC2+1,NF)-A(I,JC2,NF),A(I,JC2+1,NW),
     1               RO(I,JC2),RO(I,JC2+1 )-RO(I,JC2),RADC2)
      IF ((JC2-JC1).EQ.1)  GO TO 111
      DX1=X1(IC)-X1(IC-1)
      JJC1=JC1+1
      DO 15  J=JJC1,JC2M
15    A(IC,J,NW)=WVW(     A(IC-1,J,NF),A(IC-1,J,NW),
     1                 RO(IC,J),RO(IC-1,J)-RO(IC,J), R(J))
111   DO 10 I=1,IC
      IF(INDG.EQ.1) A(I,1,NW)=0.0
      IF(INDG.EQ.2) A(I,1,NW)=
     1          A(I,2,NW)+(X2(2)/(X2(3)-X2(2)))*(A(I,2,NW)-A(I,3,NW))
10    CONTINUE
      DO 17  J=2,JC1
17    A(IC,J,NW)=WJ(X2(J))/R(J)
      BB=YY(2.*DELX1(IN-1),X1(IN)-X1(IN-1))
      DO 18  J=JC2,JN
18    A(IN,J,NW)=BB*A(IN-1,J,NW)-(BB-1.)*A(IN-2,J,NW)
100   CONTINUE
      RETURN
C*************************************************
C   FOR SWIRL VELOCITY
C*************************************************
4     CONTINUE
      BB=YY(2.*DELX1(IN-1),X1(IN)-X1(IN-1))
      DO 41  J=JC2,JN
41    A(IN,J,NVT)=BB*A(IN-1,J,NVT)-(BB-1.)*A(IN-2,J,NVT)
      RETURN
      END
      SUBROUTINE DENSCT
      COMMON/CVP/A(33,15,9),G1(33,15),G2(33,15),RO(33,15),ZMU(33,15)
      COMMON/CINDEX/INDE(9),INDG,INDRO,INDZMU
      COMMON/CREFER/ROREF,PREF,ZMUREF,TREF,CPREF
      COMMON/CGRID/IMIN(33),IMAX(33),IN,JN,INM,JNM,IE
      COMMON/CCONST/PR(9),ZMW(3),CPJ(3),GCPM,GC,ZJC
      COMMON/CNITER/NITER
      COMMON/CNUMBR/NW,NF,NZML,NZMH,NZMF,NVT,NP
      COMMON/CHEM/STC,STOX,HC,GLOB,ZEX
      COMMON/CROWF/ROWF
C***********************************************************************
C     **DENSITY** SUBROUTINE
C     MIXTURE DENSITY CALCULATION
C***********************************************************************
      DO 40 J=1,JN
      IL=IMIN(J)
      IH=IMAX(J)
      DO 40 I=IL,IH
      AFU=A(I,J,NZML)
      IF(AFU.GT.1.)  AFU=1.0
      IF(AFU.GT.-1.0E-05) GO TO 15
      AFU=0.0
      IF (NITER.LE.40) GO TO 15
      PRINT 100, AFU, I, J
100   FORMAT(1H ,10X,4HAFU=,E12.3,5X,2HI=,I3,5X,,2HJ=,I3)
15    CONTINUE
      AFH=A(I,J,NZMH)
      TEMP=(AFH-AFU*HC)/CPREF
      IF(TEMP.GE.300.) GO TO 50
      TEMP=TREF
      IF(NITER.LE.40) GO TO 50
      PRINT 120, I, J
120   FORMAT (1H ,32HTEMP LESS THAN 300. (DENSCT)  I=,I2,2HJ=,I2)
50    CONTINUE
      AMF=A(I,J,NZMF)
      FOX=(AFU-AMF)/STOX
      IF (FOX.GT.-1.E-05) GO TO 20
      FOX=0.0
      IF (NITER.LE.40)  GO TO 20
      PRINT 110, I, J
110   FORMAT (1H ,20HFOX LESS THAN 0.0,I=,I2,2HJ=,I2)
20    CONTINUE
      FIP=1.0-FOX-AFU
      ZMW3=ZMW(3)-((0.1416-AFU)/0.1416)*3.2
      ZMEAN=1.0/(AFU/ZMW(1)+FOX/ZMW(2)+FIP/ZMW3)
      DENSTY=(ZMEAN*PREF)/(GCPM*TEMP)
      RO(I,J)=ROWF*DENSTY+(1.0-ROWF)*RO(I,J)
40    CONTINUE
      RETURN
      END
      SUBROUTINE VISCCT
      COMMON/CVP/A(33,15,9),G1(33,15),G2(33,15),RO(33,15),ZMU(33,15)
      COMMON/CINDEX/INDE(9),INDG,INDRO,INDZMU
      COMMON/CREFER/ROREF,PREF,ZMUREF,TREF,CPREF
      COMMON/CGRID/IMIN(33),IMAX(33),IN,JN,INM,JNM,IE
      COMMON/CNUMBR/NW,NF,NZML,NZMH,NZMF,NVT,NP
      COMMON/CYLI/JC1,JC2,IC,RADC1,RADC2,RADN,DCN,DN,JJC2,ICM,JC2M,JC1M
      COMMON/CPARAM/VINJ,VINP(15),TP,PP,TJ,PJ,PHIP,PHIJ
      COMMON/CZMUK/ZMUK
      COMMON/CX1X2/X1(33),X2(15),DELX1(33),DELX2(15)
C***********************************************************************
C    **VISCOSITY** SUBROUTINE
C    MIXTURE VISCOSITY
C***********************************************************************
      IF(INDZMU.EQ.1) GO TO 20
      ZMP=2.*(A(1,JN,NF)-A(1,1,NF))
      ZMJ=-2.*(A(IC,JC1,NF)-A(IC,1,NF))
      IF(INDG.EQ.2) ZMP=ZMP*3.14162
      IF(INDG.EQ.2) ZMJ=ZMJ*3.14162
      VINPSUM=0.0
      DO 40 J=1,JN
 40   VINPSUM=VINPSUM+VINP(J)
      VPMEAN=VINPSUM/FLOAT(JN)
      ZMVV=ZMP*VPMEAN**2+ZMJ*VINJ**2
      IF(INDE(NVT).EQ.1) ZMVV=ZMVV+ZMJ*(A(1,JC1-1,NVT)**2)
      ZMVV=ZMVV**0.33333
      AA=ZMUK*((2.*X2(JN))**0.666667)*ZMVV/((DCN)**0.33333)
      DO 10 J=1,JN
      IL=IMIN(J)
      IH=IMAX(J)
      DO 10 I=IL,IH
      ZMU(I,J)=AA*(RO(I,J)**0.666667)
 10   CONTINUE
      GO TO 30
 20   DO 21 J=1,JN
      IL=IMIN(J)
      IH=IMAX(J)
      DO 21 I=IL,IH
      ZMU(I,J)=ZMUREF
 21   CONTINUE
 30   CONTINUE
      RETURN
      END
      FUNCTION T(I,J)
      COMMON/CVP/A(33,15,9),G1(33,15),G2(33,15),RO(33,15),ZMU(33,15)
      COMMON/CNUMBR/NW,NF,NZML,NZMH,NZMF,NVT,NP
      COMMON/CCONST/PR(9),ZMW(3),CPJ(3),GCPM,GC,ZJC
      COMMON/CREFER/ROREF,PREF,ZMUREF,TREF,CPREF
      COMMON/CHEM/STC,STOX,HC,GLOB,ZEX
C***********************************************************************
C    TEMPERATURE CALCULATION
C***********************************************************************
      AFU=A(I,J,NZML)
      AFH=A(I,J,NZMH)
      TEMP=(AFH-AFU*HC)/CPREF
      T=TEMP
      RETURN
      END
```

```
      FUNCTION VS2(I,J)
      COMMON/CVP/A(33,15,9),G1(33,15),G2(33,15),RO(33,15),ZMU(33,15)
      VS2      =(G1(I,J)*G1(I,J)+G2(I,J)*G2(I,J))/(RO(I,J)*RO(I,J))
      RETURN
      END
      SUBROUTINE PRINCT  (ITAB)
      COMMON/CX1X2/X1(33),X2(15),DELX1(33),DELX2(15)
      COMMON/CVP/A(33,15,9),G1(33,15),G2(33,15),RO(33,15),ZMU(33,15)
      COMMON/CINDEX/INDE(9),INDG,INDRO,INDZMU
      COMMON/CNUMBR/NW,NF,NZML,NZMH,NZMF,NVT,NP
      COMMON/CGRID/IMIN(33),IMAX(33),IN,JN,INM,JNM,IE
      COMMON/CNAME/ATITLE(12),ASYMBL(12),ANAME(6,10)
      COMMON/CNITER/NITER
      COMMON/CVEXIT/VEXIT
      COMMON/CPARAM/VINJ,VINP(15),TP,PP,TJ,PJ,PHIP,PHIJ
      COMMON/CREFER/ROREF,PREF,ZMUREF,TREF,CPREF
      COMMON/CRAD/R(15)
      COMMON/CHEM/STC,STOX,HC,GLOB,ZEX
      COMMON/CYLI/JC1,JC2,IC,RADC1,RADC2,RADN,DCN,DN,JJC2,ICM,JC2M,JC1
      COMMON/CVARY/NHOT,NPUNCH,NREAD,NPRES
      DIMENSION W(33)
C***********************************************************************
C    ##PRINT## SUBROUTINE
C    THIS SUBR. PRINTS OUT PART OF THE RESULTS FOR EASY EXAMINATION
C***********************************************************************
      PRINT 500
      IQ=ITAB
      IT=6
      IF  (NHOT.EQ.0)  GO TO 80
      IF (NITER.EQ.1) GO TO 82
      DO 70 J=1,JN
      IL=IMIN(J)
      IH=IMAX(J)
      DO 70 I=IL,IH
      A(I,J,IT)=T(I,J)
70    CONTINUE
      IF(INDE(NVT).EQ.1) GO TO 80
80    IF(INDE(NP).EQ.1) IT=IT+1
      IF(INDE(NP).NE.1) GO TO 82
      IQ=IQ+1
      DO 50 J=1,JN
      IL=IMIN(J)
      IH=IMAX(J)
      DO 50 I=IL,IH
50    A(I,J,IT)=A(I,J,NP)
82    CONTINUE
      IX=1
      DO 10 K=1,IQ
      IF  ((K.EQ.NZMF).AND.(PHIP.EQ.PHIJ))  K=NZMF+1
      PRINT 100, (ANAME(L,K),L=1, 6), NITER
      DO 6 IP=1,3
      IF ((IP.EQ.2).AND.(IN.LE.21)) IP=3
      II1=12
      IF (IN.GT.21) II1=23
      IF(IP.EQ.1) IEND=11
      IF(IP.EQ.2) IEND=22
      IF (IP.EQ.3) IEND=IN
      DO 5 JJ=1,JN
      J=JN+1-JJ
      IF(IP.EQ.1) II1=1
      IF(IP.EQ.2) II1=12
      II2=IMAX(J)
      IF (IP.EQ.1) II2=11
      IF (IP.EQ.2) II2=22
      IF((K.NE.NW).AND.((INDE(K).NE.1).OR.(K.NE.NVT)))  GO TO 4
      DO 40 I=II1,II2,IX
      W(I)=A(I,J,K)
      IF((K.EQ.NVT).AND.(R(J).GT.0.0))  A(I,J,NVT)=W(I)/R(J)
 40   CONTINUE
 4    CONTINUE
      PRINT 101, J, (A(I, J, K), I = II1, II2, IX)
      IF((K.NE.NW).AND.((INDE(K).NE.1).OR.(K.NE.NVT)))  GO TO 5
      DO 41 I=II1,II2,IX
 41   A(I,J,K)=W(I)
 5    CONTINUE
      IF (IP.EQ.1) PRINT 102, (I,I=1,IEND)
      IF (IP.EQ.2) PRINT 102, (I,I=12,IEND)
      IF (IP.EQ.3) PRINT 102, (I,I=II1,IEND)
      PRINT 103
 6    CONTINUE
 10   CONTINUE
      IF (NITER.EQ.1) RETURN
      RENO=-42.750*A(1,1,2)/ZMU(1,1)
      PRINT 401, RENO
      ROSUM=0.0
      DO 20 J=JC2,JN
 20   ROSUM=ROSUM+RO(IN,J)
      ROMEAN=ROSUM/(FLOAT(JN)-FLOAT(JC2*))
      IF(INDG.EQ.1) VEXIT=-A(IN,JC2,NF)/((X2(JN)-X2(JC2))*ROMEAN)
      IF(INDG.EQ.2)  VEXIT=-2.*A(IN,JC2,NF)/((RADN*RADN-RADC2*RADC2)*
     1                ROMEAN)
      PRINT 301, VEXIT
 100  FORMAT(1H1,35X,21HTHE DISTRIBUTION OF  ,6A6//
     223H NUMBER OF ITERATION = ,I5//)
 101  FORMAT(1H ,I2,2X,11(1PE11.3))
 102  FORMAT(1H0/11I11///)
 103  FORMAT(1H0///)
 301  FORMAT(9H VEXIT = ,F8.3)
 401  FORMAT (/// 10X,
     1        55HREYNOLDS NO BASED ON MEAN MASS FLOW RATE AND MAX DIA = ,
     2     0PF7.1)
 500  FORMAT (1H7)
      RETURN
      END
      SUBROUTINE TABUCT   (ITAB)
      COMMON/CVP/A(33,15,9),G1(33,15),G2(33,15),RO(33,15),ZMU(33,15)
      COMMON/CGRID/IMIN(33),IMAX(33),IN,JN,INM,JNM,IE
      COMMON/CNAME/ATITLE(12),ASYMBL(12),ANAME(6,10)
      COMMON/CRAD/R(15)
      COMMON/CHEM/STC,STOX,HC,GLOB,ZEX
      COMMON/CYLI/JC1,JC2,IC,RADC1,RADC2,RADN,DCN,DN,JJC2,ICM,JC2M,JC1M
      COMMON/CNUMBR/NW,NF,NZML,NZMH,NZMF,NVT,NP
      COMMON/CINDEX/INDE(9),INDG,INDRO,INDZMU
      COMMON/CVARY/NHOT,NPUNCH,NREAD,NPRES
C*********************************************************************
C    **TABULATE** SUBROUTINE
C    THIS SUBR. TABULATES THE COMPLETE SET OF RESULTS
C*********************************************************************
      IT=ITAB
      IQ=IT
      IF (INDE(NP).EQ.1) IQ=IT+1
      IF  ((NHOT.EQ.0).AND.(INDE(NP).EQ.1))  IT=IQ
      IF (IE.EQ.5) IQ=IT
      IF ((IE.EQ.6).OR.(NHOT.EQ.0))  GO TO 21
      PRINT 101, (ASYMBL(K),K=1,IE),(ASYMBL(K),K=IT,IQ)
      GO TO 20
21    PRINT 101, (ASYMBL(K),K=1,IE)
20    CONTINUE
      ILINE=0
      DO 1 J=1,JN
      IL=IMIN(J)
      IH=IMAX(J)
      DO 1 I=1,IN
      ILINE=ILINE+1
      IF((I.LT.IL).OR.(I.GT.IH))  PRINT 104, I, J
      IF((I.LT.IL).OR.(I.GT.IH))  GO TO 10
      W=A(I,J,1)*R(J)
      V1=G1(I,J)/RO(I,J)
      V2=G2(I,J)/RO(I,J)
      IF(INDE(NVT).EQ.1) V3=A(I,J,NVT)
      IF(INDE(NVT).EQ.1.AND.R(J).GT.0.0) A(I,J,NVT)=V3/R(J)
      IF  ((IE.EQ.6).OR.(NHOT.EQ.0))  GO TO 22
      PRINT 102, I, J, V1, V2, RO(I,J), ZMU(I,J),W,(A(I,J,K),K=2,IE),
     1 (A(I,J,K),K=IT,IQ)
      GO TO 23
22    PRINT 102, I, J, V1, V2, RO(I,J), ZMU(I,J),W,(A(I,J,K),K=2,IE)
23    CONTINUE
      IF(INDE(NVT).EQ.1) A(I,J,NVT)=V3
   10 CONTINUE
      IF (ILINE/IN*IN.EQ.ILINE) PRINT 103
      IF ((IE.EQ.6).OR.(HC.EQ.0.0))  GO TO 24
      IF((IN.LT.33).AND.(ILINE/(2*IN)*(2*IN).EQ.ILINE))  PRINT 101,
     2(ASYMBL(K),K=1,IE),(ASYMBL(K),K=IT,IQ)
      IF((IN.EQ.33).AND.(ILINE/(  IN)*(  IN).EQ.ILINE))  PRINT 101,
     2(ASYMBL(K),K=1,IE),(ASYMBL(K),K=IT,IQ)
      GO TO 25
24    IF((IN.LT.33).AND.(ILINE/(2*IN)*(2*IN).EQ.ILINE))  PRINT 101,
     2(ASYMBL(K),K=1,IE)
      IF((IN.EQ.33).AND.(ILINE/(  IN)*(  IN).EQ.ILINE))  PRINT 101,
     2(ASYMBL(K),K=1,IE)
25    CONTINUE
1     CONTINUE
101   FORMAT(10H1    I    J,48H          V1           V2        DENSITY
     1VISC  ,6(6X,A6))
102   FORMAT(1H ,2I5,10(1PE12.3))
103   FORMAT(1H )
104   FORMAT(1H ,2I5)
      RETURN
      END
      SUBROUTINE PLOTCT  (ITAB)
      COMMON/CVP/A(33,15,9),G1(33,15),G2(33,15),RO(33,15),ZMU(33,15)
      COMMON/CGRID/IMIN(33),IMAX(33),IN,JN,INM,JNM,IE
      COMMON/CNUMBR/NW,NF,NZML,NZMH,NZMF,NVT,NP
      COMMON/CINDEX/INDE(9),INDG,INDRO,INDZMU
      COMMON/CNAME/ATITLE(12),ASYMBL(12),ANAME(6,10)
      COMMON/CYLI/JC1,JC2,IC,RADC1,RADC2,RADN,DCN,DN,JJC2,ICM,JC2M,JC1M
      COMMON/CHEM/STC,STOX,HC,GLOB,ZEX
      COMMON/CRAD/R(15)
      DIMENSION X(120),XA(9),VJ(9),C(11),Y(41)
      DATA INTVAL,NVJ1/3,7/
      DATA XEMTY,XBOUN,(XA(L),L=1,9)/1H ,1H.,1H1,1H2,1H3,1H4,1H5,1H6,
     1                                 1H7,1H8,1H9/
C***********************************************************************
C    **PLOTTING** SUBROUTINE
C    THIS SUBR. GIVES APPROX. CONTOUR-PLOTS OF THE DEPENDENT VAR.
C    ALSO OF TEMPERATURE
C***********************************************************************
C
C****      INTVAL=NUMBER OF LINE-SPACING BETWEEN TWO J-LINES
C****      NVJ=NUMBER OF CONTOUR-LINES TO BE PLOTTED FOR EACH VARIABLE
C
      DO 20 J=1,JN
      DO 20 I=1,IN
      A(I,J,NW)=A(I,J,NW)*R(J)
      IF((INDE(NVT).EQ.1).AND.(R(J).GT.0.0))  A(I,J,NVT)=A(I,J,NVT)/R(J)
 20   CONTINUE
      IX=IN/10
      JX=JN/10
      IF(IN.LT.10) IX=1
      IF(JN.LT.10) JX=1
      IQ=ITAB
      DO 900 K=1,IQ
      IF  (K.EQ.(IE+1))  K=K+1
      IF  (K.EQ.(IE+3))  K=IQ
      IF(K.EQ.NF)  GO TO 30
      NVJ=NVJ1
      IF  (K.EQ.NW)  NVJ=5
      IF(K.EQ.NZK) GO TO 900
      IF(K.EQ.NZML) GO TO 7
      IF(NVJ.EQ.1) NVJ=NVJ1
C****      FINDING MAX., MIN. AND MEAN VALUES IN THE FIELD AND
C****      HENCE DETERMINING THE INTERVALS
      VMIN=A(5,5,K)
      VMAX=A(8,8,K)
      SUM=0.
      NSUM=0
      DO 1 J=1,JN,JX
      II1=IMIN(J)
      II2=IMAX(J)
      DO 1 I=II1,II2,IX
      IF(A(I,J,K).GT.VMAX) VMAX=A(I,J,K)
      IF(A(I,J,K).LT.VMIN) VMIN=A(I,J,K)
      SUM=SUM+A(I,J,K)
1     NSUM=NSUM+1
      VMEAN=SUM/FLOAT(NSUM)
      VSTEP1=(VMEAN-VMIN)/3.
      VSTEP2=(VMAX-VMEAN)/3.
      VJ(1)=VMIN+VSTEP1
      VJ(2)=VJ(1)+VSTEP1
      VJ(3)=VMEAN
      VJ(4)=VMEAN+VSTEP2
      VJ(5)=VJ(4)+VSTEP2
      VJ(6)=0.95*VMAX
      VJ(7)=1.05*VMIN
C
C SPECIAL VJ VALUES FOR OPPOSED JET PROBLEM
C
      GO TO 8
30    VJ(1)=A(1,3,NF)
      VJ(2)=A(1,(JN-6),NF)
      VJ(3)=A(1,(JN-4),NF)
      VJ(4)=A(1,(JN-2),NF)
      VJ(5)=A(1,(JN-1),NF)
      VJ(6)=A(1,1,NF)
      VJ(7)=A(IC,JC1,NF)
      VJ(8)=1.02*A(IC,JC1,NF)
      VJ(9)=1.05*A(IC,JC1,NF)
      NVJ=9
      GO TO 8
7     NVJ=1
      VJ(1)=STC/(1.+STC)
8     CONTINUE
C  END SPECIAL VJ VALUFS FOR C-T PROBLEM
C
C****    PRINT OUT CONSTANT VALUES TO BE PLOTTED
      PRINT 101,ASYMBL(K)
      PRINT 102,(VJ(L),L=1,NVJ)
      PRINT 202
      DO 90 JJ=1,JN,JX
      J=JN+1-JJ
      II1=IMIN(J)
      II2=IMAX(J)
      L1=(IMIN(J)/IX-1/IX)*10+1
      L2=(IMAX(J)/IX-1/IX)*10+1
      L3=(IC/IX)*10-3
      IF (IN.LE.21) L3=(IC/IX)*10
      L4=(IN/IX-1/IX)*10 + 1
      IB=IX-1/IX+IMIN(J)
C****    BOUNDARIES FOR THE PRUBLEM
      DO 80 JJN=1,INTVAL
      DO 100 L=1,101
100   X(L)=XEMTY
      X(L1)=XBOUN
      IF  ((J.LE.JC1).AND.(J.GT.1))  L2=L3
      X(L2)=XBOUN
      IF((J.EQ.JN).AND.(JJN.EQ.1))  GO TO 200
      IF((J.EQ.1).AND.(JJN.EQ.1))  GO TO 200
      GO TO 300
  200 DO 201 L=L1,L4
  201 X(L)=XBOUN
      GO TO 390
  300 CONTINUE
C
C****    SPECIAL BOUNDARIES FOR THE COMBUSTION-CHAMBER PROBLEM
C
      IF (((J.LE.JC2).AND.(J.GT.JC1)).OR.((J.EQ.JC1).AND.(JJN.EQ.1)))
     1 GO TO 405
      GO TO 400
  405 DO 406 L=L3,L4
  406 X(L)=XBOUN
  400 CONTINUE
  390 CONTINUE
C****    INTERPOLATION BETWEEN TWO CONSECUTIVE J-LINES
      J1=J-JX
      IF((J.EQ.JC2).AND.(JJN.NE.1)) II2=IC
      DO 70 I=II1,II2
      IF ((J.EQ.1).OR.((J.EQ.JC2).AND.(I.GT.IC)))  GO TO 65
      DELAJ=(A(I,J1,K)-A(I,J,K))/FLOAT(INTVAL)
      GO TO 70
   65 DELAJ=0.
   70 Y(I)=A(I,J,K)+FLOAT(JJN-1)*DELAJ
C****    INTERPOLATION BETWEEN TWO I-LINES
      DO 60 I=IB,II2,IX
      IMARK=0
      I1=I-IX
      IF(IX.EQ.2) GO TO 71
      GO TO 79
   71 DELY1=(Y(I1+1)-Y(I1))/5.
      DO 72   IJK=1,6
   72 C(IJK)=Y(I1)+FLOAT(IJK-1)*DELY1
      DELY2=(Y(I)-Y(I1+1))/5.
      DO 73 IJK=7,11
   73 C(IJK)=Y(I1+1)+FLOAT(IJK-6)*DELY2
      GO TO 74
   79 CONTINUE
      DELY=(Y(I)-Y(I1))/10.
      DO 50 IJK=1,11
   50 C(IJK)=Y(I1)+FLOAT(IJK-1)*DELY
   74 CONTINUE
      DO 40 KL=1,NVJ
      DO 40 IJK=1,10
      IF((IX.EQ.2).AND.(IJK.LT.6))  DELY=DELY1
      IF((IX.EQ.2).AND.(IJK.GE.6))  DELY=DELY2
      NN=0
      IF((VJ(KL).GE.C(IJK)).AND.(VJ(KL).LE.(C(IJK)+DELY/2.))) NN=IJK
      IF((VJ(KL).GE.(C(IJK)+DELY/2.)).AND.(VJ(KL).LE.C(IJK+1))) NN=IJK+1
      IF((VJ(KL).LE.C(IJK)).AND.(VJ(KL).GE.(C(IJK)+DELY/2.))) NN=IJK
      IF((VJ(KL).LE.(C(IJK)+DELY/2.)).AND.(VJ(KL).GE.C(IJK+1))) NN=IJK+1
      IF(NN.EQ.0) GO TO 44
      GO TO 41
```

```
44     IF((IMARK.EQ.0).AND.(JJN.NE.1).AND.(IJK.EQ.10))  GO TO 45
       GO TO 40
45     DELAJ=(A(I,J1,K)-A(I,J,K))/FLOAT(INTVAL)
       CTOP =A(I,J,K)+FLOAT(JJN-2)*DELAJ
       IF((VJ(KL).LE.(CTOP+DELAJ/2.)).AND.(VJ(KL).GE.(C(11)+DELAJ/2.)))
     1    NN=11
       IF((VJ(KL).GE.(CTOP+DELAJ/2.)).AND.(VJ(KL).LE.(C(11)+DELAJ/2.)))
     1    NN=11
       IF(NN.EQ.0) GO TO 40
41     N1=(I1/IX)*10
       N2=N1+NN
       X(N2)=XA(KL)
       IMARK=1
40     CONTINUE
C****      PLOTTING OF ALL POINTS ON ONE J-LINE
60     CONTINUE
       IF((JJN.EQ.1).AND.(J.NE.JN))   GO TO 61
       GO TO 62
61     IF((K.EQ.NF).AND.(J.EQ.1))  GO TO 67
802    DO 63 L5=L1,L2,10
63     X(L5)=XBOUN
       IF((K.EQ.NF).AND.(J.EQ.JC2))  GO TO 64
       GO TO 62
64     DO 66 L5=L3,L4,2
66     X(L5)=XBOUN
       GO TO 62
67     DO 69  L5=L1,L3,2
69     X(L5)=XBOUN
62     CONTINUE
       IF (JJN.EQ.1) PRINT 104, J,(X(IP),IP=1, 101)
       IF (JJN.NE.1) PRINT 105, (X(IP),IP=1, 101)
       IF(J.EQ.1)  GO TO 90
80     CONTINUE
90     CONTINUE
       PRINT 302, (IZ,IZ=1,IN,IX)
900    CONTINUE
101    FORMAT(25H1CONSTANT-VALUE PLOT OF   ,A6//23H NUMBERS REFER TO THE
     139HCONSTANT-VALUES PLOTTED,VALUES BEING...//)
102    FORMAT(1H ,3H1= ,1PE12.4,    1H,,3X,
     1              3H2= ,1PE12.4,    1H,,3X,
     2              3H3= ,1PE12.4,    1H,,3X,
     3              3H4= ,1PE12.4,    1H,,3X,
     4              3H5= ,1PE12.4/
     5             4H 6= ,1PE12.4,    1H,,3X,
     6              3H7= ,1PE12.4,    1H,,3X,
     7              3H8= ,1PE12.4,    1H,,3X,
     8              3H9= ,1PE12.4)
103    FORMAT(1H1)
104    FORMAT(1H ,I2,10X,101A1)
105    FORMAT(1H ,12X,101A1)
202    FORMAT(1H0///)
302    FORMAT(1HZ//12X,11(I2,8X)/)
       RETURN
       END
```

```
      FUNCTION ADF(I,J,LX,KQ)
      COMMON/CVP/A(33,15,9),G1(33,15),G2(33,15),RO(33,15),ZMU(33,15)
      COMMON/CYLI/JC1,JC2,IC,RADC1,RADC2,RADN,DCN,DN,JJC2,ICM,JC2M,JC1M
      COMMON/CX1X2/X1(33),X2(15),DELX1(33),DELX2(15)
      COMMON/CGRID/IMIN(33),IMAX(33),IN,JN,INM,JNM,IE
      DIMENSION AQ(33,15,14)
      DIMENSION BENQ(20),BWSR(20),BP(20)
      EQUIVALENCE (A(1,1,1),AQ(1,1,1))
      DF(PN,BENQ,BWSR,BP,XENQ,XWSR)=((XENQ*XENQ-XWSR*XWSR)*BP+
     1      XWSR*XWSR*BENQ-XENQ*XENQ*BWSR)/(XENQ*XWSR*(PN*XENQ+XWSR))
C***********************************************************************
C   THIS FUNCTION EVALUATES FIRST DERVIATIVES ACCORDING
C   TO THE THREE-POINT QUADRATIC APPROXIMATION
C***********************************************************************
C
C****     DEPENDING ON THE POSITION OF THE POINT (I,J), THERE
C****     ARE FIVE DIFFERENT EXPRESSIONS FOR THE DERIVATIVE
C
      M=1
      IF((J.EQ.1).OR.((J.EQ.JC2).AND.(I.LE.IN).AND.(I.GE.IC))) GO TO 92
      IF(I.EQ.1)  GO TO 93
      IF ( J.EQ.JN)  GO TO 94
      IF(((I.EQ.IC).AND.(J.LE.JC2).AND.(J.GE.JC1)).OR.
     1   ((I.EQ.IN).AND.(J.LE.JN).AND.(J.GE.JC2))) M=5
      GO TO 99
92    M=2
      GO TO 99
93    M=3
      GO TO 99
94    M=4
99    CONTINUE
      GO TO (1,2,3,4,5),M
C****     M=1....FOR POINTS NOT ON ANY OF THE BOUNDARIES
1     PN=1.
      IF(LX.EQ.1) GO TO 12
13    IF((J.EQ.1).OR.(J.EQ.JC2))  GO TO 21
      IF(J.EQ.JN) GO TO 41
      DO 10 L=1,14
      BENQ(L)=AQ(I,J+1,L)
      BWSR(L)=AQ(I,J-1,L)
10    BP(L)=AQ(I,J,L)
      XENQ=X2(J+1)-X2(J)
      XWSR=X2(J)-X2(J-1)
      GO TO 100
12    IF(I.EQ.1) GO TO 31
      IF(((I.EQ.IC).AND.(J.EQ.1)).OR.(I.EQ.IN))  GO TO 51
      DO 11 L=1,14
      BENQ(L)=AQ(I+1,J,L)
      BWSR(L)=AQ(I-1,J,L)
11    BP(L)=AQ(I,J,L)
      XENQ=X1(I+1)-X1(I)
      XWSR=X1(I)-X1(I-1)
      GO TO 100
```

```
C****      M=2....FOR POINTS ON THE BOUNDARY J=1
2       IF(LX.EQ.1) GO TO 1
21      PN=-1.
        DO 20 L=1,14
        BENQ(L)=AQ(I,J+1,L)
        BWSR(L)=AQ(I,J+2,L)
20      BP(L)=AQ(I,J,L)
        XENQ=X2(J+1)-X2(J)
        XWSR=X2(J+2)-X2(J)
        GO TO 100
C****      M=3....FOR POINTS ON THE IAB-PLANE
3       IF(LX.NE.1) GO TO 1
31      PN=-1.
        DO 30 L=1,14
        BENQ(L)=AQ(I+1,J,L)
        BWSR(L)=AQ(I+2,J,L)
30      BP(L)=AQ(I,J,L)
        XENQ=X1(I+1)-X1(I)
        XWSR=X1(I+2)-X1(I)
        GO TO 100
C****      M=4....FOR POINTS ON ALL WALLS PARALLEL TO THE J-LINES,
C****      BEYONN THE IAB-PLANE
4       IF(LX.EQ.1) GO TO 1
41      PN=-1.
        DO 40 L=1,14
        BENQ(L)=AQ(I,J-1,L)
        BWSR(L)=AQ(I,J-2,L)
40      BP(L)=AQ(I,J,L)
        XENQ=X2(J-1)-X2(J)
        XWSR=X2(J-2)-X2(J)
        GO TO 100
C****      M=5....FOR POINTS ON THE WALL OF I=IC AND THOSE ON THE EXIT
5       IF(LX.NE.1) GO TO 1
51      PN=-1.
        DO 50 L=1,14
        BENQ(L)=AQ(I-1,J,L)
        BWSR(L)=AQ(I-2,J,L)
50      BP(L)=AQ(I,J,L)
        XENQ=X1(I-1)-X1(I)
        XWSR=X1(I-2)-X1(I)
100     CONTINUE
        IF(KQ.LT.15) GO TO 101
C****      EVALUATION OF DERIVATIVES FOR V1  (KQ=15) AND V2  (KQ=16)
        BENQ(15)=BENQ(10)/BENQ(12)
        BENQ(16)=BENQ(11)/BENQ(12)
        BWSR(15)=BWSR(10)/BWSR(12)
        BWSR(16)=BWSR(11)/BWSR(12)
        BP(15)=BP(10)/BP(12)
        BP(16)=BP(11)/BP(12)
C****
101     CONTINUE
        ADF=DF(PN,BENQ(KQ),BWSR(KQ),BP(KQ),XENQ,XWSR)
        RETURN
        END
```

```
      SUBROUTINE PRESCT
      COMMON/CVP/A(33,15,9),G1(33,15),G2(33,15),RO(33,15),ZMU(33,15)
      COMMON/CYLI/JC1,JC2,IC,RADC1,RADC2,RADN,DCN,DN,JJC2,ICM,JC2M,JC1M
      COMMON/CX1X2/X1(33),X2(15),DELX1(33),DELX2(15)
      COMMON/CGRID/IMIN(33),IMAX(33),IN,JN,INM,JNM,IE
      COMMON/CREFER/POREF,PREF,ZMUREF,TREF,CPREF
      COMMON/CNUMBR/NW,NF,NZML,NZMH,NZMF,NVT,NP
      COMMON/CRAD/R(15)
      COMMON/CCONST/PR(9),ZMW(3),CPJ(3),GCPM,GC,ZJC
      COMMON/CINDEX/INDE(9),INDG,INDRO,INDZMU
      DIMENSION PI(33),PJ(33),P1(33),P2(33),P3(33),P4(33),AQ(33,15,14)
      EQUIVALENCE (A(1,1,1),AQ(1,1,1))
C***********************************************************************
C    ##PRESSURE## (STATIC) SUBROUTINE
C    THIS SUBROUTINE  EVALUATES PRESSURE FIELD.  VALUES ALONG #JREF#
C    EVALUATED FIRST, THEN VALUES FOR THE RECTANGLE BOUNDED BY I1,I2,J1,
C    AND J2 DETERMINED BY INTEGRATION ALONG LINES PERPENDICULAR TO IT,
C    VALUES FOR THE REST OF THE FIELD BOUNDED BY I2,I3,J1 AND J3
C    ARE THEN EVALUATED BY INTEGRATION ALONG LINES PARALLEL TO JREF.....
C***********************************************************************
      I1=1
      I2=IC
      I3=IN
      J1=1
      J2=JC2
      J3=JN
      PP=PREF
C****     DETERMINING REFERENCE J-LINE
      JREF=JC2+3
      JK1=JREF-2
      JK2=JREF+2
CC
C****     EVALUATING P#S ALONG THE REFERENCE J-LINE, STARTING FROM
C****     THE INLET NODE......UP TO STATEMENT 6.
CC
C****     EVALUATING D(.....)/DZ TERM IN EXPRESSION FOR DP/DZ
      DO 1 J=JK1,JK2
      II2=IMAX(J)
      DO 1 I=I1,II2
1     AQ(I,J,14)=R(J)*G2(I,J)/RO(I,J)
      II2=IMAX(JREF)
      DO 2 I=I1,II2
2     AQ(I,JREF,14)=ZMU(I,JREF)*(1.33333*ADF(I,JREF,1,15)-
     1    0.66667*ADF(I,JREF,2,14)/R(JREF))-(G1(I,JREF)**2)/RO(I,JREF)
      DO 3 I=I1,I2
C****     EVALUATING  DP/DZ #S
3     A(I,JREF,NP)=ADF(I,JREF,I,14)
      DO 4 J=JK1,JK2
      II2=IMAX(J)
      DO 4 I=I1,II2
4     AQ(I,J,14)=R(J)*(ZMU(I,J)*(ADF(I,J,2,15)+ADF(I,J,1,16))
     1               -G1(I,J)*G2(I,J)/RO(I,J))
      DO 5 I=I1,I2
```

```
C****     EVALUATING P≠S ALONG THE REFERENCE J-LINE
5         A(I,JREF,NP)=(A(I,JREF,NP)+ADF(I,JREF,2,14)/R(JREF))/GC
          PI(I1)=PP
          II1=I1+1
          DO 6 I=II1,I2
C****     END FOR EVALUATION OF P≠S ALONG THE REFERENCE J-LINE
CC
CC
C****     EVALUATION OF DP/DR≠S FOR THE RECTANGLE BOUNDED BY
C****      I1, I2, J1, J3......UP TO STATEMENT 108
CC
C****     (DIV V)≠S
6         PI(I)=PI(I-1)+0.5*(A(I-1,JREF,NP)+A(I,JREF,NP))*(X1(I)-X1(I-1))
          DO 100 J=J1,J3
          DO 100 I=I1,I2
100       AQ(I,J,14)=R(J)*G2(I,J)/RO(I,J)
          DO 101 J=J1,J3
          DO 101 I=I1,I2
          A(I,J,NP)=ADF(I,J,1,15)
101       IF(J.GT.1) A(I,J,NP)=A(I,J,NP)+ADF(I,J,2,14)/R(J)
C****        EVALUATION OF (TERMS FOR CYL. CO-ORDINATES ONLY) +
C****        D(.....)/DR TERM
          DO 102 J=J1,J3
          DO 102 I=I1,I2
          AQ(I,J,14)=R(J)*(ZMU(I,J)*(2.0*ADF(I,J,2,16)-0.66667*A(I,J,NP))
         1              -(G2(I,J)**2)/RO(I,J))
          IF((INDG.EQ.2).AND.(R(J).GT.0.0)) A(I,J,NP)=ZMU(I,J)*(2.*G2(I,J)/
         1         (RO(I,J)*R(J))-0.66667*A(I,J,NP))/R(J)
          IF((INDE(NVT).EQ.1).AND.(R(J).GT.0.0)) A(I,J,NP)=
         1                RO(I,J)*(A(I,J,NVT)**2)/(R(J)**3)-A(I,J,NP)
102       CONTINUE
          JJ1=2
          DO 103 J=JJ1,J3
          DO 103 I=I1,I2
103       A(I,J,NP)=A(I,J,NP)*FLOAT(INDG-1)+ADF(I,J,2,14)/R(J)
C****        EVALUATING   DP/DR ≠S
          DO 104 J=J1,J3
          II2=IMAX(J)
          DO 104 I=I1,II2
104       AQ(I,J,14)=ZMU(I,J)*(ADF(I,J,2,15)+ADF(I,J,1,16))-
         1                GI(I,J)*G2(I,J)/RO(I,J)
          DO 105 J=JJ1,J3
          DO 105 I=I1,I2
105       A(I,J,NP)=(A(I,J,NP)+ADF(I,J,1,14))/GC
          DO 107 I=I1,I2
107       A(I,1,NP)=0.0
108       CONTINUE
C****        END EVALUATION OF DP/DR≠S.....NEXT EVALUATE P≠S .....UP TO 200
          DO 200 I=I1,I2
          PJ(JREF)=PI(I)
          JJ1=JREF+1
          DO 202 J=JJ1,J3
          PJ(J)=PJ(J-1)+0.5*(A(I,J-1,NP)+A(I,J,NP))*(X2(J)-X2(J-1))
202       A(I,J-1,NP)=PJ(J-1)/PP-1.000000
```

```
      A(I,J3,NP)=PJ(J3)/PP-1.000000
      JJ1=J1+1
      DO 250 JX=JJ1,JREF
      J=JREF-JX+1
      PJ(J)=PJ(J+1)+0.5*(A(I,J+1,NP)+A(I,J,NP))*(X2(J+1)-X2(J))
 250  A(I,J+1,NP)=PJ(J+1)/PP-1.000000
      A(I,1,NP)=PJ(J1)/PP-1.000000
 200  CONTINUE
C****    END EVALUATION OF P*S IN THE FIRST RECTANGLE.
CC
CC
C****    EVALUATING DP/DZ*S IN THE SECOND RECTANGLE BOUNDED BY
C****      I2, I3, J2, J3............UP TO STATEMENT 306
CC
C****    (DIV V)*S
      DO 300 J=J2, J3
      PJ(J)=(A(I2,J,NP)+1.000000)*PP
      P1(J)=A(I2-1,J,NP)
 300  P2(J)=A(I2-2,J,NP)
      II1=I2-2
      DO 301 J=J2, J3
      II3=IMAX(J)
      DO 301 I=II1,II3
 301  AQ(I,J,14)=R(J)*G2(I,J)/RO(I,J)
      DO 302 J=J2, J3
      II3=IMAX(J)
      DO 302 I=II1,II3
      A(I,J,NP)=ADF(I,J,1,15)
 302  IF(J.GT.1) A(I,J,NP)=A(I,J,NP)+ADF(I,J,2,14)/R(J)
C****    EVALUATING D(.....)/DZ  TERM IN EXPRESSION FOR  DP/DZ
      DO 303 J=J2,J3
      DO 303 I=II1,I3
 303  AQ(I,J,14)=ZMU(I,J)*(2.0*ADF(I,J,1,15)-0.6667*A(I,J,NP))
     1          -(G1(I,J)**2)/RO(I,J)
      DO 304 J=J2,J3
      DO 304 I=I2,I3
 304  A(I,J,NP)=ADF(I,J,1,14)
C****    EVALUATING COMPLETE  DP/DZ *S
      DO 305 J=J2, J3
      II3=IMAX(J)
      DO 305 I=I2,II3
      AQ(I,J,14)=ZMU(I,J)*ADF(I,J,1,16)-G1(I,J)*G2(I,J)/RO(I,J)
 305  IF(J.GT.1) AQ(I,J,14)=AQ(I,J,14)+ZMU(I,J)
     1                       *ADF(I,J,2,15)
      DO 306 J=J2,J3
      DO 306 I=I2,I3
      A(I,J,NP)=(A(I,J,NP)+ADF(I,J,2,14))/GC
      IF((INDG.EQ.2).AND.(R(J).EQ.0.0)) A(I,J,NP)=(A(I,J,NP)
     1          +ADF(I,J,2,14))/GC
      IF((INDG.EQ.2).AND.(R(J).GT.0.0)) A(I,J,NP)=(A(I,J,NP)
     1                 +AQ(I,J,14)/R(J))/GC
 306  CONTINUE
C****    END EVALUATION OF DP/DZ*S .....START EVALUATING P*S
      DO 307 J=J2,J3
      PI(I2)=PJ(J)
      II1=I2+1
      DO 308 I=II1,I3
      PI(I)=PI(I-1)+0.5*(A(I-1,J,NP)+A(I,J,NP))*(X1(I)-X1(I-1))
308   A(I-1,J,NP)=PI(I-1)/PP-1.000000
      A(I3,J,NP)=PI(I3)/PP-1.000000
307   CONTINUE
      DO 309 J=J2, J3
      A(I2-1,J,NP)=P1(J)
309   A(I2-2,J,NP)=P2(J)
900   CONTINUE
      RETURN
      END
```

APPENDIX E

Experimental Data Reduction Program

E.1 Introduction

Below is listed program EDIZA, the data reduction program for the raw experimental data. Comments are included throughout the program to make it self-explanatory. An explanation of the input variables procedes the program listing. The user is referred to the schematic diagram of the experimental apparatus, Figure A.1a, for assistance in clarifying the input data. Following the program listing are the actual experimental data.

E.2 Input Variables

FORTRAN Name	Definition
PHN3	fuel tank pressure (psig)
PBAR	barometric pressure (in. Hg)
TAMB	ambient temperature (°F)
PO	main air orifice pressure (psig)
P(2)	pressure upstream main air valve (psig)
P(3)	pressure downstream main air valve (psig)
T(1)	main air orifice temperature (mv)
D1,D2	left and right leg of main air metering manometer (in. H_2O)
PMNH3(1)	pressure downstream main fuel regulator (psig)
PMNH3(2)	pressure upstream main fuel valve (psig)
PMNH3(3)	main fuel rotometer pressure (psig)
T(2)	main fuel rotometer temperature (mv)

FORTRAN Name	Definition
DMNH3	main fuel rotometer deflection (cm)
PJAIR(2)	pressure upstream jet air valve (psig)
PJAIR(3)	jet air rotometer pressure (psig)
T(3)	jet air rotometer temperature (mv)
DJAIR	jet air rotometer deflection (cm)
PJNH3(1)	pressure downstream jet fuel valve (psig)
PJNH3(2)	pressure upstream jet fuel valve (psig)
PJNH3(3)	jet fuel rotometer pressure (psig)
T(4)	jet fuel rotometer temperature (mv)
DS	jet fuel rotometer deflection, steel ball (cm)
DG	jet fuel rotometer deflection, glass ball (cm)
PJET	pressure of combined jet fuel and air (psig)
T(6)	temperature of combined jet fuel and air (mv)
T(7)	temperature of jet at nozzle entry (mv)
PAPR	pressure at inlet to Vycor (in. H_2O)
T(5)	temperature at inlet to Vycor (mv)
T(8),T(9), T(10),T(11)	temperature in asbestos lagging (mv)
TE(I)	temperature of reacting flow (mv)

E.3 EDIZA Listing

```
      PROGRAM EDIZA (INPUT,OUTPUT)
      DIMENSION T(11),PMNH3(3), PJNH3(3), PJAIR(3), PMAIR(3)
      DIMENSION RTE(10), TE(10)
C
C***********************************************************************
C
C
C
10    READ 100,IRUN, PNH3, PBAR, TAMB, COMM
      IF (PNH3.EQ.0.0) STOP
C
      READ 101, PO, PMAIR(2), PMAIR(3), T(1), D1, D2, PMNH3(1),
     1 PMNH3(2), PMNH3(3), T(2), DMNH3
C
      READ 101, PJAIR(2), PJAIR(3), T(3), DJAIR, PJNH3(1), PJNH3(2),
     1 PJNH3(3), T(4), DJNH3S, DJNH3G
C
      READ 101, PJET, T(6), T(7), PAPR, T(5), (T(I),I=8,11)
      T(7)=22.00
      IF  (IRUN.LE.12)  T(7)=T(6)
C
C
      DO 1  I=1,11
1     T(I)=CHRMAL(T(I))
      ORFCJ=0.063
C
      PRINT 103,IRUN, COMM, ORFCJ, PNH3, TAMB, PBAR
C
      PBAR=PBAR/2.036
      PPMAIR=(PMAIR(2)+PBAR)/(PMAIR(3)+PBAR)
      PPMNH3=(PMNH3(2)+PBAR)/(PMNH3(3)+PBAR)
      PPJNH3=(PJNH3(2)+PBAR)/(PJNH3(3)+PBAR)
      PPJAIR=(PJAIR(2)+PBAR)/(PJAIR(3)+PBAR)
C
      PRINT 104, PO, PMNH3(1), PJNH3(1), PJAIR(2), PJET, PMAIR(2),
     1PMNH3(2), PJNH3(2), PJAIR(3), T(6), PMAIR(3), PMNH3(3), PJNH3(3),
     2T(3),T(7),T(1), T(2), T(4), DJAIR, D1, DMNH3, DJNH3S, D2, DJNH3G,
     3 PPMAIR, PPMNH3, PPJNH3, PPJAIR
C
      IF(IRUN.EQ.23) GO TO 52
      IF ((IRUN.GT.23).AND.(IRUN.LE.35))  GO TO 53
      GO TO 50
52    READ 110, (RTE(L), TE(L), L=1,10)
      DO 2 L=1,10
2     TE(L)=PT13RO(TE(L))
53    PRINT 105, (RTE(L), L=1,10), PAPR, (TE(L),L=1,10), T(8), T(5),
     1 T(9), T(10), T(11)
      GO TO 51
50    CONTINUE
      PRINT 112, PAPR, T(8), T(5), T(9), T(10), T(11)
51    CONTINUE
C
      DO 8 I=1,7
```

```
8     T(I)=T(I)+460.
C
C*****APPROACH**********************************************************
C
      I=0
      PAPR=PAPR/27.73 + PBAR
      CALL  NH3 (PBAR, PMNH3(3), T(2), DMNH3, 0.0, I, FSM, QMNH3)
      CALL MAIR (PBAR, PO, T(1), D1, D2, ASM, QMAIR)
      TREY=T(1)-460.
      VISC=.00001*(1.1+TREY*(.0018-4.99E-07*TREY))
      RE=ASM*48./(VISC*3.1416*2.067)
      PHIP=FSM/(ASM*.165)
      AREAP=3.1416*(5.7/2.54)**2/(4.*144.)
      ZMEANP=(ASM+FSM)/(ASM/28.97+FSM/17.03)
      RHOP=PAPR*144.*ZMEANP/(1545.*T(5))
      TSM=ASM+FSM
      VINP=TSM/(AREAP*RHOP)
C
C*****JET***************************************************************
C
      I=1
      CALL  NH3 (PBAR, PJNH3(3), T(4), DJNH3S, DJNH3G, I, FSJ, QJNH3)
      CALL JAIR (PBAR, PJAIR(3),  T(3), DJAIR, ASJ, QJAIR)
      TSJ=FSJ+ASJ
      PHIJ=FSJ/(ASJ*.165)
      AJRAT=(TSJ/TSM)*100.
C
C*****JET EXIT**********************************************************
C
      PJET=PJET+PBAR
      RATAREA=(0.125/ORFCJ)**2
      GKJ=(ASJ*1.4+FSJ*1.29)/TSJ
      ZMEANJ=TSJ/(ASJ/28.97+FSJ/17.03)
      RHOJ2=PJET*144.*ZMEANJ/(1545.*T(7))
      AREAJ2=(3.1416*(0.125)**2)/(4.*144.)
      A2=SQRT(GKJ*1545.*T(7)*32.2/ZMEANJ)
      VJET2=TSJ/(AREAJ2*RHOJ2)
      AMACH2=VJET2/A2
      AREAJE=(3.1416*(ORFCJ)**2)/(4.*144.)
      AMACHE=AMACH2+.05
      GKEX=(GKJ+1.)/(2.*(GKJ-1.))
      XX=.05
      GO TO 32
33    XX=.005
      AMACHE=AMACHE-.05
32    ICT=0
30    ICT=ICT+1
      AMACHE=AMACHE+XX
      IF (ICT.EQ.20) GO TO 34
      TRATE=(1.+(GKJ-1.)/2.*AMACH2**2)/(1.+(GKJ-1.)/2.*AMACHE**2)
      GARNET=AMACHE*TRATE**GKEX/(RATAREA*AMACH2)
      IF (GARNET-1.0) 30,31,31
31    IF (XX.EQ..05) GO TO 33
34    PRINT 111, GARNET, AMACH2, AMACHE
```

```
      TJETE=TRATE*T(7)
      GKEX=1./(1.-GKJ)
      RHOJE=RHOJ2*TRATE**GKEX
      VINJ=TSJ/(RHOJE*AREAJE)
      PJETE=RHOJE*1545.*TJETE/(144.*ZMEANJ)
      TJETE=TJETE-460.
      T(5)=T(5)-460.
C
C***********************************************************************
C
      PRINT 106, ASM, FSM, FSJ, ASJ, QMAIR, QMNH3, QJNH3, QJAIR, RE
C
      PRINT 107,                 TSM, TSJ, VINP, VINJ, T(5), TJETE, PAPR,
     1 PJETE, RHOP, RHOJE, PHIP, PHIJ
      PRINT 108, AJRAT
      PRINT 102
      GO TO 10
C
100   FORMAT (I5, 3F5.0, A10)
101   FORMAT (16F5.2)
102   FORMAT (1H ,*NOTE - P(1)...REGULATOR PRESSURE, P(2)...UPSTREAM VAL
     2VE PRESSURE, P(3)..DOWNSTREAM VALVE AND METERING PRESSURE* )
103   FORMAT (1H1,4HRUN ,I5,3X,A10,35X,19HGENERAL INFORMATION //
     140X,40HORFCJ, JET ORIFICE ID, IN.................,F6.3/
     240X,40HPNH3, AMMONIA TANK PRESSURE, PSIG........,F6.0/
     240X,40HTAMB, AMBIENT TEMPERATURE, F..............,F6.0/
     240X,40HPBAR, BAROMETRIC PRESSURE, IN HG.........,F6.2 ///)
104   FORMAT(1H , *         MAIN AIR                       MAIN NH3
     1      JET NH3                         JET AIR                    JET * //
     11X,15HP, PSIG.........,F5.1,4X,15HP(1), PSIG.....,F5.1,4X,
     2    15HP(1), PSIG.....,F5.1,4X,15HP(2), PSIG.....,F5.1,4X,
     3    15HP, PSIG.........,F5.1  /
     11X,15HP(2), PSIG.....,F5.1,4X,15HP(2), PSIG.....,F5.1,4X,
     2    15HP(2), PSIG.....,F5.1,4X,15HP(3), PSIG.....,F5.1,4X,
     3    15HT(6), F.........,F5.1  /
     11X,15HP(3), PSIG.....,F5.1,4X,15HP(3), PSIG.....,F5.1,4X,
     2    15HP(3), PSIG.....,F5.1,4X,15HT, F............,F5.1,4X ,
     3 15HT(7), F........., F8.1 /
     11X,15HT, F............,F5.1,4X,15HT, F............,F5.1,4X,
     2    15HT, F............,F5.1,4X,15HD, CM...........,F5.1  /
     11X,15HD1, IN H2O.....,F5.2,4X,15HD, CM...........,F5.1,4X,
     2    15HDS, CM..........,F5.1  / 1X,15HD2, IN H2O.....,F5.2,
     2 28X,15HDG, CM..........,F5.1 /
     11X,15HP/P.............,F5.1,4X,15HP/P.............,F5.1,4X,
     2    15HP/P.............,F5.1,4X,15HP/P.............,F5.1 ///)
105   FORMAT (11X,8HAPPROACH, 44X,19HTEMPERATURE PROFILE, 38X,5HVYCOR/
     1 26X,7HR, IN.., 10F7.3 /
     1 1X,15HP, IN H2O......,F5.3,5X, 7HT, F...,        1X,10F7.1,
     2 5X,11HT(8), F....,F5.1 /
     2  1X,15HT, F............,F5.1,88X,11HT(9), F....,F5.1 / 109X,
     2 11HT(10), F...,F5.1 / 109X,11HT(11), F...,F5.1 //)
106   FORMAT (  // 20X,*MAIN AIR                       MAIN NH3
     1   JET NH3                         JET AIR *// 1X,*FLOW RATES*/
     23X,*LBM/SEC*,E18.4,3E25.4 /  6X,*SCFM*,F18.3,3F25.3 /
```

```
      31X,*ORIFICE RE*,E18.4 ///)
107    FORMAT (1H ,34X,8HAPPROACH,19X8HJET EXIT // 11X,
      119HTOTAL FLOW, LBM/SEC, E12.4,E27.4/   11X,19HVELOCITY, FPS
      2F12.1,F27.1  / 11X, 19HT, F                     , F12.1,F27.1 /  11X,
      319HP, PSIA            ,F12.2,F27.2  / 11X, 19HRHO, LBM/FT3
      4F12.4, F27.4 /  11X,19HPHI                      ,F12.4,F27.4//)
108    FORMAT (1H ,*PERCENT MASS FLOW OF JET =*,F6.2 )
110    FORMAT (16F5.2)
111    FORMAT (14H GARNET,M2;ME=,3F5.3)
112    FORMAT (11X,8HAPPROACH,10X,5HVYCOR/ 1X,15HP, IN H2O......,F5.3,
      15X,11HT(8), F....,F5.1 / 1X,15HT, F...........,F5.1,5X,
      2 11HT(9), F....,F5.1 / 26X,11HT(10), F...,F5.1 / 26X,
      3 11HT(11), F...,F5.1 //)
       END
      SUBROUTINE JAIR(PBAR, P, T, D, ASJ, Q)
C CALCULATES MASS FLOW OF AIR (LBM/SEC) IN FISCHER-PORTER ROTAMETER,
C TUBE 8-3A25, FLOAT BSX-33(SS)
      P=P+PBAR
      DNS=0.075
      CORR=SQRT(P*530./(14.7*T))
      CALL FITLAG (D,2.0,5.0,10.0,0.25,0.416,0.67,Q)
      QA=Q*CORR
      ASJ=QA*DNS/60.
      RETURN
      END
      SUBROUTINE MAIR (PBAR, P, T, D1, D2, ASM, Q)
C CALCULATES AIR MASS FLOW FOR FLANGE-TAPPED CONCENTRIC SQUARE-EDGE ORIF
C 2-INCH PIPE, USING METER COEFFICIENTS FROM ASME FLOWMETER HANDBOOK, 1
C P. 14-16.  COMPRESSIBILITY FACTORS GOOD FOR SUB- OR SUPER-CRITICAL FL
C CUNNINGHAM, ASME TRANSACTIONS VOL. 73, P. 625, 1951.
      OD=0.600
      CI=18.121
      P=P+PBAR
      DP=D1+D2
      P2=P-DP*(62.31/62.37)/27.70
      RHO=P*144./(53.34*T)
      BETA=OD/2.067
      GK=1.4
      RAT=P2/P
      IF (RAT .LT. .63) GO TO 1
      Y=1.-(.41+.35*(BETA**4))*(1.-RAT)/GK
      GO TO 2
1     Y63=1.-(.41+.35*(BETA**4))*(1.-.63)/GK
      Y=Y63-.3501*(.63-RAT)
2     CONTINUE
      ASM=2.067**2*SQRT(DP*RHO)
      ASM=(CI*ASM/3600.)*Y
      CORR=SQRT(P*530./(14.696*T))
      Q=ASM*60./(CORR*0.0765)
      RETURN
      END
      SUBROUTINE NH3 (PBAR, P, T, D, DG, I, FS, Q)
C CALCULATES MAIN AMMONIA MASS FLOW RATE IN FISCHER-PORTER ROTAMETER,
C TUBE B4N-25-A, FLOAT BSX-41-A(SS) (I=0) AND JET AMMONIA MASS FLOW IN
C 604 (I=1)
CALCULATES SPECIFIC VOLUME OF AMMONIA VAPOR FROM BEATTIE-BRIDGMAN EQUATI
       PP(V) = R*T*((1.-(C/(V*T**3)))/V**2)* (V+BB*(1.-B/V)) - AA*(1.-A/
     1 V) /V**2
       VSTD = 22.48
       R = .73023
       AA = 613.91
      A=2.729
       BB=.547
       B=3.062
       C=445600000.
      P=(P+PBAR)/PBAR
       V = R*T/P
       ICT = 0
       DV = .2
    5  DIF = PP(V) - P
       V2=V+DV
       DEL = PP(V2) - P
       IF (DEL - DIF) 6,7,8
    6  V3 = V + (V2 - V) * DIF/(DIF - DEL)
       GO TO 9
    8  V3 = V2 + (V2 - V) * DEL/(DIF - DEL)
    9  DE=ABS((V3-V2)/2.)
       IF (DE.LT. .005) GO TO 7
       DV = AMIN1 (.2,DE)
       V = V3
       ICT=ICT+1
       IF (ICT .GT. 10) GO TO 7
       GO TO 5
    7  CONTINUE
      PPX=PP(V3)
       PRINT 20, V3, V2, P, PPX
       VOLNH3 = V3/17.03
       DNS = 1./VSTD
       CORR = SQRT( VSTD/VOLNH3)
      IF(I) 40,40,50
40    CALL FITLAG (D,5.0,15.0,25.0,1.26,2.64,4.04,Q)
      GO TO 51
50    CALL FITLAG (D,2.0,4.0,6.0,0.0813,0.168,0.256,Q)
      CALL FITLAG (DG,2.0,3.7,5.0,0.0345,0.0813,0.112,QG)
      PRINT 100, Q, QG
100   FORMAT (6H Q,QG=,2F6.4)
      Q=(Q+QG)/2.
51    CONTINUE
      Q=Q*SQRT(0.075/DNS)
      FS=Q*DNS/60.*CORR
   20  FORMAT (45X, 21H V3, V2, P, PP(V3) = , 4F15.4)
       RETURN
       END
      SUBROUTINE FITLAG (X, X1, X2, X3, Y1, Y2, Y3, Y )
C LAGRANGE SECOND-ORDER INTERPOLATION (3-PT PARABOLIC FIT)
C X IS ABSCISSA, LOCATED BETWEEN X1, X2, AND X3.  Y IS DESIRED ORDINATE.
      AA = Y1/((X1-X2) * (X1-X3))
      BB = Y2/((X2-X1) * (X2-X3))
      CC = Y3/((X3-X1) * (X3-X2))
      A = AA + BB + CC
      B = - ((X2+X3)*AA + (X1+X3)*BB + (X1+X2)*CC)
      C = X2*X3*AA + X1*X3*BB + X1*X2*CC
      Y = (A*X + B) * X + C
      RETURN
      END
      FUNCTION CHRMAL (VV)
C CONVERTS MILLIVOLT OUTPUT OF CHROMEL-ALUMEL THERMOCOUPLE TO DEG F.
      DIMENSION Z(20), W(20)
      DATA (Z(I), W(I), I=1,20) / 32.,0.,40.,.18,60.,.62,80.,1.06,100.,
     11.52,150.,2.66,200.,3.82,300.,6.09,400.,8.31,500.,10.57,600.,
     212.86,700.,15.18,800.,17.53,900.,19.89,1000.,22.26,1250.,
     328.15,1500.,33.93,1750.,39.53,2000.,44.91,2500.,54.92/
      DO 10 J=1,20
      I=J
10    IF (VV.LE.W(I)) GO TO 11
11    CALL FITLAG (VV,W(I-1),W(I),W(I+1),Z(I-1),Z(I),Z(I+1),CHRMAL)
      CHRMAL = CHRMAL
      RETURN
      END
      FUNCTION PT13RO (VV)
C CONVERTS MILLIVOLT OUTPUT OF PT-PT 13 PCT RHO THERMOCOUPLE TO DEG F,
C WITH REFERENCE JUNCTION OF 32 DEG F.
      DIMENSION Z(20), W(20)
      DATA (Z(I), W(I), I=1,20)/ 40.,.02,300.,1.03,600.,2.55,900.,4.26,
     11200.,6.13,1400.,7.44,1600.,8.81,1800.,10.24,2000.,11.73,
     22100.,12.49,2200.,13.26,2300.,14.03,2400.,14.80,2500.,15.57,
     32600.,16.34,2700.,17.11,2800.,17.88,2900.,18.64,3000.,19.39,
     43100.,20.15 /
      DO 10 J=1,20
      I=J
10    IF (VV.LE.W(I)) GO TO 11
11    CALL FITLAG (VV,W(I-1),W(I),W(I+1),Z(I-1),Z(I),Z(I+1),TEMP)
      PT13RO = TEMP
      RETURN
      END
     15115. 29.7371.  R=0.8
48.1 46.0 8.75 0.8164.80 3.20 59.0 53.0 40.0 0.65218.05
30.0 2.00 0.8273.20 59.0 53.0 1.00 0.8751.60 3.00
1.50 0.8750.00 0.32 0.7632.6001.9031.2912.246
     16120. 29.7372.  R=0.9
49.0 46.0 8.75 0.8184.80 3.20 63.0 57.0 39.6 0.89718.05
30.0 2.80 0.8753.20 63.0 57.0 2.50 0.9211.60 3.00
2.10 0.8870.00 0.36 0.791 0.00 0.00 0.00 0.00
     17130. 29.7371.5 R=0.7
49.1 47.0 8.75 0.8334.80 3.20 63.0 57.0 39.6 0.89918.05
30.0 3.20 0.8883.20 63.0 57.0 3.00 0.9271.60 3.00
2.60 0.9050.00 0.40 0.801 0.00 0.00 0.00 0.00
     18130. 29.7372.  R=0.6
48.5 46.0 8.75 0.8294.80 3.20 63.0 56.0 40.4 0.89518.05
30.0 4.00 0.8953.20 63.0 56.0 3.70 0.9401.60 3.00
3.50 0.9200.00 0.43 0.8203.0822.7321.4743.549
     19120. 29.7372.  R=0.5
48.8 46.0 8.75 0.8224.80 3.20 62.0 56.0 40.0 0.91418.05
30.0 4.80 0.9033.20 62.0 56.0 4.40 0.9621.60 3.00
4.00 0.9220.00 0.45 0.8050.00 0.00 0.00 0.00
     20115. 29.7372.  R=0.4
49.0 47.0 8.75 0.8474.80 3.20 61.0 55.0 40.0 0.93218.05
30.0 5.40 0.9143.20 61.0 55.0 5.00 0.9531.60 3.00
4.60 0.9280.00 0.47 0.8254.6213.2931.7864.022
     21105. 29.7372.  R=0.3
48.9 47.0 8.75 0.8674.80 3.20 61.0 55.0 40.1 0.95018.05
30.0 5.90 0.9203.20 61.0 55.0 5.50 0.9431.60 3.00
5.20 0.9110.00 0.47 0.8094.8123.4671.9334.008
     22102. 29.7372.  R=0.2
49.2 47.0 8.75 .852 4.80 3.20 61.0 55.0 40.0 0.98018.05
30.0 5.90 0.9193.20 61.0 55.0 5.50 0.9351.60 3.00
5.20 0.916 0.000.47 0.8250.00 0.00 0.00 0.00
     23 75. 29.8861.  R=0.6
48.0 46.0 8.75 0.7004.80 3.20 62.0 56.0 40.4 0.56518.05
30.0 2.10 0.6933.20 62.0 56.0 1.80 0.7391.60 3.00
1.50 0.7150.00 0.33 0.6000.00 0.00 0.00 0.00
 .1858.77 0.20 9.29 0.30 9.87 0.40 9.04 0.50 7.44 0.60
 .90 1.37 1.00 0.93
     24 90. 29.8863.  R=0.7
47.2 45.0 8.75 0.6904.80 3.20 67.0 62.0 39.8 0.70018.05
30.0 2.50 0.7103.20 67.0 62.0 2.10 0.7301.60 3.00
1.80 0.6920.00 0.35 0.6010.00 0.00 0.00 0.00
     25115. 29.8863.  R=0.8
48.0 46.0 8.75 0.6804.80 3.20 69.0 65.0 39.0 0.73518.05
30.0 2.50 0.7353.20 69.0 65.0 2.10 0.7201.60 3.00
2.00 0.6950.00 0.35 0.6100.00 0.00 0.00 0.00
     26135. 29.8863.  R=0.9
47.2 45.0 8.75 0.6854.80 3.20 70.0 65.0 39.6 0.77518.05
30.0 2.50 0.7753.20 70.0 65.0 2.30 0.7351.60 3.00
2.10 0.7150.00 0.35 0.6300.00 0.00 0.00 0.00
     27148. 29.8863.  R=0.5
48.0 46.0 8.75 0.6854.80 3.20 70.0 65.0 39.9 0.78018.05
30.0 2.80 0.7803.20 70.0 65.0 2.50 0.7281.60 3.00
     28150. 29.8863.5 R=0.4
47.2 45.0 8.75 0.7004.80 3.20 70.0 65.0 39.9 0.74118.05
30.0 3.10 0.7413.20 70.0 65.0 2.80 0.7321.60 3.00
2.50 0.6900.00 0.38 0.6223.0282.0121.3122.462
```

```
   1180. 29.6061.   R=0.1
47.8 46.0 8.75 0.63 4.80 3.20 61.0 56.0 39.5 0.81 18.05
30.0 1.50 0.63 3.20 44.0 44.0 0.00 0.62 1.60 3.00
 .75 0.62 0.00 0.05 0.55 0.00 0.00 0.00 0.00
   2160. 29.6061.   R=0.025
47.1 45.0 8.75 0.64 4.80 3.20 61.0 56.0 39.0 0.82 18.05
30.0 1.50 0.63 3.20 44.0 44.0 0.00 0.63 1.60 3.00
 .75 0.62 0.00 0.05 0.57 0.00 0.00 0.00 0.00
   3150. 29.6061.   R=0.2
47.1 45.0 8.75 0.63 4.80 3.20 61.0 56.0 39.1 0.79 18.05
30.0 1.50 0.63 3.20 44.0 44.0 0.00 0.65 1.60 3.00
 .75 0.61 0.00 0.05 0.54 0.00 0.00 0.00 0.00
   4135. 29.6061.   R=0.3
47.9 45.0 8.75 0.63 4.80 3.20 61.0 56.0 39.5 0.80 18.05
30.0 1.50 0.64 3.20 44.0 44.0 0.00 0.66 1.60 3.00
 .75 0.63 0.00 0.05 0.56 0.00 0.00 0.00 0.00
   5130. 29.6061.   R=0.4
47.5 46.0 8.75 0.63 4.80 3.20 61.0 56.0 39.6 0.86 18.05
30.0 1.50 0.65 3.20 44.0 44.0 00.0 0.66 1.60 3.00
 .75 0.62 0.00 0.05 0.57 0.00 0.00 0.00 0.00
   6145. 29.6062.   R=0.5
47.2 45.0 8.75 0.63 4.80 3.20 62.0 57.0 39.4 0.93 18.05
30.0 1.50 0.64 3.20 44.0 44.0 0.00 0.65 1.60 3.00
 .75 0.63 0.00 0.05 0.57 0.00 0.00 0.00 0.00
   7155. 29.6062.   R=0.6
48.0 46.0 8.75 0.65 4.80 3.20 62.0 57.0 39.4 0.93 18.05
30.0 1.50 0.64 3.20 44.0 44.0 0.00 0.66 1.60 3.00
 .75 0.63 0.00 0.05 0.60 0.00 0.00 0.00 0.00
   8145. 29.6063.   R=0.7
48.0 46.0 8.75 0.63 4.80 3.20 62.0 56.0 39.2 0.91 18.05
30.0 1.50 0.65 3.20 44.0 44.0 0.00 0.65 1.60 3.00
 .75 0.64 0.00 0.05 0.58 0.00 0.00 0.00 0.00
   9130. 29.6063.   R=0.8
47.8 46.0 8.75 0.64 4.80 3.20 61.0 56.0 39.1 0.90 18.05
30.0 1.50 0.65 3.20 44.0 44.0 0.00 0.65 1.60 3.00
 .75 0.63 0.00 0.05 0.59 0.00 0.00 0.00 0.00
   10120. 29.6062.   R=0.865
47.5 45.0 8.75 0.65 4.80 3.20 61.0 55.0 39.2 0.92 18.05
30.0 1.50 0.65 3.20 44.0 44.0 0.00 0.65 1.60 3.00
 .75 0.62 0.00 0.05 0.59 0.00 0.00 0.00 0.00
   11127. 29.6063.   R=0.5
48.0 46.0 8.75 0.65 4.80 3.20 61.0 56.0 39.2 1.02 18.05
30.0 1.50 0.65 3.20 44.0 44.0 0.00 0.67 1.60 3.00
 .75 0.64 0.00 0.05 0.60 0.00 0.00 0.00 0.00
   12145. 29.6063.   R=0.2
48.0 46.0 8.75 0.66 4.80 3.20 62.0 56.0 39.0 1.06 18.05
30.0 1.50 0.66 3.20 44.0 44.0 0.00 0.66 1.60 3.00
 .75 0.63 0.00 0.05 0.61 0.00 0.00 0.00 0.00
   13130. 27.7261.   JETEMP
47.8 46.0 8.75 0.63 4.80 3.20 71.0 66.0 39.6 0.53 18.05
30.0 1.60 0.65 3.20 38.0 38.0 0.40 0.65 1.60 3.00
1.10 0.64 22.000.30 0.55 0.00 0.00 0.00 0.00
   14120. 29.8770.   R=0.6
48.0 45.0 8.75 0.70 4.80 3.20 59.0 54.0 39.5 0.71 18.05
30.0 3.10 0.64 3.20 59.0 54.0 2.80 0.89 1.60 3.00
2.50 0.85 0.00 0.36 0.74 4.77 7.15 8.73 9.62
```

Reproduced from
best available copy.

```
   29150. 29.8864.  R=0.3
47.8 45.0 8.75 0.7004.80 3.20 70.0 65.0 39.9 0.74218.05
30.0 3.30 0.7423.20 70.0 65.0 3.00 0.7281.60 3.00
2.80 0.7100.00 0.39 0.6323.0282.0121.3122.462
   30150. 29.8864.2 R=0.2
48.1 45.0 8.75 0.6504.80 3.20 70.0 65.0 39.7 0.75118.05
30.0 3.50 0.7513.20 70.0 65.0 3.20 0.7411.60 3.00
3.00 0.7100.00 0.40 0.6283.0282.0121.3122.462
   31150. 29.8864.5 R=0.4
47.8 45.0 8.75 0.7124.80 3.20 70.0 65.0 39.6 0.76518.05
30.0 3.60 0.7093.20 70.0 65.0 3.40 0.7381.60 3.00
3.20 0.7250.00 0.40 0.6823.5982.3611.4582.952
   32145. 29.8865.  R=0.7
48.1 46.0 8.75 0.7104.80 3.20 70.0 65.0 39.6 0.77818.05
30.0 3.90 0.7213.20 70.0 65.0 3.60 0.7381.60 3.00
3.40 0.7180.00 0.41 0.6283.5982.3611.4582.952
   33145. 29.8865.5 R=1.00
47.5 45.0 8.75 0.6954.80 3.20 70.0 65.0 39.6 0.78518.05
30.0 4.30 0.7223.20 70.0 65.0 4.00 0.7381.60 3.00
3.80 0.7320.00 0.4250.6353.5982.3611.4582.952
   34145. 29.8865.8 R=1.10
48.0 46.0 8.75 0.7124.80 3.20 70.0 65.0 39.6 0.78518.05
30.0 5.00 0.7403.20 70.0 65.0 4.60 0.7441.60 3.00
4.40 0.7300.00 0.4250.6383.0482.6301.6203.285
   35138. 29.8866.5 R=0.185
47.8 45.0 8.75 0.6924.80 3.20 70.0 65.0 39.6 0.82418.05
30.0 5.90 0.7253.20 70.0 65.0 5.60 0.7491.60 3.00
5.30 0.7350.00 0.4750.6534.0282.8351.7453.460
   36130. 29.8057.   LBL02
48.  48.  1.3  .56  1.8  0.2  73.  65.   7.0 .10  8.0
30.0 4.0  .57  3.2  73.  65.  2.5  .57  1.6  3.0
3.0  .57  0.0  .27  .53
   37130. 29.8057.   RBL02
47.5 48.  1.5  .56  1.8  0.2  74.  73.  22.0 .12  13.9
30.0 4.0  .57  3.2  74.  73.  3.5  .58  1.6  3.0
3.2  .56  0.0  .27  .54
   38134. 29.8057.   LBL03
47.0 46.  2.6  .57  2.3  0.7  74.  74.  11.1 .12  10.2
30.0 4.0  .57  3.2  74.  74.  3.5  .58  1.6  3.0
3.2  .56  0.0  .32  .54
   39140. 29.8057.   RBL03
47.0 46.  2.5  .56  2.3  0.7  76.  75.  22.0 .15  15.6
30.0 4.0  .57  3.2  76.  75.  3.0  .57  1.6  3.0
3.5  .56  0.0  .32  .54
   40145. 29.8057.   LBL04
47.0 46.  4.0  .56  2.8  1.2  77.  75.  14.0 .15  11.2
30.0 4.0  .56  3.2  77.  75.  3.5  .57  1.6  3.0
3.1  .55  0.0  .32  .52
   41145. 29.8057.   RBL04
47.0 46.  4.0  .56  2.8  1.2  77.  75.  35.0 .15  17.0
30.0 4.0  .56  3.2  77.  75.  3.5  .57  1.6  3.0
3.1  .55  0.0  .32  .52  6.66 4.16 2.10 5.08
   42130. 29.8057.   LBL05
47.5 46.  5.9  .57  3.3  1.7  76.  75.  18.5 .22  12.8
30.0 4.0  .56  3.2  76.  75.  3.5  .56  1.6  3.0
3.1  .55  0.0  .30  .50
```

```
    43130. 29.8057.   RBL05
47.5 46.  5.9  .57   3.3  1.7  76.  75.  39.9 .22  18.0
30.0 4.0  .56  3.2   76.  75.  3.5  .56  1.6  3.0
    44115. 29.8057.   LBL06
47.1 46.  6.5  .57   3.8  2.2  74.  72.  21.4 .30  13.9
30.0 3.8  .57  3.2   74.  72.  3.3  .57  1.6  3.0
3.1  .56  0.0  .36   .50
    45115. 29.8057.   RBL06
47.1 46.  6.5  .57   3.8  2.2  74.  72.  45.0 .30  19.0
30.0 3.8  .57  3.2   74.  72.  3.3  .57  1.6  3.0
3.1  .56  0.0  .36   .50
    46115. 29.8058.   LBL07
47.0 45.  7.75 .58   4.3  2.7  74.  70.  25.5 .46  14.8
30.0 3.8  .58  3.2   74.  70.  3.5  .58  1.6  3.0
3.3  .57  0.0  .38   .50
    47115. 29.8058.   RBL07
47.0 45.  7.75 .58   4.3  2.7  74.  70.  48.0 .46  19.5
30.0 3.8  .58  3.2   74.  70.  3.5  .58  1.6  3.0
3.3  .57  0.0  .38   .50  4.36 2.96 1.65 3.46
    48130. 29.8058.   LBL08
47.5 46.  8.75 .58   4.8  3.2  76.  68.  29.5 .60  15.8
30.0 3.8  .58  3.2   73.  68.  3.5  .58  1.6  3.0
3.4  .56  0.0  .38   .50
    49130. 29.8058.   RBL08
47.5 46.  8.75 .58   4.8  3.2  73.  68.  52.0 .60  20.3
30.0 3.8  .58  3.2   73.  68.  3.5  .58  1.6  3.0
3.4  .56  0.0  .38   .50
    50135. 29.8058.   LBL09
47.5 45.  9.9  .58   5.3  3.7  76.  70.  32.4 .65  16.5
30.0 4.0  .58  3.2   76.  70.  3.6  .58  1.6  3.0
3.4  .57  0.0  .42   .50
    51135. 29.8058.   RBL09
47.5 45.  9.9  .58   5.3  3.7  76.  70.  53.0 .65  20.5
30.0 4.0  .58  3.2   76.  70.  3.6  .58  1.6  3.0
3.4  .57  0.0  .42   .50
    52120. 29.8058.   LBL09 1/2
47.1 44.  10.25.58   5.55 3.95 78.  74.  35.0 .58  17.0
30.0 4.0  .58  3.2   78.  74.  3.5  .58  1.6  3.0
3.3  .57  0.0  .42   .50
    53120. 29.8058.   RBL09 1/2
47.1 44.  10.25.58   5.55 3.95 78.  74.  53.5 .58  20.5
30.0 4.0  .58  3.2   78.  74.  3.5  .58  1.6  3.0
3.3  .57  0.0  .43   .50
    54110. 29.8058.   LBL010
47.0 44.  10.7 .59   5.8  4.2  80.  74.  35.9 .68  17.2
30.0 4.0  .58  3.2   80.  74.  3.5  .58  1.6  3.0
3.2  .57  0.0  .43   .49  2.93 2.10 1.34 2.44
    55110. 29.8058.   RBL010
47.0 44.  10.7 .59   5.8  4.2  80.  74.  56.0 .68  20.9
30.0 4.0  .58  3.2   80.  74.  3.5  .58  1.6  3.0
3.2  .57  0.0  .43   .49
    56120. 29.8058.   LBL012
47.5 44.  12.5 .58   6.7  5.2  80.  74.  42.2 .81  18.6
30.0 3.8  .58  3.2   80.  74.  3.4  .58  1.6  3.0
3.2  .57  0.0  .43   .50  1.96 1.28 1.24 2.25
```

```
   57120. 29.8058.   MXBLO
47.5 44.   13.5 .58   7.4  5.0  80.   77.   54.5 .81  20.7
30.0 3.8   .58  3.2   80.  77.  4.3  .58   1.6  3.0
3.2  .57   0.0  .43   .50
   58125. 29.8059.   LBLO1
47.5 48.   0.0  .60   1.35 -.30 77.   77.    4.0 .38   5.6
30.0 4.5   .58  3.2   77.  77.  4.3  .58   1.6  3.0
3.2  .57   0.0  .26   .56
   59125. 29.8059.   RBLO1
47.5 48.   0.0  .60   1.35 -.30 77.   77.   14.0 .38  11.1
30.0 4.5   .58  3.2   77.  77.  4.3  .58   1.6  3.0
3.2  .57   0.0  .26   .56
   60130. 29.8059.   LBLO11S
47.5 46.0 11.6 .60    6.3  4.7  77.0 76.0 40.5 .75  18.1
30.0 4.5   .58  3.2   77.0 76.0 4.3  .58   1.6  3.0
3.2  .57   0.0  .42   .50
   61130. 29.8059.   RBLO11S
47.5 46.0 11.5 .60    6.3  4.7  77.0 76.0 58.0 .75  21.2
30.0 4.5   .58  3.2   77.0 76.0 4.3  .58   1.6  3.0
3.2  .57   0.0  .42   .50
   62125. 29.8059.   RBLO12S
47.5 45.0 12.5 .60    6.7  5.2  79.0 75.0 56.6 .79  21.4
30.0 4.5   .58  3.2   79.0 75.0 4.3  .58   1.6  3.0
3.2  .57   0.0  .43   .50
   63125. 29.8059.   LBLO13S
47.5 45.0 13.3 .60    7.3  5.7  78.0 76.0 50.5 .79  20.0
30.0 4.5   .58  3.2   78.0 76.0 4.3  .58   1.6  3.0
3.2  .57   0.0  .43   .50
   64125. 29.8059.   RBLO13S
47.5 45.0 13.3 .60    7.3  5.7  78.0 76.0 58.2 .79  21.3
30.0 4.5   .58  3.2   78.0 76.0 4.3  .58   1.6  3.0
3.2  .57   0.0  .43   .50
```